THE REMOVAL OF D-ALANINE FROM THE CELL WALL TEICHOIC ACIDS OF *STAPHYLOCOCCUS AUREUS* BY THE FMTA PROTEIN DRIVES STRAIN-SPECIFIC VIABILITY ALTERATIONS UNDER ENVIRONMENTAL STRESS CONDITIONS

MATTHEW CAPOTA

A THESIS SUBMITTED TO
THE FACULTY OF GRADUATE STUDIES
IN PARTIAL FULFILMENT OF THE REQUIREMENTS
FOR THE DEGREE OF
MASTER OF SCIENCE

GRADUATE PROGRAM IN BIOLOGY
YORK UNIVERSITY
TORONTO, ONTARIO

March 2025

Abstract

Antibiotic resistance of highly infectious *Staphylococcus aureus* makes eliminating this microorganism increasingly difficult, contributing to hospitalizations and severe infections worldwide. Wall teichoic acids (WTAs), linked to the bacterial cell wall, play key roles in resistance, cell lysis, and survival. WTAs are modified by the addition of D-alanine (D-Ala), which helps control bacterial surface charge and antibiotic resistance. *S. aureus* naturally cleaves D-Ala using the enzyme FmtA. We investigated whether purified FmtA could influence bacterial growth and survival by removing D-Ala from WTAs *in vivo* under favourable or unfavourable environments. Our findings confirmed that FmtA removes D-Ala from *S. aureus* and other Gram-positive bacteria. While *S. aureus* viability remained stable under favourable conditions, strain-specific responses emerged under variable stress. Notably, methicillin-resistant strains became more sensitive to oxacillin when exposed to FmtA. These results suggest that targeting WTA modifications could be a strategy to alter *S. aureus* viability under specific stress-inducing conditions.

Acknowledgments

During this particular chapter of my life, I was constantly reminded of the kindness, dependability, and determination of those around me. To all of you, I would like to extend my deepest gratitude. This thesis would not have been possible without your support.

Under the supervision and instruction of Dr. Golemi-Kotra, I was able to achieve a goal I set for myself as a child: contributing to the further advancement of scientific knowledge in hopes of helping others. She instilled in me a valuable work ethic that I will carry with me in my personal life and as I further my career. I could always rely on her support even when things seemed unexplainable.

Sap and Sai, my lab colleagues whom I now have the privilege to call friends, I would like to thank you both for teaching me and being patient with me as I undoubtably asked many questions. I pray for your continued success and look forward to hearing about your many exploits.

To my parents, John and Monica Capota, I would like to dedicate this thesis. They have supported me my entire life and have been excellent role models. Their acts of devotion and kindness have truly been inspiring, and as I go on to further my career, I will keep in mind the valuable lessons they have taught me.

Jessica, I will always cherish the support and encouragement you've given me. Thank you for keeping me in your prayers and sticking by my side all these years.

To all of my friends who pushed me to strive for success and stood by me through the ups and downs, I thank you.

"Commit to the Lord whatever you do, and he will establish your plans" – Proverbs 16:3

Table of Contents

List of Tables

List of Figures

Chapter One

Chapter Two

Chapter Three

List of Abbreviations

A.U.: Absorbance Units

BPEI: Branched Polyethylenimine

CFU/ml: Colony Forming Units/milliliter

D-Ala: D-Alanine

DAO: Diamine Oxiadase

ddH_2O: Double Distilled Water

DSS: Sodium 2,2-Dimethyl-2-Silapentane-5-Sulfonate

FAD: Flavin Adenine Dinucelotide

GlcNAc: N-Acetylglucosamine

HCl: Hydrochloric Acid

^{1}H-NMR: Proton Nuclear Magnetic Resonance

HRP: Horseradish Peroxidase

IgG: Immunoglobulin G

LB Broth: Luria Bertani Broth

LTA: Lipoteichoic Acid

MIC: Minimum Inhibitory Concentration

MRS: de Man, Rogosa, and Sharpe Broth

MRSA: Methicillin-Resistant *Staphylococcus aureus*

MSSA: Methicillin-Sensitive *Staphylococcus aureus*

OD_{600}: Optical Density (600nm)

PBP: Penicillin Binding Proteins

PBS: Phosphate Buffered Saline

Pi: Inorganic Phosphate

PGRP: Peptidoglycan Recognition Proteins

RCF: Relative Centrifugal Force

RPM: Revolutions Per Minute

Tris: Tris(Hydroxymethyl)aminomethane

TSB: Tryptic Soy Broth

VISA: Vancomycin Intermediate *S. aureus*

WTA: Wall Teichoic Acid

Chapter One:

Introduction

The Implication of Staphylococcus aureus as an Infectious Organism

Gram-positive bacteria, such as *Staphylococcus*, are indigenous to human individuals, inhabiting various niches within and on the human body, including the skin and the nasal passages, without the cause of health-related issues (Wertheim et al., 2005; Findley et al., 2013). However, the *Staphylococcus aureus* (*S. aureus*) organism can lead to life-threatening infections, necessitating immediate medical intervention and hospitalization, with an associated mortality rate estimated to reach values over 30% (Pastagia et al., 2012). They are not only deadly, but these infections can affect diverse areas of the human anatomy, including, but not limited to, the cardiovascular system and the skin. For instance, fatal toxic shock syndrome represents one of many life-threatening outcomes associated with *S. aureus* infections (Todd et al., 1978; Fowler et al., 2003).

Treatments for *S. aureus* infections, that provide successful outcomes for patients, are achievable; however, accurate identification of the infecting strain and selection of appropriate therapeutic strategies significantly influence patient outcomes. Higher rates of recovery are also reached through the availability of a robust immune system and younger patient age (Guillamet et al., 2018).

S. aureus exhibits elevated virulence as the antibiotics that were developed to eradicate their infection, particularly β-lactam antibiotics, are inhibited from limiting peptidoglycan cell wall biosynthesis due to resistance properties emerging in these organisms (Assis et al., 2017; Barber and Rozwadowska-Dowzenko, 1948; Georgopapadakou and Liu, 1980). Furthermore, Methicillin-resistant *S. aureus* (MRSA) strains have acquired an additional layer of resistance to antibiotics saved exclusively for highly virulent and persistent infections, like antibiotic vancomycin (Hort et al., 2021; Ersoy et al., 2022; Singh et al., 2017). The first case of an *S. aureus* infection responding poorly to vancomycin treatment was documented in the late 1900s (Hiramatsu et al. 1997).

Of great significance to modern microbial research endeavours, *S. aureus* employs specific cell wall teichoic acids (WTA) to manifest the aforementioned virulence and antibiotic resistance properties (Hort et al. 2021, Ersoy et al. 2022, Singh et al. 2017). This introduction elucidates the role of *S. aureus* WTA in promoting bacterial survival in hostile environments, including exposure to antibiotics, and defines how WTA facilitates *S. aureus* virulence and regulates peptidoglycan synthesis. Furthermore, current therapeutic approaches against *S. aureus* infections are examined, emphasizing the requirement for innovative, more effective strategies.

What Is WTA? What Makes It Significant for S. aureus?

WTAs are linear polymers of repeating ribitol-phosphate subunits that are covalently attached to the cell envelope, particularly to the peptidoglycan at the surface of the cell wall (Kojima et al., 1985). They play essential roles in cellular processes, including antibiotic resistance, cell division, and the proper localization of enzymes. These enzymes include penicillin-binding proteins (PBPs), which facilitate peptidoglycan biosynthesis; AtlA, responsible for peptidoglycan lysis; and FmtA, which modifies WTAs, altering electrostatic properties at the cell surface (Brown et al., 2013; Ersoy et al., 2022; Hill et al., 2019; Qamar and Golemi-Kotra, 2012; Schlag et al., 2010; Wyke et al., 1981; Rahman et al., 2016). The ribitol-phosphate subunits form a 40-unit-long polymer through phosphodiester bonds creating the WTA backbone (Kojima et al., 1985). The presence of phosphate groups renders these polymers negatively charged, imparting a negative charge to both the WTA backbone and the overall cell wall (Brown et al., 2013).

The ribitol subunits of WTAs are decorated with D-alanine (D-Ala) amino acids covalently bound to the second carbon of the ribitol structure (Mirelman et al., 1970). The presence of D-Ala modifications serves crucial functions within the *S. aureus* cell, including its role in virulence, autolysis, and antibiotic resistance (Peschel et al., 1999; Bertsche et al., 2013; Qamar and Golemi-Kotra, 2012; Wecke et al., 1997; Baur et al., 2014). Furthermore, when bound to WTAs, the D-Ala amino group becomes protonated, resulting in a positive charge. As a result, the negative charge conferred on the *S. aureus* cell wall by the WTA backbone groups is reduced (Neuhaus and Baddiley, 2003). The *dltABCD* operon encodes the Dlt proteins, which collaboratively facilitate the addition of D-Ala to the lipoteichoic acids (LTAs) attached to the cell membrane (Peschel et

al. 1999). These proteins function by transporting the D-Ala from within the cell, making it available for attachment onto the LTA extracellularly (Neuhaus and Baddiley, 2003). Notably, evidence suggests that the D-Ala content made available for teichoic acids is shared between LTA and WTA, as LTA absence in *S. aureus* leads to WTAs lacking D-Ala. It is believed that the LTA is modified initially and subsequently undergoes dealanylation providing the D-Ala amino acids needed for WTA modification. However, the mechanism underlying the transfer of D-Ala remains unclear (Reichmann et al., 2013; Rahman et al., 2016). One proposed mechanism for the initial modification step of WTAs with D-Ala is the facilitated hydrolysis of the bond between D-Ala and LTA by a protein native to *S. aureus* called FmtA (Rahman et al., 2016; Qamar and Golemi-Kotra, 2012).

The ribitol subunits of WTAs can undergo glycosylation through the addition of N-Acetylglucosamine residues. These sugar molecules, when bound to WTA, have been linked to antibiotic resistance properties in *S. aureus* (Brown et al. 2012), as well as the bacterium's ability to bind to host receptors during invasion and withstand changes in environmental conditions (Mistretta et al., 2019; Winstel et al., 2015). There are two primary configurations in which N-Acetylglucosamine residues can be attached to WTAs: α and β configurations. The regulation of which N-Acetylglucosamine configuration is added to WTAs is mediated by the TarM and TarS proteins. The α-N-Acetylglucosamine variant is added to the WTA following synthesis of the TarM protein, while TarS adds this sugar molecule in the β configuration (Mistretta et al., 2019). Different clinical and reference strains of *S. aureus* exhibit diverse expression profiles for the TarM and TarS proteins. Experimental evidence suggests that not all strains of *S. aureus* possess the TarM protein, as they do the TarS protein. This leads to WTAs exhibiting sugar modifications lacking the α configuration entirely. If the strain harbors both *tarS* and *tarM* genes, both β-N-Acetylglucosamine and α-N-Acetylglucosamine WTAs are observed on the peptidoglycan surface (Mistretta et al., 2019). As discussed in this section, the physiological implications of WTAs are critical for the survival and viability of *S. aureus* in various environmental conditions. The modifications of WTAs and their interactions with different cellular proteins establish WTAs as essential components for *S. aureus* viability, as will be further discussed in subsequent sections.

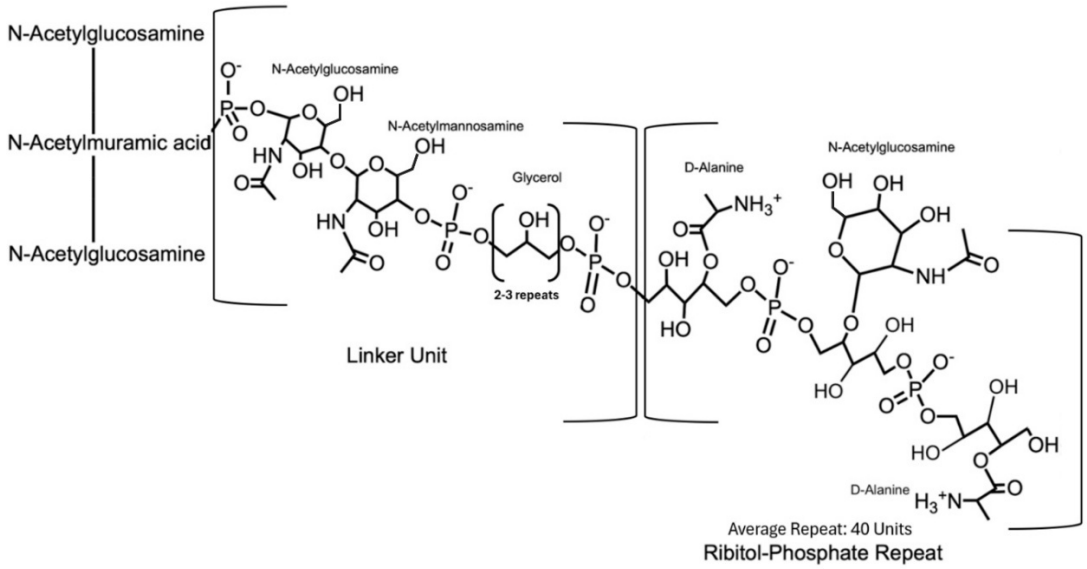

Figure 1. Depiction of the structure of a typical *S. aureus* WTA polymer complete with the linker unit and partial repeats of the ribitol-phosphate subunits. The WTA backbone consists majorly of ribitol-phosphate repeats estimated to consist of an average of 40 units. D-alanine and glucose modifications, bound to the ribitol-phosphate, are also present and labelled.

Insite Into the WTA-Bound Cell Wall Assembly Providing Structural Support and Protection

Peptidoglycan, the essential architectural unit of *S. aureus* cell walls, is organized into a net-like structure beyond the cell membrane. Several N-Acetylmuramic acid and N-Acetylglucosamine molecules are joined through glycosidic bonds to create this peptidoglycan (Schleifer and Kandler, 1972; Ghuysen, 1968). The N-Acetylmuramic acid units are connected together via crosslinking regions within the stacked cell wall layers, facilitating cohesion between adjacent layers. These N-Acetylmuramic acid subunits contain pentapeptide segments that extend between the strands of peptidoglycan, enabling the formation of these crosslinking regions between closely oriented subunits by means of a pentaglycine bridge. The pentapeptide is composed of various amino acids, including L- and D-Alanine, L-Lysine, and D-glutamic acid (Schleifer and Kandler, 1972; Ghuysen, 1968). The WTAs of *S. aureus* play a crucial task in

regulating the activities of autolysins, like AtlA, and peptidoglycan-synthesizing proteins PBP4, and PBP2a. (Qamar and Golemi-Kotra 2012, Schlag et al. 2010, Atilano et al. 2010, Łęski and Tomasz 2005).

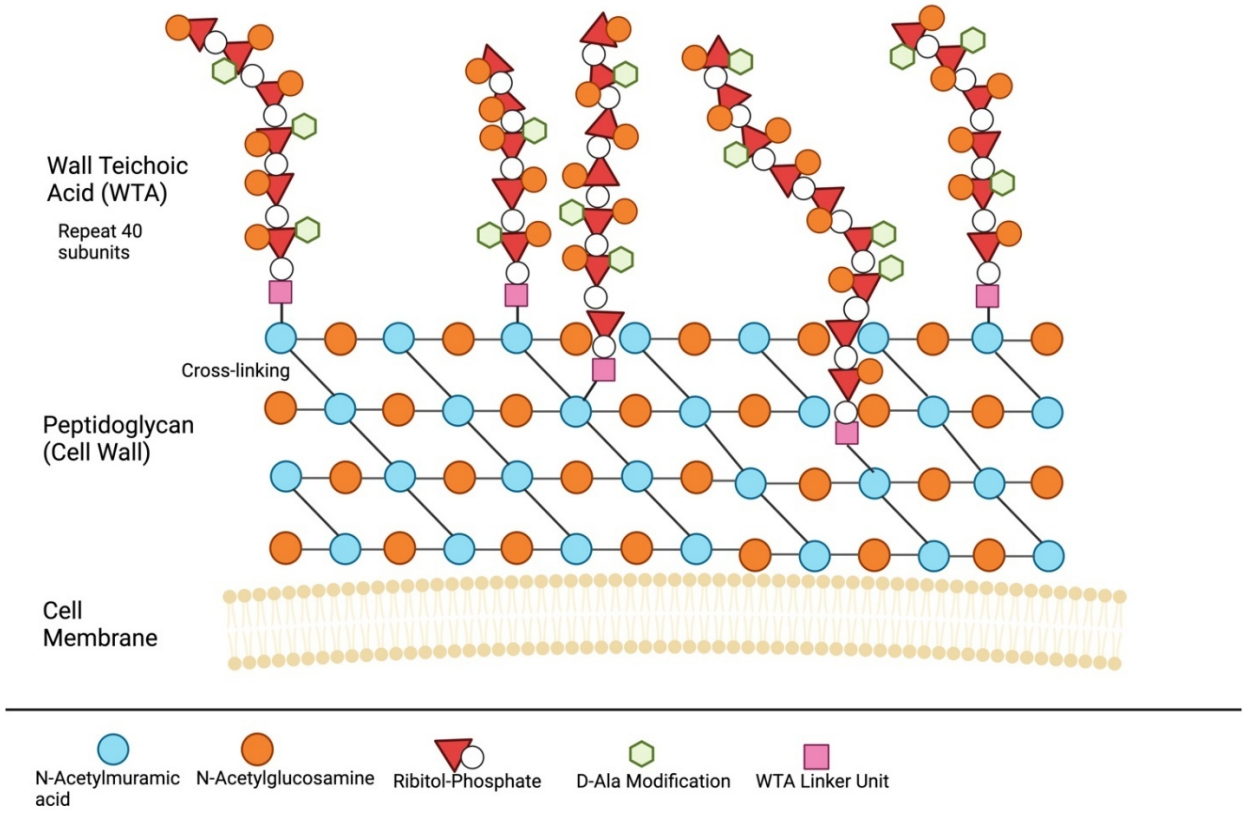

Figure 2. A schematic representation of the cell surface of the *S. aureus* organism subdivided into two primary structural components: the cell membrane and the cell wall. The cell wall consists of multiple layers of peptidoglycan, comprising repeating units of N-Acetylmuramic acid and N-Acetylglucosamine. These layers are interconnected via cross-linking regions. Additionally, WTAs are covalently attached to the peptidoglycan, forming polymers. WTAs contain both D-alanine and glucosamine modifications. Created in BioRender.com

WTA Regulation of Vital Peptidoglycan Lysis Through Proper AtlA Localization

Autolysis of the peptidoglycan cell wall in *S. aureus* is facilitated by the protein AtlA, synthesized by the expression of the *atl* gene, which plays a critical role in lysing the peptidoglycan at the cell division septa enabling cell division to occur as intended (Biswas et al., 2006; Oshida et al., 1995). Genetic mutation, preventing AtlA protein synthesis, impedes proper cell division, resulting in cells that are disproportionate in size compared to their wildtype counterparts, and a higher proportion of clustered cells that remain interconnected and have difficulty separating (Biswas et al., 2006). AM and GL hydrolase proteins, each with specific enzymatic functions, originate from the cleavage of the AtlA protein, following AtlA synthesis and extracellular transport (Oshida et al., 1995). The first protein, AM, possesses amidase activity and is responsible for cleaving the bond between N-Acetylmuramic acid and L-Alanine in the peptidoglycan peptide chain (Oshida et al., 1995). The second protein, GL, exhibits glycosaminidase activity, targeting the covalent bond of the peptidoglycan at the N-Acetylglucosamine subunit (Oshida et al., 1995; Karamanos, 1997).

WTA plays a pivotal role in regulating peptidoglycan lysis and cell division by modulating the activity of the AtlA protein. The presence of WTAs on the cell wall seems to decrease the intensity of cell wall autolysis, whereas their apparent deficiency at the cell division septa promotes AtlA localization and activity in this region (Schlag et al., 2010). In particular, this localization of the AtlA protein can be facilitated by various modifications of WTA (Hort et al., 2021). Notably, there appears to be a correlation between β-N-Acetylglucosamine modified WTA and cell wall autolysis induced by AtlA. Antibiotic-resistant *S. aureus* strains, such as the laboratory strain VC40, synthesize the β-N-Acetylglucosamine variant of WTA over the α variant, with 75% of the N-Acetylglucosamine synthesized by VC40 being in the β configuration. This leads to decreased peptidoglycan autolysis as a result of restricted AtlA-peptidoglycan interaction. It is noteworthy to mention, and subsequently discussed in detail, that decreased peptidoglycan crosslinking is observed in some antibiotic-resistant strains, prompting these cells to avoid additional peptidoglycan weakening by limiting cell wall autolysis (Hort et al., 2021).

Furthermore, D-Ala modifications on WTA also influence autolysis activity. The overall charge of the cell wall is impacted by the presence of the D-Ala residues on WTA, shifting the charge due to these positive residues (Wecke et al., 1997). In *Bacillus subtilis*, another Gram-

positive organism, the modification of WTAs with D-Ala contributes to limiting cell wall autolysis. In other words, the presence of WTAs devoid of D-Ala enhances autolysin action by guiding them to the cell wall through electrostatic attraction between the WTA backbone and the autolysins, as the latter display a net positive charge (Wecke et al., 1997). In contrast to the findings of Wecke et al. (1997) regarding *Bacillus subtilis*, a study by Peschel et al. (2000) investigating vancomycin-tolerant *S. aureus* cells revealed a distinct difference in autolysis patterns. In this study, it was believed that the electrostatic attraction between the WTA backbone and the autolysins prevented the latter from reaching the cell wall, decreasing its activity. This was evident upon removal of the D-Ala content from WTA through the elimination of the *dlt* operon (Peschel et al., 2000). Vancomycin-resistant *S. aureus* strains, along with how they differ from MRSA strains, will be further discussed in subsequent sections.

Hesser et al. (2020) demonstrated that WTAs are not the only regulators of autolysis, as the D-Ala bound LTA in MRSA *S. aureus* also exhibit an impact on autolysis. An elevation in peptidoglycan autolysis was linked to the inhibition of the early stages of LTA synthesis due to improper glycolipid anchor production and transportation, resulting in LTA production lacking this membrane anchor. This inhibition was achieved by genetic alterations leading to the removal of the *ugtP* and *ltaA* genes. Further prevention of D-Ala incorporation in these mutants also played a role in the elevated cell wall lysis observed. Interestingly, evidence confirmed that a mechanism in *S. aureus* cells, which ensures proper regulation of autolysis, is activated to increase WTA synthesis if LTA synthesis is ever inhibited. Although Hesser et al. (2020) did not specifically address alterations in D-Ala content on WTA, they proposed that when the synthesis of either WTA or LTA is compromised, *S. aureus* offsets this loss by increasing the synthesis of the unaffected teichoic acid through an unknown process (Hesser et al., 2020). Therefore, it is plausible that D-Ala modification could also be redirected to WTA when LTA synthesis is impaired. While the role of D-Ala modification in regulating WTA-mediated autolysis is evident, it appears that the conservation of WTA D-Ala regulation of autolysis may vary depending on the Gram-positive organism, *S. aureus* strain, or the presence of mutations in cell surface components, as discussed.

Interestingly, WTAs have been shown to regulate the pH of the cell peptidoglycan, thereby exerting control over the localization of the AtlA protein (Biswas et al., 2012). Evidence suggests a charge-dependent attraction between extracellularly released protons and the WTA backbone, facilitating a decrease in the cell surface pH and subsequently a decrease in AtlA function. This

phenomenon, along with the speculated absence of protons at the cell division septa, regulates AtlA-mediated peptidoglycan lysis at the cell division septa by maintaining proper AtlA localization (Biswas et al., 2012). This region is speculated to contain WTA (Atilano et al., 2010); however, the density of WTA on the peptidoglycan outside of this region is far greater (Schlag et al., 2010). The intricate role of WTA in cell wall autolysis, particularly in conjunction with the AtlA protein, highlights the complexity of bacterial cell wall dynamics. The precise mechanisms by which WTA controls the localization and activity of AtlA, including the implications of the D-Ala modifications, remain a subject of ongoing microbiological research.

Localization of PBPs to the Division Septa by WTA Promotes Peptidoglycan Biosynthesis

The survival and viability of *S. aureus* is highly dependent upon Penicillin-binding proteins (PBPs). The various types of PBPs identified in *S. aureus* are PBP1, PBP2, PBP4, and non-native PBP2a. These proteins play a crucial role in facilitating the cross-linking bridge formed between the different layers of the peptidoglycan as the cell wall is synthesized. This process is referred to as transpeptidation. Cross-linking leads to enhanced structural integrity and provides protection against environmental stressors, including antibiotics (Wada and Watanabe, 1998; Wacnik et al., 2022; Pinho et al., 2001; Wyke et al., 1981; Lim and Strynadka, 2002).

As mentioned, PBP2a is a non-native *S. aureus* protein synthesized from the expression of the *mec* gene acquired by genetic transfer between organisms (Fuda et al., 2004). This protein is a PBP variant present in *S. aureus*, conferring the β-lactam resistance phenotypes observed particularly in MRSA strains. Resistance arises as a result of the inability of readily accessible antibiotics to interact with and suppress PBP2a activity (Hartman and Tomasz, 1984; Lim and Strynadka, 2002). WTAs have been reported to affect PBP4 and may further influence PBP2a, indicating WTA's significance in cell wall biosynthesis. However, no direct relationship has been observed between WTA and other native PBPs of *S. aureus*. WTA plays a decisive role in PBP4 function by maintaining PBP4 positioning at the site of peptidoglycan synthesis (Atilano et al., 2010; Hill et al., 2019). Moreover, the report that PBP2a directly associates with WTA (Qamar and

Golemi-Kotra, 2012) suggests that the absence or inhibition of WTA may lead to the delocalization of PBP2a, impacting antibiotic resistance and peptidoglycan cross-linking in *S. aureus*.

Interactions among PBP2, PBP2a, and PBP4 have been documented, as experimental evidence suggests these proteins do not operate independently to form complete peptidoglycan synthesis. Łęski and Tomasz (2005) demonstrated that in order to ensure adequate cross-linking, these proteins were required to collaborate and function synergistically. This may explain the increased activity of antibiotics targeting PBP2 against *S. aureus* when PBP4 function is limited. Although a direct link between WTA and PBP2 is not apparent, the absence of WTA appears to affect PBP2 activity (Farha et al., 2012). WTA synthesis impediment results in the formation of an incomplete and structurally deficient cell wall. While not yet confirmed to our knowledge, it is plausible that preventing WTA synthesis or removing it from the cell wall could result in the loss of PBP4 recruitment to the site of peptidoglycan synthesis, thereby reducing the activity of PBP2, especially if their collaborative action is required (Farha et al., 2012). Additionally, the loss of PBP4 function, in WTA-deficient cells, increases the sensitivity of *S. aureus* to cefuroxime leading to subsequent cell death. This antibiotic specifically targets PBP2 and is more effective under these conditions (Farha et al., 2012).

Suppressing WTA activity induces structural changes in the cell wall of *S. aureus*. In a study conducted by G C et al. (2019), elucidating the function of the *msaABCR* operon led to the discovery that WTA attachment to the cell wall is dependent on the expression of this operon. Diminished WTA levels were observed following operon deletion, accompanied by a reduction in peptidoglycan cross-linking, presumably stemming from the reduced WTA activity. This morphological change in the cell wall further resulted in a significant thinning of the *S. aureus* peptidoglycan (G C et al., 2019). Moreover, the division septa, where new peptidoglycan is synthesized, exhibits irregular and misshapen characteristics when WTA synthesis and activity are impeded by environmental factors such as sodium bicarbonate and synthetic molecules like branched polyethylenimine (BPEI). These molecules bind to WTA or WTA synthesizing factors, thereby preventing proper localization and function of PBP proteins (Ersoy et al., 2022; Hill et al., 2019). Under conditions involving sodium bicarbonate, WTA absence prevents efficient daughter cell separation, leading to the formation of numerous division septa and cell aggregation. Additionally, the angles at which these septa formed differed from those of untreated or non-susceptible cells (Ersoy et al., 2022). In the presence of charged molecules such as BPEI, two

characteristics become apparent. Cells have a greater abundance of division septa, and these septa appear broader than cells that are not incubated with the BPEI molecule (Hill et al., 2019).

As WTAs are polymers that direct PBPs and AtlA to the site of cellular division, their exclusion results in the loss of activity and positioning of these proteins within the cell due to delocalization. Consequently, both the autolysis and complete synthesis of the cell wall are impaired (Ersoy et al., 2022; Schlag et al., 2010), leading to dividing cells with an expanded size (Schlag et al., 2010) that remain bound to each other at the division site (Ersoy et al., 2022). Furthermore, the production of course, rather than smooth, cell walls when WTA synthesis is impeded or completely prevented is also observed (Brignoli et al., 2022; Schlag et al., 2010).

WTA Regulating Cell Wall Lysis, Charge, and Biofilm Through Localization of FmtA Protein

FmtA, a native protein of *S. aureus*, will be the final protein discussed in this chapter, alongside PBPs and AtlA, that is dependent on WTA production for activity and localization within the cell (Qamar and Golemi-Kotra, 2012; Rahman et al., 2016). FmtA functions by binding to WTAs and subsequently facilitating D-Ala excision from the WTA. The alpha-helix and alpha/beta domain structure of FmtA harbours an active site serine (Ser127) that directly interacts with FmtA, catalyzing D-Ala removal through a bond-breaking process called hydrolysis. The D-Ala-WTA substrate of FmtA, particularly the cleavage of this bond (Dalal et al., 2019), indicates FmtA's probable participation in development of biofilms and autolysis (Brown et al., 2013). The removal of cationic D-Ala amino acids by FmtA from WTA significantly alters the electrostatic properties of the cell surface. A transition of the cell wall toward a more negative charge is expected as only the ribitol-phosphate backbone groups remain (Brown et al., 2013; Neuhaus and Baddiley, 2003). This alteration in cell wall charge aids the cell in adapting to changes in its environment, as further discussed in subsequent sections.

Since FmtA controls the level of D-Ala-WTA substitutions (Rahman et al., 2016), the synthesis of this protein can further regulate the cell's ability to undergo peptidoglycan autolysis (Qamar and Golemi-Kotra, 2012) and contribute to *S. aureus* virulence, as D-Ala has been implicated in both of these cellular characteristics (Brown et al., 2013). It is neither confirmed nor

believed that FmtA is able to directly bind with the AtlA to induce autolysis in dividing cells. However, it is established that as FmtA removes D-Ala from the WTA, there appears to be an indirect change in autolysis occurring, potentially as a result of the alterations in cell wall charge that follow (Qamar and Golemi-Kotra, 2012). As mentioned earlier, AtlA's task at the division septa is dependent upon WTA (Schlag et al., 2010). Further evidence linking FmtA to cell wall autolysis comes from the deletion of the *fmtA* gene, which leads to dysregulation of autolysis of the cell wall, with mutated strains exhibiting an elevated rate of lysis (Boles et al., 2010). These studies verify that D-Ala on WTAs is essential for proper autolysis regulation in *S. aureus.*

Furthermore, the development of an *S. aureus* biofilm community relies on proper regulation of the *fmtA* gene expression, which plays a role in maintaining and directing cell autolysis (Qamar and Golemi-Kotra, 2012). The capability of bacterial species to form biofilms represents a fundamental aspect of their physiology and, in certain cases, is crucial for survival and viability. A biofilm begins to take shape when motile cells called planktonic cells bind to a surface via specific components on their cell envelope. Upon attachment, these cells are no longer planktonic and instead transition to a non-motile state due to their adhesion. As the population of non-motile cells increases, the cells are observed to cluster together, allowing for intercellular collaboration and eventual cell division and reproduction, ultimately forming a colony. The final aspect of biofilm establishment involves the production of an extracellular matrix, which encapsulates the bacterial colony and is composed from the release of bacterial cellular materials (Sharma et al., 2023). For *S. aureus* in particular, the extracellular matrix may be of a different composition than other species. In *S. aureus*, this matrix is composed of proteins, extracellular DNA, WTAs and LTAs, and polysaccharides, including the N-Acetylglucosamine sugar (Karygianni et al., 2020). Biofilms, particularly as a result of the extracellular matrix, offer heightened protection against several antimicrobials, including antibiotics. The persistence and location of these biofilms makes them a threat for infection even in the hospital setting (Sharma et al., 2023). The *fmta* gene was reported by Tu Quoc et al. (2007) in being essential for *S. aureus* to develop biofilm, with removal or mutation of this gene leading to deficiencies in biofilm formation, prompting additional investigations into FmtA. FmtA-regulated *S. aureus* biofilm exhibits a clear trend at 0.2 μM of FmtA incubation: biofilm formation was suppressed at higher concentrations, whereas lower concentrations promoted biofilm formation. This further

demonstrates the connection between FmtA, autolysis, and biofilm, as the autolysis trend was comparable to that of the biofilm (Qamar and Golemi-Kotra, 2012).

Additionally, *in vitro* studies have demonstrated FmtA's ability to not only remove D-Ala from WTA but also from LTA (Rahman et al., 2016). The potential benefit that arises from FmtA acting on both teichoic acids is the resultant adaptation of *S. aureus*, due to surface charge alterations, to variations in its environmental factors. LTA or WTA can be modified with D-Ala, allowing FmtA to alter the positive charges at the cell wall surface, either increasing or decreasing them depending on which teichoic acid is more heavily modified (Rahman et al., 2016). In this thesis, we further explore the FmtA protein and its implication in *S. aureus* physiology under different environmental conditions.

Modification of WTA in Response to a High Salt Stress Environment

The environment in which *S. aureus* develops is capable of shaping its physiology and viability, with changes to protein synthesis observed under certain circumstances. For instance, environmental composition leads to variations in the synthesis of TarS and TarM, allowing for the modification of α or β glucose variants on WTA (Mistretta et al., 2019). High salt concentration in the environment imposes stress on the bacteria cell, as it experiences a decrease in viability due to its incapability to maintain an optimal volume of water intracellularly. This condition is known as plasmolysis, and it leads to alterations in morphology and eventual cell death (Wijnker et al., 2006). However, experimental evidence indicates the salt content has a marginal impact on *S. aureus* survival, as *S. aureus* can develop purposeful alterations to cellular structures to battle against salt-induced damage (Feng et al., 2022).

Although the precise mechanism by which β-N-Acetylglucosamine modification contributes to bacterial salt stress tolerance is not fully understood, the enhanced activity of TarS indicates a pronounced shift toward β-N-Acetylglucosamine modifications on WTA under sub-optimal, salt containing environments (Mistretta et al., 2019). This shift in modification was further supported *in vivo* upon exposure of *S. aureus* to predominant infection loci in experimental rodent models. The results support the notion that alterations to cellular structures, such as elevated β-N-Acetylglucosamine WTAs, occur in order to amplify the potential role for WTA in bacterial

virulence. This study highlights that variable modification of WTA represents one of the strategies employed by the bacterium to achieve adaptation (Mistretta et al., 2019).

Role of WTA in the Viability of S. aureus Under Nutrient Limiting Conditions

The *S. aureus* organism requires adequate nutrition for cellular metabolism and growth. However, this optimal condition is often limited in *S. aureus*-occupied hosts, necessitating the development of bacterial survival mechanisms. Although not entirely absent, nutrients available within microbial niches of the host, such as the nose, require *S. aureus* and the surrounding diverse bacteria to contend for survival and nutritional viability (Jorge et al., 2018).

S. aureus are not the only bacterial species to synthesize WTAs, leading to a fascinating discovery that *S. aureus* present in a diverse microbial environment cause the breakdown of WTA from other microbials (Jorge et al., 2018). The protein responsible for catalyzing this breakdown is GlpQ, which the researchers describe as a teichoicase. The structural composition of WTAs from these organisms differs from those of *S. aureus*, as they consist of glycerol and phosphate chains. Therefore, the observed specificity of GlpQ for these glycerol WTAs facilitates two advantages for *S. aureus*. The first involves the breakdown of the WTAs into fragments for utilization as nutrients in cellular metabolism. The second advantage is that *S. aureus* ensures its own WTA safety, as these distinct WTAs are composed of ribitol and phosphate chains and are therefore not targeted. However, there is a caveat to the use of GlpQ for WTA breakdown. Segments of WTAs containing D-Ala and N-Acetylglucosamine remain intact as GlpQ activity is limited. In other words, GlpQ catalyzes unmodified segments only. This conclusion was further supported by the observation that when cultured in the presence of unmodified WTA as the sole nutritional source, *S. aureus* was capable of growing (Jorge et al., 2018).

Sodium Bicarbonate in the Environment Leads to Impediment of WTA Synthesis

The TarO protein, in conjunction with several other proteins, synthesizes WTA and is vital for this process. There are various unfavourable environments that can impose constraints on the

physiology of MRSA *S. aureus* bacterial strains, particularly on the TarO protein (Ersoy et al., 2022). It is speculated that in MRSA strains MW2 and MRSA 11/11, this protein is restricted from performing its WTA synthesis role on account of sodium bicarbonate in the immediate surrounding. Conversely, not all MRSA strains depict this characteristic decline in cell surface WTA density. Ultimately, the consequential impact of sodium bicarbonate-targeted WTA decline becomes evident as MW2 and MRSA 11/11 strains exhibit impaired growth at oxacillin and cefuroxime concentrations that would normally permit growth in the absence of sodium bicarbonate. This phenomenon indicates a decrease in resistance potential for these MRSA strains (Ersoy et al., 2022).

WTA synthesis is a multi-step process mediated by several proteins, each promoting polymer assembly and transport by facilitating the binding of distinct structural components. TarO is primarily involved in the binding of N-Acetylglucosamine-1-phosphate to the undecaprenyl-phosphate carrier intracellularly at the membrane surface, triggering WTA synthesis. Consequently, the abundance of WTA on the peptidoglycan is intrinsically linked to TarO synthesis (D'Elia et al., 2006). Ersoy et al. (2022) employ a distinct WTA-inhibiting technique: sodium bicarbonate. In addition to the decrease in antibiotic resistance mentioned, they provide further compelling data that the WTA polymer coordinates vital intracellular processes, namely autolysis and peptidoglycan cross-linking, the regulation of which also decreases in sodium bicarbonate-impaired WTA conditions (Ersoy et al., 2022).

Bactericidal Daptomycin Activity Impaired Under Larger WTA Synthesis

Antibiotics are the fundamental aspect of combating bacterial infections, and they predominantly target essential processes involved in bacterial growth and viability, serving as remedial agents. They can be designed and manufactured to act either as bacteriostatic or bactericidal agents. Bactericidal antibiotics are designed to effectively destroy bacteria within the host. In contrast, bacteriostatic antibiotics permit cell survival, alternatively contributing to the detriment of bacterial viability factors, namely protein synthesis, respiration, and metabolism, triggering a hindrance of microbial growth (Pankey and Sabath, 2004; Lobritz et al., 2015).

However, a decrease in susceptibility to bactericidal antibiotics may develop if bacteria experience growth arrest as a result of initial bacteriostatic antibiotic presence (Ocampo et al., 2014).

Daptomycin is designed to be positioned and exert an effect on cellular membrane, thereby acting as a bactericidal antibiotic. A daptomycin subunit initially inserts into the membrane surface in the presence of calcium ions located at this region, subsequently forming an oligomer with repeating daptomycin subunits acting in concert. Consequently, the daptomycin oligomer leads to compromised membrane structural integrity, causing the release of cellular material, particularly ions, into the extracellular space, ultimately damaging the bacterial cell (Muraih et al., 2011; Muraih et al., 2012). Ledger and Edwards (2023) demonstrated that, following the utilization of tetracycline,—a bacteriostatic, ribosomal-targeting antibiotic (Chopra and Roberts, 2001)—an increase in the resistance potential of MRSA cells to daptomycin was achieved, as the cells maintained their metabolic activity. The growth-inhibited cells prevented daptomycin from binding to its target under two conditions. First, the longer the cells were exposed to tetracycline, the stronger their survival when subsequently exposed to daptomycin; no cell death was observed after 16 hours. Second, due to their ongoing metabolism, the inclusion of nutrients, such as glucose, further enabled the cells to resist the effects of daptomycin (Ledger and Edwards, 2023).

Ledger and Edwards (2023) concluded that excess peptidoglycan synthesis, which led to a thickening of the cell wall, resulted from cell growth impairment, consequently hindering daptomycin from reaching its cell membrane target to promote cell death. Together with this physical change observed at the cell wall, higher WTA substitutions with D-Ala were also detected. This culminated in the belief that the WTA substitutions allow for potentially more interaction with cell wall synthesizing and autolyzing proteins, facilitating peptidoglycan thickening. The effectiveness of daptomycin differs from that of other bactericidal antibiotics. MRSA cells treated with bacteriostatic antibiotics can develop tolerance to these bactericidal antibiotics at different rates. In the case of daptomycin, it appears to become more effective as the *S. aureus* organism is given less time to synthesize enlarged peptidoglycan. Therefore, when using both bacteriostatic and bactericidal antibiotics, such as daptomycin, as part of a therapeutic regimen, minimizing the duration between doses may lead to a more successful outcome (Ledger and Edwards, 2023).

WTA Contribution to β-lactam Antibiotic Resistance

The predominant bacterial stressors utilized within healthcare are antibiotics, which constitute a vast array of chemical entities, each characterized by distinct structural configurations, function, and specific bacterial target sites. Of notable interest are the cell envelope-weakening antibiotics, classified as β-lactam antibiotics, which act upon Gram-positive organisms such as *S. aureus* (Bush and Bradford, 2016). The weakening of the cell envelope, particularly of the peptidoglycan, leads to a compromised cell wall and ensuing cell death. PBP action induces strengthening of the cell wall through the facilitation of peptidoglycan strand cross-links; therefore, the β-lactam affinity for the active site of PBPs obstructs their activity. The earliest discovered β-lactam, penicillin, was utilized by Alexander Fleming in the 1900s. Remarkably, the bacterial organisms initiated a counter-response to early β-lactams, emerging resistant due to the synthesis of β-lactamases—enzymes that target the β-lactams for destruction. The successive design of β-lactam antibiotics with decreased affinity for β-lactamases became imperative, resulting in the classification of β-lactams into two principal groups: penicillins and cephalosporins (Bush and Bradford, 2016). Although both penicillins and cephalosporins target PBPs, they exhibit variability in structure and efficiency. These antibiotics are designed with a communal β-lactam ring at the core of the structure, and differences in efficacy potential against bacterial strains arise from modifications to the side chains extending from the core (Chaudhry et al., 2019).

As β-lactam antibiotics designed to evade β-lactamase activity became widely used in healthcare, the introduction of *mecA*, an exogenous genetic element, into *S. aureus* subsequently gave rise to decreased sensitivity to β-lactam antibiotics, such as oxacillin, across several strains (Dien Bard et al., 2014). Consequently, the *S. aureus* organism was classified into two groups: Methicillin-Sensitive *Staphylococcus aureus* (MSSA) and Methicillin-Resistant *Staphylococcus aureus* (MRSA). The *mecA*-deficient MSSA strains lack resistance properties, allowing for efficient infection-management strategies based on available treatments (Dien Bard et al., 2014). MRSA strains employ the PBP2a protein, synthesized through the transcription and translation of the *mecA* gene, to perform a similar function as native *S. aureus* PBPs when these enzymes are functionally compromised by β-lactams. Resistance emerges as PBP2a continues to function in the presence of these antibiotics maintaining cell wall cross-linking (Dien Bard et al., 2014; Hartman and Tomasz, 1984; Lim and Strynadka, 2002). Horizontal gene transfer of *mecA* is believed to

have facilitated its distribution between various *S. aureus* strains. Although the precise donor organism was difficult to uncover, compelling evidence presented by Tsubakishita et al. (2011) suggests that *Staphylococcus fleurettii* may have been the original source.

It is highly likely that WTA plays a direct role in antibiotic resistance because of its predicted influence on PBP2a activity. Although experimental evidence depicts a direct WTA-PBP2a relationship (Qamar and Golemi-Kotra, 2012), additional data reveals that the sugar modification on the WTA is a key factor likely associated with this process, contingent upon the specific variant with which the WTA is modified (Brown et al., 2012). The Minimum Inhibitory Concentrations (MIC) of β-lactam antibiotics, like oxacillin, decrease upon the removal of β-N-Acetylglucosamine-modified WTA, whereas inhibition of the α variant shows no such alteration. Hence, the modification with the β variant, as opposed to the α glycosylation variant, enables WTA to protect the cell against antibiotics, likely resulting from enhanced affinity for PBP2a. The cells are reliant on the synthesis and variable glycosylation of WTA for PBP2a-induced survival (Brown et al., 2012).

WTA and D-Ala as Resistance Components of Vancomycin and other Glycopeptide Antibiotics

Although not classified as a β-lactam, the traditionally employed antibiotic vancomycin similarly targets peptidoglycan synthesis, albeit via an unrelated functional pathway, making it a vital treatment option for use against β-lactam resistant *S. aureus* strains (Cong et al., 2020). As a consequence of genetic adaptation, *S. aureus* continues to pose a challenge to the health care industry, with vancomycin-resistant *S. aureus* (VRSA) and vancomycin-intermediate *S. aureus* (VISA) strains emerging (Singh et al., 2017; Hort et al., 2021; Cong et al., 2020). In MRSA cells, a severely compromised and incomplete cell wall, accompanied by D-Ala-deficient WTA, is formed as a result of the high-affinity binding of vancomycin to lipid II. This leads to a significant reduction in *S. aureus* viability, as active peptidoglycan transglycosylation is disrupted following vancomycin-induced interference with lipid II's engagement in this cell wall synthesis process. Lipid II refers to the precursors of peptidoglycan, which consist of a single N-Acetylmuramic acid bound to an N-Acetylglucosamine, along with the pentapeptide chain that ultimately participates

in the cross-linking of the cell wall. Notably, this pentapeptide chain serves as the target region of vancomycin, as it binds to the D-Ala-D-Ala terminus. (Cong et al., 2020; Singh et al., 2017).

In *S. aureus*, histidine kinase proteins such as VraS and WalK, along with response regulators like GraR, are involved in maintaining the cell wall architecture and facilitating cell wall synthesis (Howden et al., 2011; Berscheid et al., 2014; Neoh et al., 2008). These proteins belong to two-component systems and are specifically mentioned, because studies show that mutations in their corresponding genes result in physiological alterations. These alterations distinguish VISA from typical MRSA strains (Howden et al., 2011; Berscheid et al., 2014; Neoh et al., 2008). As this distinction between VISA and vancomycin-sensitive strains is further explored, changes in cell wall morphology and abundance of peptidoglycan-bound WTA become apparent in VISA strains. This correlates with reduced vancomycin efficacy against such strains. As observed, these prominent features include increased peptidoglycan and WTA accumulation at the cell envelope (Cui et al., 2003; Hort et al., 2021), and overall fewer sections of the cell wall that are cross-linked between the peptidoglycan strands (Hort et al., 2021).

The capability of VISA strains to isolate vancomycin from its natural binding site by presenting alternative, less harmful binding sites is a key feature of vancomycin resistance in these strains. An increased amount of free pentapeptide sequences that mimic the antibiotic's original target arise as a direct consequence of fewer cross-linked sections throughout the cell wall (Cui et al., 2000, 2006). The structure of the highly essential peptidoglycan synthesis molecule, lipid II, includes a pentapeptide sequence containing the D-Ala-D-Ala region recognized by vancomycin (Cong et al., 2020). Pentapeptide chains in the cell wall that are not involved in cross-linking also retain this region, providing binding sites for vancomycin, which contribute to limiting its antimicrobial efficacy, thereby protecting lipid II from inhibition. As a result, the cell can continue transglycosylation even in the presence of vancomycin (Cui et al., 2000, 2006).

The final characteristics of VISA strains associated with vancomycin resistance that will be discussed are the abundant incorporation of WTA and D-Ala into the cell wall and WTAs, respectively (Hort et al., 2021). These traits are exemplified by strains such as VC40. As previously mentioned, autolysis and WTA synthesis are interrelated within the cell; a greater abundance of WTA interferes with AtlA's interaction with peptidoglycan. This provides an advantage to the cell, as autolytic activity can be detrimental to VISA strains and may lead to cell death (Hort et al., 2021). An increase in D-Ala can be favourable not only for VISA strains, but also for MRSA and

MSSA strains as well. WTA-bound D-Ala acts as a countermeasure against positively charged antibiotics and antimicrobial peptides by defending the cell through electrostatic repulsion. Positively charged antimicrobial agents include vancomycin, as well as peptides synthesized by bacteria and animals, such as defensins and protegrin (Peschel et al., 1999; Hort et al., 2021). The interaction between these agents and the negatively charged cell wall is driven by charge-based affinity. However, positively charged D-Ala residues limit this charge attraction, consequently decreasing the cell lytic potential of these agents. As proposed, the higher the abundance of D-Ala, the stronger the resulting force of repulsion (Peschel et al., 1999).

Bacterial resistance drives innovation in antibiotic design, exemplified by oritavancin, a promising antibiotic with antibacterial functions that are both similar to and distinct from those of vancomycin. The difference in activity stems from the incorporation of a hydrophobic chlorobiphenyl side chain in oritavancin, making it a more viable option than vancomycin for the clearance of VISA and VRSA infections (Kim et al., 2008a; Kim et al., 2008b; Singh et al., 2017). Similar to how vancomycin binds lipid II, oritavancin also interacts with this precursor, promoting the development of severely compromised peptidoglycan due to inefficient transglycosylation. However, unlike vancomycin, oritavancin diminishes the viability of *S. aureus* by increasing spatial restriction between peptidoglycan strands, physically obstructing their crosslinking via the limitations imposed by its characteristic side chain. This transpeptidation process is disrupted by oritavancin, which directly binds to other strands at the established pentaglycine bridges. (Kim et al., 2008a; Kim et al., 2008b; Singh et al., 2017). Despite our efforts toward antimicrobial innovation, bacterial adaptation persists. Peptidoglycan synthesis takes precedence over WTA synthesis for survival. The D-Ala made available intracellularly is utilized in both processes. However, during oritavancin incubation*, S. aureus* primarily reserves D-Ala for peptidoglycan synthesis. While the regulatory mechanisms remain unclear, the cell is speculated to prioritize cell wall synthesis over WTA D-Ala modification (Singh et al. 2017).

The change in D-Ala quantity made available to different synthesis pathways is likely controlled by tighter regulation of several processes under stress. The bacterium employs a survival strategy, optimizing its resources to fortify the peptidoglycan cell wall at the expense of WTA modifications (Singh et al. 2017). However, there is a limit to how much D-Ala can be reallocated without compromising cell viability. Although *S. aureus* can survive with decreased D-Ala on WTA, this decrease cannot exceed the 12% threshold of total D-Ala that must remain bound to

WTA to prevent structural defects and ensure cell survival. Further depletion of D-Ala beyond the threshold could result in deficiencies of vital cellular processes (Singh et al., 2017).

Using Innovative Procedures to Increase S. aureus Susceptibility via the Targeting of WTA

Studies exploring the use of environmental factors, as well as drug treatments co-administered with molecular agents targeting bacterial viability, show potential in advancing innovative solutions for controlling antibiotic resistant *S. aureus* infections (Ersoy et al., 2022; Hill et al., 2019). Theoretically, in comparison to monotherapies, multi-drug treatments may exhibit a higher success rate in countering MRSA strains, owing to the probable synergistic interactions between antibacterial agents. BPEI is a molecule studied for its antibacterial potential, as it directly associates with WTA through charge attraction following incubation in MRSA cultures (Hill et al., 2019). Adverse physiological alterations in peptidoglycan synthesis are observed as BPEI interferes with WTA-regulated PBP4 activity upon binding. Consequently, a synergistically mediated increase in MRSA susceptibility to antibiotics such as oxacillin and ampicillin occurs as BPEI operates in conjunction with these antibiotics to promote cell death. Notably, despite D-Ala-modified WTAs, electrostatic repulsion does not significantly impede BPEI binding capability (Hill et al., 2019).

The utilization of newly synthesized antibiotics or synergistic antibiotic cocktails is not the sole approach to potentially counteract MRSA or VISA strains. Elucidating the functions of specific genes and operons can provide insight into previously unknown mechanisms of bacterial resistance, enabling the development of strategies to restore antibiotic efficacy (G C et al. 2019). For instance, a mutation in the *S. aureus* genome, achieved by the deletion of the *msaABCR* operon, informed researchers of this operon's functional significance in bacterial resistance characteristics. In particular, impediment of WTA binding to the cell wall was associated with the loss of this operon, likely contributing to the ensuing reduction in vancomycin and oxacillin MICs against the *S. aureus* strain. Additionally, the *msaABCR*-deficient *S. aureus* displayed a structurally vulnerable cell envelope (G C et al. 2019). In our pursuit of formulating strategies aimed at increasing MRSA susceptibility, the WTA polymer bound to peptidoglycan remains a key structure of interest.

The Virulence of S. aureus During an Immune Response Attributed to WTA and D-Ala

WTA polymers are integral to maintaining cellular homeostasis and regulation, as discussed thus far, and during *S. aureus* host infection, they also play a critical role in promoting virulence. At the onset of *S. aureus* infection in the host, the human immune system responds with a countermeasure in the form of antibodies that target the pathogen for destruction. To facilitate pathogen extermination, these immunoglobulins must directly interact with precise bacterial regions (Kurokawa et al., 2016). In particular, the synthesis of bacterial WTAs generates antibody-accessible binding regions on *S. aureus*, enabling antibody coating of the bacterial envelope and prompting further immune signalling to promote bacterial cell phagocytosis. This phenomenon is known as opsonophagocytosis. WTAs act as the bacterial antigen, with the β-N-Acetylglucosamine modification serving as the precise epitope required for Immunoglobulin G2 (IgG2) recognition, which subsequently triggers bacterial digestion via phagocytosis. This process is the outcome of an active immune complement system (Jung et al., 2012; Kurokawa et al., 2016).

IgG antibodies exhibit discernible discrepancies in binding affinity towards the different variants of modified WTA. Although the explanation behind α-N-Acetylglucosamine's limited contribution to opsonophagocytosis is not fully understood, it is speculated that β-N-Acetylglucosamine-modified WTAs maintain their structural composition and anchoring to the cell wall, reducing the likelihood of separation compared to their α counterparts (Kurokawa et al., 2013). Moreover, during a host infection with *S. aureus*, β-N-Acetylglucosamine-modified WTAs may be synthesized more extensively compared to α-N-Acetylglucosamine-modified WTAs (Kurokawa et al., 2013). The speculative role of WTA charge in influencing the degree of IgG antibody attraction merits consideration. Charge alteration may restrict or permit IgG binding to WTAs, which can be regulated by the presence or absence of D-Ala (Di Carluccio et al., 2022). Despite the apparent ability of the human immune system to discern WTAs, the persistence of several *S. aureus* strain infections remains. This aberration may be partially rationalised by the fact that IgG antibodies do not singularly target WTA, with Mannose-Binding Lectin (MBL) also exhibiting affinity towards these cell wall polymers. Persistent infections by certain antibiotic-resistant *S. aureus* strains, such as MW2, appear to be facilitated by the coexistence of MBL and IgG in the host, where MBL-induced interference with IgG results in a sustained and damaging

infection. This phenomenon potentially allows *S. aureus* MBL-bound WTAs to act as a shield against IgG and other immune system constituents (Takahashi et al., 2013). An alternative rationale for the persistence of *S. aureus* infections suggests that IgG antibodies may become overwhelmed, failing to effectively counteract the infectious dose of *S. aureus* cells (Gautam et al., 2015; Takahashi et al., 2013).

The human immune system is a highly complex, infection-combating system, and IgG antibodies remain a staple of this system, especially during *S. aureus* infections. To assist the immune system during infection, effective vaccine design and treatment strategies rely in part on a thorough understanding of WTA segments, specifically how these segments bind to human antibodies (Di Carluccio et al., 2022). For this purpose, researchers began utilizing monoclonal antibodies, which, as the name implies, are antibodies produced by cloning immunoglobulin antibodies originally generated by the immune system (Fong et al., 2018). IgG antibodies are composed of characteristic heavy and light chains, and the precise orientation of these chains leads to the emergence of a pocket between them where the detection and binding of N-Acetylglucosamine occurs. Notably, it was observed that antibodies do not exclusively recognize β-N-Acetylglucosamine, as some also target the α variant and are produced by the immune system. An interesting discovery was that the remaining WTA subunits further promote the stability of the N-Acetylglucosamine-IgG interaction (Di Carluccio et al., 2022; Fong et al., 2018).

Although WTAs may initially seem detrimental to *S. aureus* during infection, as outlined above, they also serve to enhance the survival and virulence of the bacterium. The immune system produces and releases a vast array of antibodies aimed at eliminating pathogens, some of which have precise affinity for the peptidoglycan in the cell envelope. The exclusion of these antibodies from the peptidoglycan is facilitated by WTAs, which directly restrict their association, thereby promoting *S. aureus* viability and acting as a major deterrent against this immune response (Gautam et al., 2015). Gautam et al. (2015) postulate that this limitation imposed on the antibodies is attributable to two features of WTA: their spatial dimensions and abundant incorporation into the cell wall, as well as their net charge conferred by D-Ala and phosphate subunits.

In humans, a protein with apparent parallels to peptidoglycan recognition proteins (PGRPs) whose activity is influenced by the incorporation of WTA into the cell wall is serum amyloid P component (SAP) (An et al., 2013). As SAPs travel toward the peptidoglycan of invading *S. aureus* cells, their access is physically obstructed upon first encounter with WTAs, thereby leading to

SAP's incapability to function as a detection element and to recruit polymorphonuclear leukocytes for cell breakdown and death (An et al., 2013). This impediment of PGRP binding is not confined to humans but is also observed in other organisms. In the species *Drosophila melanogaster*, *S. aureus* employs WTAs and the Atl protein as defense mechanisms against Peptidoglycan Recognition Protein-SA (PGRP-SA), which is synthesized and deployed to target *S. aureus* (Atilano et al., 2011, 2014). After entering the host, *S. aureus* uses both the Atl protein and the WTA polymer to ensure a PGRP-free cell wall. As peptidoglycan-targeting PGRP-SA approaches the cell wall, WTA acts as a direct hindrance (Atilano et al., 2011), while hydrolysis by Atl is directed toward the peptidoglycan (Atilano et al., 2014). Through segment excision by hydrolysis, the Atl protein limits the propensity of specific peptidoglycan segments, originally presented to PGRP-SA immune surveillance proteins, to bind (Atilano et al., 2014). In light of the previously mentioned regulatory role of WTAs on AtlA (Schlag et al., 2010; Hort et al., 2021), it is plausible that WTAs indirectly promote *S. aureus* survival by facilitating the removal of these peptidoglycan segments through AtlA regulation. A similar theory linking WTA to AtlA activity during an immune response was proposed by Gautam et al. (2015), drawing upon the findings of Atilano et al. (2014). Although Atilano et al. (2014) did not address this possibility, it warrants consideration.

In addition to its involvement in promoting *S. aureus* survival by reducing PGRP and PGRP-like-induced immune responses, WTA is instrumental in *S. aureus*-mediated lysis of host cells, primarily through damage resulting from toxins. For toxins produced in the cytoplasm to gain access to host cells, they must first rely on the Sec pathway and charged WTAs to ensure their capability to traverse the membrane and cell wall, respectively (Brignoli et al., 2022; Sibbald et al., 2006). Researchers discovered that AB leukocidins and alpha- or gamma- hemolysins are partially dependent on WTA for this purpose (Brignoli et al., 2022), exhibiting common but also distinct targets. Through the insertion of pores into white blood cells (WBCs), both LukAB and alpha- or gamma- hemolysin toxins trigger subsequent death of WBCs, such as neutrophils. Although termed hemolysins for their ability to target erythrocytes, these toxins also affect platelets (DuMont et al., 2013; Seilie and Wardenburg, 2017) and have been implicated in physiological challenges in mice, such as arthritis (Nilsson et al., 1999). The influence of a reduction or gain in cell wall WTA density, achieved experimentally or via genetic mutations, on the extracellular concentration of these cytolytic toxins is inversely correlated. Unlike effective WTA-abundant cells, bacteria with WTA-deficient peptidoglycan that continue to synthesize

toxins are unable to fully utilize these toxins for their intended function. In this instance, the toxins are devoid of the necessary force of attraction required to ensure efficient traversal across the cell peptidoglycan and consequently experience membrane-associated sequestration. This phenomenon can be attributed to the navigation of the positively charged toxins across the peptidoglycan, a process made possible only by the charge-based attraction induced by the availability of WTA. The impact of D-Ala modifications on the transport of these toxins remains to be revealed (Brignoli et al., 2022).

In the context of specific, invasive infections, infiltrating *S. aureus* organisms have been detected in the blood of their hosts (Fowler et al., 2003). The discovery of the LOX-1 receptor, located on the inner lining of host blood vessels, has further elucidated the fundamental native components employed by *S. aureus* to ensure efficient colonization within this region (Slavetinsky et al., 2023). Data indicate that *S. aureus* is highly dependent on WTA and its attachment to the cell wall for this process. This bacteria takes full advantage of the direct association between LOX-1 and synthesized WTAs, promoting its sustained localization at the inner layer of host blood vessels following polymer binding. This association between WTA and the recognition region of LOX-1 is likely driven by electrostatic attraction, wherein the predominantly negatively charged WTA is drawn toward the oppositely charged LOX-1 recognition region. In the host blood vessels, this resulting adherence constitutes a relevant preliminary step in maintaining the operational viability of *S. aureus* (Slavetinsky et al., 2023).

The impact of WTA synthesis and accessibility on the *S. aureus* colonization of the bloodstream is not restricted to this site, as a similar infection-inducing pathway is also observed in the nasal cavity. Depending on the receptors in this host region, association with WTA appears to be largely contingent upon the two WTA substitutions present on its backbone repeats, as evidenced by SREC-I recognition (Baur et al., 2014; Winstel et al., 2015). As mentioned, the interaction between the LOX-1 recognition region and WTA is driven by electrostatic attraction between opposite charges (Slavetinsky et al., 2023), which correlates, to some extent, with attachment to SREC-I. Unlike LOX-1, enhanced association of SREC-I and WTA is attributed to a reduction in the negative charge of WTA, which is directly regulated by D-Ala levels. Increased D-Ala substitutions may lead to enhanced binding of SREC-I (Baur et al., 2014). Less is known about N-Acetylglucosamine, although recognition of this WTA substitution appears to occur, promoting persistence irrespective of the conformational variant synthesized (Winstel et al., 2015).

Significance of this Research

S. aureus are pathogenic microorganisms that, upon entry into the host, have the potential to infect several sites within the body leading to impairment of proper function and, in some cases, mortality. These microorganisms are extensively studied for the purpose of understanding their intricate physiology and developing preventative therapeutic measures against potential infections. However, due to specific cell wall-associated components, such as D-Ala modified WTAs, and continuous genetic adaptations, including horizontal gene transfer, *S. aureus* and other bacterial organisms are able to multiply within the host and achieve resistance to numerous antibiotics. Antibiotics that were efficient years ago are now ineffectual at successfully treating *S. aureus* infections caused by resistant strains. Utilizing the D-Ala removal enzyme, notably FmtA, can shed some light regarding the physiological and viability impact on this organism when loss of WTA-bound D-Ala is experienced. This focus could potentially offer an alternative therapeutic treatment, in the form of FmtA, that can be used on its own or in synergy with other antibiotics or antimicrobial molecules.

Accordingly, this thesis outlines three main objectives. The first aim was to demonstrate that FmtA is capable of hydrolyzing the bond between D-Ala and WTA *in vivo* in *S. aureus*, as well as other gram-positive organisms, such as *B. subtilis* and *L. plantarum*. The second aim was to discover whether the use of FmtA to remove D-Ala *in vivo* resulted in an alteration in *S. aureus* cell physiology, particularly in its viability, both in nutrient-rich optimal environments and stress-inducing unfavourable conditions. The third and final aim was to investigate whether the susceptibility of *S. aureus* to β-lactam antibiotics, such as oxacillin, changed as a result of D-Ala exclusion from WTA via FmtA. The data obtained will enhance our understanding of whether the use of FmtA can remove D-Ala *in vivo* and if this loss of D-Ala from the WTAs of *S. aureus* results in physiological alterations, particularly antibiotic resistance and viability alterations, in optimal and suboptimal laboratory-controlled environments. We hypothesized that the physiology of *S. aureus*, in terms of growth, antibiotic susceptibility, and rate of cell lysis, is negatively influenced by the esterase activity of FmtA on D-Ala bound to WTA. This influence would lead to a decrease in growth and an increase in antibiotic susceptibility and cell lysis rates. Additionally, the native *S. aureus* FmtA protein can hydrolyze D-Ala from other Gram-positive organisms *in vivo*.

References

An, J.-H., Kurokawa, K., Jung, D.-J., Kim, M.-J., Kim, C.-H., Fujimoto, Y., Fukase, K., Coggeshall, K. M., & Lee, B. L. (2013). Human sap is a novel peptidoglycan recognition protein that induces complement-independent phagocytosis of *Staphylococcus aureus*. *The Journal of Immunology*, *191*(6), 3319–3327.

Assis, L. M., Nedeljković, M., & Dessen, A. (2017). New strategies for targeting and treatment of multi-drug resistant *Staphylococcus aureus*. *Drug Resistance Updates*, *31*, 1–14.

Atilano, M. L., Pereira, P. M., Vaz, F., Catalão, M. J., Reed, P., Grilo, I. R., Sobral, R. G., Ligoxygakis, P., Pinho, M. G., & Filipe, S. R. (2014). Bacterial autolysins trim cell surface peptidoglycan to prevent detection by the drosophila innate immune system. *eLife*, *3*, e02277.

Atilano, M. L., Pereira, P. M., Yates, J., Reed, P., Veiga, H., Pinho, M. G., & Filipe, S. R. (2010). Teichoic acids are temporal and spatial regulators of peptidoglycan cross-linking in *Staphylococcus aureus*. *Proceedings of the National Academy of Sciences*, *107*(44), 18991–18996.

Atilano, M. L., Yates, J., Glittenberg, M., Filipe, S. R., & Ligoxygakis, P. (2011). Wall teichoic acids of *Staphylococcus aureus* limit recognition by the drosophila peptidoglycan recognition protein-SA to promote pathogenicity. *PLoS Pathogens*, *7*(12).

Barber, M., & Rozwadowska-Dowzenko, M. (1948). Infection by penicillin-resistant *Staphylococci*. *The Lancet*, *252*(6530), 641–644.

Baur, S., Rautenberg, M., Faulstich, M., Grau, T., Severin, Y., Unger, C., Hoffmann, W. H., Rudel, T., Autenrieth, I. B., & Weidenmaier, C. (2014). A nasal epithelial receptor for *Staphylococcus aureus* WTA governs adhesion to epithelial cells and modulates nasal colonization. *PLoS Pathogens*, *10*(5).

Berscheid, A., Francois, P., Strittmatter, A., Gottschalk, G., Schrenzel, J., Sass, P., & Bierbaum, G. (2014). Generation of a vancomycin-intermediate *Staphylococcus aureus* (VISA) strain by two amino acid exchanges in vras. *Journal of Antimicrobial Chemotherapy*, *69*(12), 3190–3198.

Bertsche, U., Yang, S.-J., Kuehner, D., Wanner, S., Mishra, N. N., Roth, T., Nega, M., Schneider, A., Mayer, C., Grau, T., Bayer, A. S., & Weidenmaier, C. (2013). Increased cell wall teichoic acid production and D-Alanylation are common phenotypes among

daptomycin-resistant methicillin-resistant *Staphylococcus aureus* (MRSA) clinical isolates. *PLoS ONE*, *8*(6).

Biswas, R., Martinez, R. E., Göhring, N., Schlag, M., Josten, M., Xia, G., Hegler, F., Gekeler, C., Gleske, A.-K., Götz, F., Sahl, H.-G., Kappler, A., & Peschel, A. (2012). Proton-binding capacity of *Staphylococcus aureus* wall teichoic acid and its role in controlling Autolysin activity. *PLoS ONE*, *7*(7).

Biswas, R., Voggu, L., Simon, U. K., Hentschel, P., Thumm, G., & GÖtz, F. (2006). Activity of the major staphylococcal autolysin Atl. *FEMS Microbiology Letters*, *259*(2), 260–268.

Boles, B. R., Thoendel, M., Roth, A. J., & Horswill, A. R. (2010). Identification of genes involved in polysaccharide-independent *Staphylococcus aureus* biofilm formation. *PLoS ONE*, *5*(4).

Brignoli, T., Douglas, E., Duggan, S., Fagunloye, O. G., Adhikari, R., Aman, M. J., & Massey, R. C. (2022). Wall teichoic acids facilitate the release of toxins from the surface of *Staphylococcus aureus*. *Microbiology Spectrum*, *10*(4).

Brown, S., Santa Maria, J. P., & Walker, S. (2013). Wall teichoic acids of gram-positive bacteria. *Annual Review of Microbiology*, *67*(1), 313–336.

Brown, S., Xia, G., Luhachack, L., Campbell, J., Meredith, T., Chen, C., Winstel, V., Gekeler, C., Irazoqui, J., Peschel, A., & Walker, S. (2012). Methicillin resistance in *Staphylococcus aureus* requires glycosylated wall teichoic acids. *Proceedings of the National Academy of Sciences*, *109*(46), 18909–18914.

Bush, K., & Bradford, P. A. (2016). B-lactams and β-lactamase inhibitors: An overview. *Cold Spring Harbor Perspectives in Medicine*, *6*(8).

Chaudhry, S. B., Veve, M. P., & Wagner, J. L. (2019). Cephalosporins: A focus on side chains and β-lactam cross-reactivity. *Pharmacy*, *7*(3), 103.

Chopra, I., & Roberts, M. (2001). Tetracycline antibiotics: Mode of action, applications, molecular biology, and epidemiology of bacterial resistance. *Microbiology and Molecular Biology Reviews*, *65*(2), 232–260.

Cong, Y., Yang, S., & Rao, X. (2020). Vancomycin resistant *Staphylococcus aureus* infections: A review of case updating and clinical features. *Journal of Advanced Research*, *21*, 169–176.

Cui, L., Iwamoto, A., Lian, J.-Q., Neoh, H., Maruyama, T., Horikawa, Y., & Hiramatsu, K. (2006). Novel mechanism of antibiotic resistance originating in vancomycin-intermediate *Staphylococcus aureus*. *Antimicrobial Agents and Chemotherapy*, *50*(2), 428–438.

Cui, L., Ma, X., Sato, K., Okuma, K., Tenover, F. C., Mamizuka, E. M., Gemmell, C. G., Kim, M.-N., Ploy, M.-C., El Solh, N., Ferraz, V., & Hiramatsu, K. (2003). Cell wall thickening is a common feature of vancomycin resistance in *Staphylococcus aureus*. *Journal of Clinical Microbiology*, *41*(1), 5–14.

Cui, L., Murakami, H., Kuwahara-Arai, K., Hanaki, H., & Hiramatsu, K. (2000). Contribution of a thickened cell wall and its glutamine nonamidated component to the vancomycin resistance expressed by *Staphylococcus aureus* MU50. *Antimicrobial Agents and Chemotherapy*, *44*(9), 2276–2285.

Dalal, V., Kumar, P., Rakhaminov, G., Qamar, A., Fan, X., Hunter, H., Tomar, S., Golemi-Kotra, D., & Kumar, P. (2019). Repurposing an ancient Protein core structure: Structural studies on FMTA, a novel esterase of *Staphylococcus aureus*. *Journal of Molecular Biology*, *431*(17), 3107–3123.

Di Carluccio, C., Soriano-Maldonado, P., Berni, F., de Haas, C. J., Temming, A. R., Hendriks, A., Ali, S., Molinaro, A., Silipo, A., van Sorge, N. M., van Raaij, M. J., Codee, J. D., & Marchetti, R. (2022). Antibody recognition of different *Staphylococcus aureus* wall teichoic acid glycoforms. *ACS Central Science*, *8*(10), 1383–1392.

Dien Bard, J., Hindler, J. A., Gold, H. S., & Limbago, B. (2014). Rationale for eliminating *Staphylococcus* breakpoints for β-lactam agents other than penicillin, oxacillin or cefoxitin, and ceftaroline. *Clinical Infectious Diseases*, *58*(9), 1287–1296.

DuMont, A. L., Yoong, P., Surewaard, B. G., Benson, M. A., Nijland, R., van Strijp, J. A., & Torres, V. J. (2013). *Staphylococcus aureus* elaborates leukocidin ab to mediate escape from within human neutrophils. *Infection and Immunity*, *81*(5), 1830–1841.

D'Elia, M. A., Pereira, M. P., Chung, Y. S., Zhao, W., Chau, A., Kenney, T. J., Sulavik, M. C., Black, T. A., & Brown, E. D. (2006). Lesions in teichoic acid biosynthesis in *Staphylococcus aureus* lead to a lethal gain of function in the otherwise dispensable pathway. *Journal of Bacteriology*, *188*(12), 4183–4189.

Ersoy, S. C., Gonçalves, B., Cavaco, G., Manna, A. C., Sobral, R. G., Nast, C. C., Proctor, R. A., Chambers, H. F., Cheung, A., & Bayer, A. S. (2022). Influence of sodium bicarbonate on

wall teichoic acid synthesis and β-lactam sensitization in NaHCO3-responsive and nonresponsive methicillin-resistant *Staphylococcus aureus*. *Microbiology Spectrum*, *10*(6).

Farha, M. A., Leung, A., Sewell, E. W., D'Elia, M. A., Allison, S. E., Ejim, L., Pereira, P. M., Pinho, M. G., Wright, G. D., & Brown, E. D. (2012). Inhibition of WTA synthesis blocks the cooperative action of pbps and sensitizes MRSA to β-lactams. *ACS Chemical Biology*, *8*(1), 226–233.

Feng, Y., Ming, T., Zhou, J., Lu, C., Wang, R., & Su, X. (2022). The response and survival mechanisms of *Staphylococcus aureus* under high salinity stress in Salted Foods. *Foods*, *11*(10), 1503.

Findley, K., Oh, J., Yang, J., Conlan, S., Deming, C., Meyer, J. A., Schoenfeld, D., Nomicos, E., Park, M., Kong, H. H., & Segre, J. A. (2013). Topographic diversity of fungal and bacterial communities in human skin. *Nature*, *498*(7454), 367–370.

Fong, R., Kajihara, K., Chen, M., Hotzel, I., Mariathasan, S., Hazenbos, W. L. W., & Lupardus, P. J. (2018). Structural investigation of human *S. aureus*-targeting antibodies that bind wall teichoic acid. *mAbs*, *10*(7), 979–991.

Fowler, V. G., Olsen, M. K., Corey, G. R., Woods, C. W., Cabell, C. H., Reller, L. B., Cheng, A. C., Dudley, T., & Oddone, E. Z. (2003). Clinical identifiers of complicated *Staphylococcus aureus* bacteremia. *Archives of Internal Medicine*, *163*(17), 2066-2072.

Fuda, C., Suvorov, M., Vakulenko, S. B., & Mobashery, S. (2004). The basis for resistance to β-lactam antibiotics by penicillin-binding protein 2A of methicillin-resistant *Staphylococcus aureus*. *Journal of Biological Chemistry*, *279*(39), 40802–40806.

G C, B., Sahukhal, G. S., & Elasri, M. O. (2019). Role of the *msaABCR* operon in cell wall biosynthesis, autolysis, integrity, and antibiotic resistance in *Staphylococcus aureus*. *Antimicrobial Agents and Chemotherapy*, *63*(10).

Gautam, S., Kim, T., Lester, E., Deep, D., & Spiegel, D. A. (2015). Wall teichoic acids prevent antibody binding to epitopes within the cell wall of *Staphylococcus aureus*. *ACS Chemical Biology*, *11*(1), 25–30.

Georgopapadakou, N. H., & Liu, F. Y. (1980). Penicillin-binding proteins in bacteria. *Antimicrobial Agents and Chemotherapy*, *18*(1), 148–157.

Ghuysen, J. M. (1968). Use of bacteriolytic enzymes in determination of wall structure and their role in cell metabolism. *Bacteriological Reviews*, *32*(4_pt_2), 425–464.

Guillamet, M. C., Vazquez, R., Deaton, B., Shroba, J., Vazquez, L., & Mercier, R.-C. (2018). Host-pathogen-treatment triad: Host factors matter most in methicillin-resistant *Staphylococcus aureus* bacteremia outcomes. *Antimicrobial Agents and Chemotherapy*, *62*(2).

Hartman, B. J., & Tomasz, A. (1984). Low-affinity penicillin-binding protein associated with beta-lactam resistance in *Staphylococcus aureus*. *Journal of Bacteriology*, *158*(2), 513–516.

Hesser, A. R., Matano, L. M., Vickery, C. R., Wood, B. M., Santiago, A. G., Morris, H. G., Do, T., Losick, R., & Walker, S. (2020). The length of lipoteichoic acid polymers controls *Staphylococcus aureus* cell size and envelope integrity. *Journal of Bacteriology*, *202*(16).

Hill, M. A., Lam, A. K., Reed, P., Harney, M. C., Wilson, B. A., Moen, E. L., Wright, S. N., Pinho, M. G., & Rice, C. V. (2019). BPEI-induced delocalization of PBP4 potentiates β-lactams against MRSA. *Biochemistry*, *58*(36), 3813–3822.

Hiramatsu, K., Hanaki, H., Ino, T., Yabuta, K., Oguri, T., & Tenover, F. C. (1997). Methicillin-resistant *Staphylococcus aureus* clinical strain with reduced vancomycin susceptibility. *Journal of Antimicrobial Chemotherapy*, *40*(1), 135–136.

Hort, M., Bertsche, U., Nozinovic, S., Dietrich, A., Schrötter, A. S., Mildenberger, L., Axtmann, K., Berscheid, A., & Bierbaum, G. (2021). The role of β-glycosylated wall teichoic acids in the reduction of vancomycin susceptibility in vancomycin-intermediate *Staphylococcus aureus*. *Microbiology Spectrum*, *9*(2).

Howden, B. P., McEvoy, C. R., Allen, D. L., Chua, K., Gao, W., Harrison, P. F., Bell, J., Coombs, G., Bennett-Wood, V., Porter, J. L., Robins-Browne, R., Davies, J. K., Seemann, T., & Stinear, T. P. (2011). Evolution of multidrug resistance during *Staphylococcus aureus* infection involves mutation of the essential two component regulator walkr. *PLoS Pathogens*, *7*(11).

Jorge, A. M., Schneider, J., Unsleber, S., Xia, G., Mayer, C., & Peschel, A. (2018). *Staphylococcus aureus* counters phosphate limitation by scavenging wall teichoic acids from other staphylococci via the teichoicase GlpQ. *Journal of Biological Chemistry*, *293*(38), 14916–14924.

Jung, D.-J., An, J.-H., Kurokawa, K., Jung, Y.-C., Kim, M.-J., Aoyagi, Y., Matsushita, M., Takahashi, S., Lee, H.-S., Takahashi, K., & Lee, B. L. (2012). Specific serum IG

recognizing staphylococcal wall teichoic acid induces complement-mediated opsonophagocytosis against *Staphylococcus aureus*. *The Journal of Immunology*, *189*(10), 4951–4959.

Karamanos, Y. (1997). Endo-N-acetyl-β-D-glucosaminidases and their potential substrates: Structure/function relationships. *Research in Microbiology*, *148*(8), 661–671.

Karygianni, L., Ren, Z., Koo, H., & Thurnheer, T. (2020). Biofilm matrixome: Extracellular components in structured microbial communities. *Trends in Microbiology*, *28*(8), 668–681.

Kim, S. J., Cegelski, L., Stueber, D., Singh, M., Dietrich, E., Tanaka, K. S. E., Parr, T. R., Far, A. R., & Schaefer, J. (2008). Oritavancin exhibits dual mode of action to inhibit cell-wall biosynthesis in *Staphylococcus aureus*. *Journal of Molecular Biology*, *377*(1), 281–293.

Kim, S. J., Matsuoka, S., Patti, G. J., & Schaefer, J. (2008). Vancomycin derivative with damaged d-ala-d-ala binding cleft binds to cross-linked peptidoglycan in the cell wall of *Staphylococcus aureus*. *Biochemistry*, *47*(12), 3822–3831.

Kojima, N., Araki, Y., & Ito, E. (1985). Structure of the linkage units between ribitol teichoic acids and peptidoglycan. *Journal of Bacteriology*, *161*(1), 299–306.

Kurokawa, K., Jung, D.-J., An, J.-H., Fuchs, K., Jeon, Y.-J., Kim, N.-H., Li, X., Tateishi, K., Park, J. A., Xia, G., Matsushita, M., Takahashi, K., Park, H.-J., Peschel, A., & Lee, B. L. (2013). Glycoepitopes of staphylococcal wall teichoic acid govern complement-mediated opsonophagocytosis via human serum antibody and mannose-binding lectin. *Journal of Biological Chemistry*, *288*(43), 30956–30968.

Kurokawa, K., Takahashi, K., & Lee, B. L. (2016). The staphylococcal surface-glycopolymer wall teichoic acid (WTA) is crucial for complement activation and immunological defense against *Staphylococcus aureus* infection. *Immunobiology*, *221*(10), 1091–1101.

Ledger, E. V., & Edwards, A. M. (2023). Growth arrest of *Staphylococcus aureus* induces daptomycin tolerance via cell wall remodelling. *mBio*, *14*(1).

Lim, D., & Strynadka, N. C. J. (2002). Structural basis for the β lactam resistance of pbp2a from Methicillin-resistant *Staphylococcus aureus*. *Nature Structural Biology*, *9*(11), 870-876

Lobritz, M. A., Belenky, P., Porter, C. B., Gutierrez, A., Yang, J. H., Schwarz, E. G., Dwyer, D. J., Khalil, A. S., & Collins, J. J. (2015). Antibiotic efficacy is linked to bacterial cellular respiration. *Proceedings of the National Academy of Sciences*, *112*(27), 8173–8180.

Mirelman, D., Beck, B. D., & Shaw, D. R. D. (1970). The location of the D-alanyl ester in the ribitol teichoic acid of *Staphylococcus aureus*. *Biochemical and Biophysical Research Communications*, *39*(4), 712–717.

Mistretta, N., Brossaud, M., Telles, F., Sanchez, V., Talaga, P., & Rokbi, B. (2019). Glycosylation of *Staphylococcus aureus* cell wall teichoic acid is influenced by environmental conditions. *Scientific Reports*, *9*(1).

Muraih, J. K., Harris, J., Taylor, S. D., & Palmer, M. (2012). Characterization of daptomycin oligomerization with perylene excimer fluorescence: Stoichiometric binding of phosphatidylglycerol triggers Oligomer Formation. *Biochimica et Biophysica Acta (BBA) - Biomembranes*, *1818*(3), 673–678.

Muraih, J. K., Pearson, A., Silverman, J., & Palmer, M. (2011). Oligomerization of daptomycin on membranes. *Biochimica et Biophysica Acta (BBA) - Biomembranes*, *1808*(4), 1154–1160.

Neoh, H., Cui, L., Yuzawa, H., Takeuchi, F., Matsuo, M., & Hiramatsu, K. (2008). Mutated response regulator *grar* is responsible for phenotypic conversion of *Staphylococcus aureus* from heterogeneous vancomycin-intermediate resistance to vancomycin-intermediate resistance. *Antimicrobial Agents and Chemotherapy*, *52*(1), 45–53.

Neuhaus, F. C., & Baddiley, J. (2003). A continuum of anionic charge: structures and functions of d-alanyl-teichoic acids in gram-positive bacteria. *Microbiology and Molecular Biology Reviews*, *67*(4), 686–723.

Nilsson, I.-M., Hartford, O., Foster, T., & Tarkowski, A. (1999). Alpha-toxin and gamma-toxin jointly promote *Staphylococcus aureus* virulence in murine septic arthritis. *Infection and Immunity*, *67*(3), 1045–1049.

Ocampo, P. S., Lázár, V., Papp, B., Arnoldini, M., Abel zur Wiesch, P., Busa-Fekete, R., Fekete, G., Pál, C., Ackermann, M., & Bonhoeffer, S. (2014). Antagonism between bacteriostatic and bactericidal antibiotics is prevalent. *Antimicrobial Agents and Chemotherapy*, *58*(8), 4573–4582.

Oshida, T., Sugai, M., Komatsuzawa, H., Hong, Y. M., Suginaka, H., & Tomasz, A. (1995). A *Staphylococcus aureus* autolysin that has an N-acetylmuramoyl-L-alanine amidase domain and an endo-beta-N-acetylglucosaminidase domain: Cloning, sequence analysis, and characterization. *Proceedings of the National Academy of Sciences*, *92*(1), 285–289.

Pankey, G. A., & Sabath, L. D. (2004). Clinical relevance of bacteriostatic versus bactericidal mechanisms of action in the treatment of gram-positive bacterial infections. *Clinical Infectious Diseases*, *38*(6), 864–870.

Pastagia, M., Kleinman, L. C., Lacerda de la Cruz, E. G., & Jenkins, S. G. (2012). Predicting risk for death from MRSA Bacteremia. *Emerging Infectious Diseases*, *18*(7), 1072–1080.

Peschel, A., Otto, M., Jack, R., Kalbacher, H., Jung, G., & Götz, F. (1999). Inactivation of the *dlt* operon in *Staphylococcus aureus* confers sensitivity to Defensins, Protegrins, and other antimicrobial peptides. *Journal of Biological Chemistry*, *274*(13), 8405–8410.

Peschel, A., Vuong, C., Otto, M., & Götz, F. (2000). The D-alanine residues of *Staphylococcus aureus* teichoic acids alter the susceptibility to vancomycin and the activity of autolytic enzymes. *Antimicrobial Agents and Chemotherapy*, *44*(10), 2845–2847.

Pinho, M. G., Filipe, S. R., de Lencastre, H., & Tomasz, A. (2001). Complementation of the essential peptidoglycan transpeptidase function of penicillin-binding protein 2 (PBP2) by the drug resistance protein PBP2A in *Staphylococcus aureus*. *Journal of Bacteriology*, *183*(22), 6525–6531.

Qamar, A., & Golemi-Kotra, D. (2012). Dual roles of FmtA in *Staphylococcus aureus* cell wall biosynthesis and autolysis. *Antimicrobial Agents and Chemotherapy*, *56*(7), 3797–3805.

Rahman, M. M., Hunter, H. N., Prova, S., Verma, V., Qamar, A., & Golemi-Kotra, D. (2016). The *Staphylococcus aureus* methicillin resistance factor FmtA is a d-amino esterase that acts on teichoic acids. *mBio*, *7*(1).

Reichmann, N. T., Cassona, C. P., & Gründling, A. (2013). Revised mechanism of D-alanine incorporation into cell wall polymers in gram-positive bacteria. *Microbiology*, *159*(Pt_9), 1868–1877.

Schlag, M., Biswas, R., Krismer, B., Kohler, T., Zoll, S., Yu, W., Schwarz, H., Peschel, A., & Götz, F. (2010). Role of staphylococcal wall teichoic acid in targeting the major autolysin Atl. *Molecular Microbiology*, *75*(4), 864–873.

Schleifer, K. H., & Kandler, O. (1972). Peptidoglycan types of bacterial cell walls and their taxonomic implications. *Bacteriological Reviews*, *36*(4), 407–477.

Scientific Image and Illustration Software. BioRender. (n.d.). https://www.biorender.com

Seilie, E. S., & Bubeck Wardenburg, J. (2017). *Staphylococcus aureus* pore-forming toxins: The interface of pathogen and host complexity. *Seminars in Cell & Developmental Biology*, *72*, 101–116.

Sharma, S., Mohler, J., Mahajan, S. D., Schwartz, S. A., Bruggemann, L., & Aalinkeel, R. (2023). Microbial Biofilm: A review on formation, infection, antibiotic resistance, control measures, and innovative treatment. *Microorganisms*, *11*(6), 1614.

Sibbald, M. J., Ziebandt, A. K., Engelmann, S., Hecker, M., de Jong, A., Harmsen, H. J., Raangs, G. C., Stokroos, I., Arends, J. P., Dubois, J. Y., & van Dijl, J. M. (2006). Mapping the pathways to staphylococcal pathogenesis by comparative secretomics. *Microbiology and Molecular Biology Reviews*, *70*(3), 755–788.

Singh, M., Chang, J., Coffman, L., & Kim, S. J. (2017). Hidden mode of action of glycopeptide antibiotics: Inhibition of wall teichoic acid biosynthesis. *The Journal of Physical Chemistry B*, *121*(16), 3925–3932.

Slavetinsky, J., Lehmann, E., Slavetinsky, C., Gritsch, L., van Dalen, R., Kretschmer, D., Bleul, L., Wolz, C., Weidenmaier, C., & Peschel, A. (2023). Wall teichoic acid mediates *Staphylococcus aureus* binding to endothelial cells via the scavenger receptor LOX-1. *ACS Infectious Diseases*, *9*(11), 2133–2140.

Takahashi, K., Kurokawa, K., Moyo, P., Jung, D.-J., An, J.-H., Chigweshe, L., Paul, E., & Lee, B. L. (2013). Intradermal immunization with wall teichoic acid (WTA) elicits and augments an Anti-WTA IgG response that protects mice from methicillin-resistant *Staphylococcus aureus* infection independent of mannose-binding lectin status. *PLoS ONE*, *8*(8).

Todd, J., Fishaut, M., Kapral, F., & Welch, T. (1978). Toxic-shock syndrome associated with phage-group-I staphylococci. *The Lancet*, *312*(8100), 1116–1118.

Tsubakishita, S., Kuwahara-Arai, K., Sasaki, T., & Hiramatsu, K. (2011). Origin and molecular evolution of the determinant of methicillin resistance in Staphylococci. *Antimicrobial Agents and Chemotherapy*, *55*(2), 946–946.

Tu Quoc, P. H., Genevaux, P., Pajunen, M., Savilahti, H., Georgopoulos, C., Schrenzel, J., & Kelley, W. L. (2007). Isolation and characterization of biofilm formation-defective mutants of *Staphylococcus aureus*. *Infection and Immunity*, *75*(3), 1079–1088.

Wacnik, K., Rao, V. A., Chen, X., Lafage, L., Pazos, M., Booth, S., Vollmer, W., Hobbs, J. K., Lewis, R. J., & Foster, S. J. (2022). Penicillin-binding protein 1 (PBP1) of *Staphylococcus aureus* has multiple essential functions in cell division. *mBio*, *13*(4).

Wada, A., & Watanabe, H. (1998). Penicillin-binding protein 1 of *Staphylococcus aureus* is essential for growth. *Journal of Bacteriology*, *180*(10), 2759–2765.

Wecke, J., Madela, K., & Fischer, W. (1997). The absence of D-alanine from lipoteichoic acid and wall teichoic acid alters surface charge, enhances autolysis and increases susceptibility to methicillin in Bacillus subtilis. *Microbiology*, *143*(9), 2953–2960.

Wertheim, H. F., Melles, D. C., Vos, M. C., Leeuwen, W. van, Belkum, A. van, Verbrugh, H. A., & Nouwen, J. L. (2005). The role of nasal carriage in *Staphylococcus aureus* infections. *Lancet Infectious Diseases*, *5*(12), 751–762.

Wijnker, J. J., Koop, G., & Lipman, L. J. A. (2006). Antimicrobial properties of salt (NaCl) used for the preservation of natural casings. *Food Microbiology*, *23*(7), 657–662.

Winstel, V., Kühner, P., Salomon, F., Larsen, J., Skov, R., Hoffmann, W., Peschel, A., & Weidenmaier, C. (2015). Wall teichoic acid glycosylation governs *Staphylococcus aureus* nasal colonization. *mBio*, *6*(4).

Wyke, A. W., Ward, J. B., Hayes, M. V., & Curtis, N. A. C. (1981). A role *in vivo* for penicillin-binding protein-4 of *Staphylococcus aureus*. *European Journal of Biochemistry*, *119*(2), 389–393.

Łęski, T. A., & Tomasz, A. (2005). Role of penicillin-binding protein 2 (PBP2) in the antibiotic susceptibility and cell wall cross-linking of *Staphylococcus aureus*: Evidence for the cooperative functioning of PBP2, PBP4, and PBP2A. *Journal of Bacteriology*, *187*(5), 1815–1824.

Chapter Two:

In vitro and *in vivo* Removal of D-Alanine from Gram-Positive Organisms Utilizing the *S. aureus*-native FmtA Enzyme

Introduction

The study of FmtA raises numerous questions that require experimental investigation. A segment of this chapter addresses the possibility and quantity of D-Ala released from living Gram-positive bacterial cells upon incubation with exogenous FmtA. The organisms that were examined were *S. aureus*, which naturally produces FmtA, *Bacillus subtilis (B. subtilis)*, and *Lactiplantibacillus plantarum (L. plantarum)*. All three of these Gram-positive bacteria contain WTAs; however, the WTA structure varies among them. *S. aureus* WTA consists of ribitol-phosphate backbone units (Kojima et al., 1985), whereas both *B. subtilis* 168 and *L. plantarum* NCIMB 8826 have WTA composed of glycerol-phosphate backbone units (Bhavsar et al., 2004; Tomita et al., 2010). A previous study conducted in Dr. Golemi-Kotra's lab discovered that isolated LTA, composed of glycerol-phosphate units, underwent D-Ala cleavage, separating it from the LTA backbone upon incubation with FmtA (Rahman et al., 2016). LTAs are polymers that share structural similarities with WTAs and are believed to be the initial teichoic acid carriers of the D-Ala, which is subsequently seen on WTAs in *S. aureus* (Rahman et al., 2016). The structures of LTAs are similar in composition to the D-Ala bound WTA backbone of both *B. subtilis* and *L. plantarum.*

The focus on WTA isolation and its functional significance in cellular processes has become a staple in the study of *S. aureus* bacterial strains. Discovering as much as can be discernable of WTA composition and organization in *S. aureus* is imperative to understanding changes that may occur as a result of mutations involving the peptidoglycan or WTA directly. As mentioned in the first chapter, WTA plays a diverse role in cell viability. This polymer is composed of a linker unit made up of three main components, N-Acetylglucosamine, N-Acetylmannosamine, and glycerol-phosphate that join to the N-Acetylmuramic acid of the peptidoglycan. The main structure of the *S. aureus* WTA is the ribitol-phosphate repeats that follow. It is estimated that on average, this main backbone unit is repeated 40 times (Kojima et al., 1985). Having an enhanced

perception of how D-Ala is spatially organized onto WTA plays a further part in uncovering the organizational mysteries of WTA. The remainder of this chapter aims to demonstrate how D-Ala is spaced, on average, across the WTA polymer of *S. aureus* RN4220. Of particular interest is that the growth environment of the organism appears to change the level of D-Ala modifications on the LTA. A modification in pH, temperature, and even salt concentration can influence the total amount, such that an increase in either of the three mentioned parameters can lead to a decrease in the overall D-Ala substitutions on LTA (Hurst et al., 1975; Koch et al., 1985; MacArthur and Archibald, 1984). It is probable that the WTA D-Ala is originally transferred from LTA (Rahman et al., 2016). Therefore, if environmental factors alter the D-Ala substitution on LTA, it will stand to reason that there is a comparable change of D-Ala on WTA as well. In our study, the growth environment of the RN4220, *B. subtilis*, and *L. plantarum* cells was created for optimal growth and was kept consistent to determine D-Ala spatial orientation on the WTA of cells grown under optimal conditions. One benefit to accurately estimating D-Ala special arrangement, as discussed here, is to more accurately be able to estimate the molecular weight of WTA and compare D-Ala modifications between organisms.

Materials and Methods

Confirmation and Quantification of D-Ala Removal from WTA of *S. aureus* RN4220, *B. subtilis 168*, and *L. plantarum NCIMB 8826 in vivo* using ^{1}H-NMR

A 1 mL aliquot of an overnight bacterial culture, incubated at 37°C with agitation at 200 rpm, was inoculated into two separate flasks, each containing 99 mL of Tryptic Soy Broth (TSB) purchased from Sigma-Aldrich. The cultures were further incubated at 37°C with shaking at 170 rpm until the optical density at 600 nm (OD_{600}) reached 1.0 absorbance units (A.U.). For *L. plantarum*, which was purchased from Cedarlane Labs, MRS broth (Sigma-Aldrich) was used instead of TSB. Upon reaching an OD_{600} of 1.0 A.U., 50 mL of each bacterial suspension was collected and centrifuged at 5000 x g for 15 minutes at 22°C. The supernatant was discarded, and the pellets were washed twice with 20 mL of 50 mM sodium phosphate buffer (pH 7.2) and centrifuged again at 5000 x g for 15 minutes at 22°C to remove the buffer. The buffer was created based on an established protocol with chemicals purchased from Fisher Chemical. The buffer was filtered prior using Sarstedt Filtropur 0.2 μm syringe filters. The weights of the pellets were

recorded and normalized to ensure uniformity across samples, as each FmtA concentration required an equal amount of bacterial weight. FmtA solutions at concentrations of 10 μM, 15 μM, and 20 μM were prepared in 50 mM sodium phosphate buffer (pH 7.2), and each bacterial pellet was resuspended in one of these FmtA solutions for a total of 650 μl of solution. The suspensions were incubated for 1 hour on a three-dimensional rotator at 22°C. Following incubation, the samples were centrifuged at 10,200 RCF for 10 minutes at 22°C, and the supernatant, containing unbound D-Ala, was collected and stored at 4°C for subsequent analysis. Analysis was performed using Bruker AV III 700 series Proton Nuclear Magnetic Resonance (^{1}H-NMR) spectrometer set to a standard "zgesgp" pulse program using 32768 data points, a 16-ppm spectral width, a relaxation delay of 7 seconds, and a total of 64 scans.

Following the acquisition of the ^{1}H-NMR data, the D-Ala peak for each FmtA concentration was quantitatively compared to the D-Ala peaks of previously prepared D-Ala solution standards. The preparation of these standard solutions involved dissolving varying concentrations of the D-Ala amino acid (Sigma-Aldrich) in a 50 mM sodium phosphate buffer (pH 7.2). The standard concentration created for *S. aureus* experiments was 40 μM D-Ala, the concentration created for *B. subtilis* experiments was 80 μM D-Ala, and the standard D-Ala concentration for *L. plantarum* experiments was 150 μM and 1 mM. ^{1}H-NMR was performed on each standard concentration, yielding spectra with peaks corresponding to different concentrations of D-Ala. These peaks were integrated using Bruker TopSpin software to quantify their respective size. The integration values obtained for each standard peak were normalized to a reference value of 1.0. Each standard concentration was repeated a total of three times to ensure reproducibility and elevate confidence in the data, with the 1 mM standard being the only exclusion. The comparison between D-Ala standard peaks and FmtA released D-Ala involved calculating the ratio between the two peaks and given that the concentration of the standard D-Ala peaks was known, the concentration of the unknown D-Ala was determined from this ratio. For each FmtA concentration, the experiment was conducted in triplicate for each organism. The three unknown D-Ala peaks generated at each FmtA concentration were initially compared to one of the standard D-Ala trials to calculate the mean D-Ala released from the three unknown peaks. This process was then repeated for the second and third D-Ala standard trials, resulting in three mean values corresponding to a single FmtA concentration. These mean values were subsequently averaged to determine the total D-Ala release for each FmtA concentration. This was performed for each

organism to enhance the reliability of the data. Direct comparison of the D-Ala peaks to this standard was necessary because the internal standard, 50 µg/ml sodium 2,2-dimethyl-2-silapentane-5-sulfonate (DSS) purchased from Thermo Fisher Scientific, displayed variability in peak size, rendering it unreliable for accurate peak size determination. This analysis was performed for all three different gram-positive organisms tested. The 1 mM standard implemented for *L. plantarum* D-Ala was used to verify the values determined using the 150 µM standard.

Determining Quantity of Phosphate from Isolated WTA

Phosphate quantification was employed to determine the phosphate content in a defined concentration of isolated WTA from *S. aureus* RN4220, *B. subtilis* 168, and *L. plantarum* NCIMB 8826 as identified via ^{1}H-NMR spectroscopy. These values were subsequently compared to the D-Ala content within the same WTA sample or concentration. The total phosphate content served as an indicator of the WTA abundance present on the peptidoglycan of these Gram-positive organisms. For *S. aureus*, WTA was isolated twice. The first isolation was used to quantify phosphate content and directly compare those values to the D-Ala content, determined using a fluorescent enzyme coupled assay, from the same WTA concentration. The WTA isolated for these experiments was aliquoted into 0.75 mg samples. The second isolation was performed by Saptarshi Sengupta and utilized to quantify phosphate and D-Ala content using ^{1}H-NMR for a dissolved 300 µl sample obtained from a 1 L culture of cells. *L. plantarum* and *B. subtilis* samples were subjected to the same procedure. For both *S. aureus* WTA experiments, a BioAssay Systems QuantiChrom Phosphate Assay Kit (DIPI-500) was utilized to quantify the phosphate.

To quantify the phosphate content of varying WTA concentrations, WTA was isolated from 1 L culture of *S. aureus*, *B. subtilis, and L. plantarum* using a previously established protocol. In brief, following the isolation protocol, the entire WTA sample was dissolved in 300 µl solution and run on ^{1}H-NMR to determine the amount of WTA. For this purpose, the ratio between the WTA N-Acetylglucosamine peak and the DSS peak was calculated and subsequently compared to the N-Acetylglucosamine/DSS ratio of a WTA sample with a known concentration, 5 mg/ml. Based on this comparison, the concentration of WTA in the unknown sample was calculated. The difference in DSS peaks was also accounted for.

For *S. aureus* RN4220 phosphate quantification utilized for fluorescent enzyme coupled assay D-Ala comparison, the 300 µl WTA sample was aliquoted and stored into individual

Eppendorf tubes, each containing 0.75 mg WTA. One aliquot was subsequently used to prepare a 1.0 µg/µl WTA stock solution in double distilled water (ddH_2O). From this stock, the volumes of 5.5 µl, 11 µl, 22.5 µl, 35 µl, and 40 µl were pipetted into separate glass tubes. For *L. plantarum* and *B. subtilis* phosphate quantification, the 300 µl dissolved WTA samples, 2.8 mg/ml and 1.0 mg/ml respectively, were directly used to create a 1 µg/µl WTA stock in double distilled water (ddH_2O). From this stock, the volumes of 2.5 µl and 5 µl were pipetted into separate glass tubes. Each solution was incubated at 150°C for 10 minutes in a dry bath to ensure complete evaporation of water, resulting in the drying of the tubes and the retention of the WTA polymers. Hence, following the completion of the dry bath, 5.5 µg, 11 µg, 22.5 µg, 35 µg, and 40 µg of WTA remained for the RN4220 samples and 2.5 µg and 5 µg of WTA remained for the *L. plantarum* and *B. subtilis* samples. An aliquot of 40 µl of 70% perchloric acid (Sigma-Aldrich) was added to each sample, and the samples were incubated again at 150°C for 2 hours (the solutions do not dry out). Subsequently, 1 ml of ddH_2O was added to dilute the samples resulting in the final concentrations of WTA: 0.005 µg/µl, 0.01 µg/µl, 0.02 µg/µl, 0.03 µg/µl, and 0.04 µg/µl for *S. aureus* and 0.0024 µg/µl and 0.0048 µg/µl for *L. plantarum* and *B. subtilis*. From these dilutions, 50 µl was transferred to a 96-well culture plate (SPL Life Sciences). A BioAssay Systems QuantiChrom Phosphate Assay Kit (DIPI-500) was utilized following the manufacturer's protocol to quantify inorganic phosphate released. Briefly, 100 µl of the kit reagent was added to each sample in the wells and incubated at 22°C for 30 minutes. The reagent, consisting of malachite green dye and molybdate, produces a colorimetric response in the presence of inorganic phosphate. Consequently, the OD_{620} was measured, and the phosphate concentration was determined using the equation provided by the kit. A water blank and phosphate standard were also included for calibration. The dilutions performed for the *L. plantarum* and *B. subtilis* samples were calculated and utilized to determine the phosphate concentration in the undiluted 300 µl isolated WTA sample. For *S. aureus*, the average phosphate concentration was calculated and listed based on WTA concentrations of 0.05 µg/µl, 0.1 µg/µl, 0.15 µg/µl, 0.2 µg/µl, and 0.25 µg/µl to compare to the D-Ala content recorded using the fluorescent enzyme coupled assay. The *S. aureus* data for comparison to *L. plantarum* and *B. subtilis* samples was provided by Saptarshi Sengupta and Sai Sundararaman, obtained exactly as described for *L. plantarum* and *B. subtilis*.

Determining D-Ala Content from Isolated WTA

To quantify the D-Ala content in varying concentrations of isolated WTA from *S. aureus* RN4220, five samples were prepared, each containing a different concentration of WTA and a constant concentration of exogenous FmtA. The samples consisted of 5 µg, 10 µg, 15 µg, 20 µg, or 25 µg of WTA, 10 µM FmtA, and 50 mM sodium phosphate buffer (pH 7.2) to a total volume of 100 µl per sample. The buffer was filtered prior using 0.2 µm syringe filters. Consequently, the WTA concentrations were 0.05 µg/µl, 0.1 µg/µl, 0.15 µg/µl, 0.2 µg/µl, and 0.25 µg/µl. The samples were incubated for 2 hours to allow FmtA to remove the D-Ala from the WTA. A working solution was prepared containing 0.56 µl Flavin adenine dinucleotide (FAD) (2 mg/ml stock), 8.66 µl Diamine oxidase (DAO) (2 mg/ml stock), 1.69 µl Horseradish Peroxidase (HRP) (1 Unit/µl stock), 0.9 µl Invitrogen Amplex Red (10 mM stock), and 438.19 µl 0.1 M Tris-HCl buffer (pH 8.6). The enzymes used in the working solution were purchased from Sigma-Aldrich and the Amplex Red was purchased from Thermo Fisher Scientific. After the initial 2-hour incubation, 20 µl of each WTA sample was added to 20 µl of the working solution in separate wells of a 96-well culture plate, with three replicates performed for each trial. A further 1-hour incubation was conducted in the dark to protect the light-sensitive Amplex Red reagent. Following this incubation, fluorescence was measured using a Synergy H4 Hybrid microplate reader at an excitation wavelength of 563 nm and an emission wavelength of 584 nm. The fluorescence readings were recorded, averaged, and plotted using Excel, and the amount of D-Ala released was calculated from a standard curve of known D-Ala concentrations ranging from 5-50 µM D-Ala. A solution without WTA was used as a blank. The standard curve was plotted based on data recorded from two trials, each with three replicates (Figure 27 in Appendix A). The standard curve was generated using the same working solution as previously described. However, D-Ala amino acid was substituted for the isolated WTA and FmtA and was dissolved in a 50 mM sodium phosphate buffer (pH 7.2) to prepare a series of solutions with varying D-Ala concentrations. Fluorescence readings were subsequently recorded for each solution. Given the known concentrations of D-Ala, a standard curve was constructed by plotting fluorescence intensity against D-Ala concentration.

Determining D-Ala content from WTA isolated from *L. plantarum* and *B. subtilis* was achieved using ^{1}H-NMR spectroscopy to estimate the total WTA concentration from each organism. The ^{1}H-NMR was set to a standard “zgesgp” pulse program using 32768 data points, a 16-ppm spectral width, a relaxation delay of 7 seconds, and a total of 64 scans. Based on these

concentrations, WTA samples of 200 µg and 300 µg were prepared from *L. plantarum* in 300 µl of solution, while a single 200 µg sample was prepared for *B. subtilis* in 300 µl of solution. These samples were created by diluting the original WTA stock solution. Each 300 µl solution contained WTA, 50 µg/ml DSS, D_2O, 0.1 M NaOH, and ddH_2O. NaOH was added to completely separate the D-Ala from the WTA, and its addition resulted in a shift of the D-Ala peak from approximately 1.47 ppm to 1.2 ppm in the NMR spectra. The samples were subjected to ^{1}H-NMR spectroscopy, and the D-Ala concentration for each sample was determined based on the integration of the D-Ala peak relative to the DSS peak using Bruker TopSpin software. The resultant ratios were compared to a standard D-Ala curve generated following the integration of D-Ala solutions of known concentrations (ranging from 200 µM to 10 mM) with a DSS peak (Figure 28 in Appendix B). A single DSS peak was used to integrate all standard D-Ala peaks to account for potential variability in DSS signal intensity across spectra. This approach ensured consistency in D-Ala peak integration across all samples for the standard curve. After the D-Ala concentrations in the diluted WTA samples were determined, the values were multiplied by their respective dilution factors to calculate the total D-Ala content in the original undiluted WTA samples. For *L. plantarum*, the D-Ala concentrations obtained from the 200 µg and 300 µg samples were averaged to determine the final value. The final phosphate and D-Ala concentrations (in the stock solutions of isolated WTA from 1 L cultures and suspended in 300 µl), including D-Ala/phosphate ratios, were subsequently compared between *L. plantarum* and *B. subtilis*, as well as with those for *S. aureus* RN4220 provided by lab colleague Sai Sundararaman, to compare the differences in the isolated WTA from these cultures.

Results

Confirmation and Quantification of D-Ala Removal from WTA of *S. aureus* RN4220, *B. subtilis* 168, and *L. plantarum* NCIMB 8826 *in vivo* using ^{1}H-NMR

The experiments summarized in this section aimed to investigate whether FmtA can hydrolyze the bond between D-Ala and WTA from *S. aureus* organisms *in vivo*, as well as other Gram-positive organisms such as *B. subtilis* and *L. plantarum*. The objectives also included the quantification of the D-Ala released from these bacteria. The amount of D-Ala released from the

different organisms, using various concentrations of exogenous FmtA, was quantified using a standard D-Ala peak generated from known D-Ala concentrations using ^{1}H-NMR. All organisms were cultured to the same OD_{600} to ensure consistency across the different studies. On average, 50 ml of *S. aureus* and *B. subtilis* cell cultures grown to an OD_{600} of 1.0 yielded between 50-60 mg of bacterial pellet. In contrast, *L. plantarum* produced an average of 76 mg of bacterial pellet per 50 ml, although the OD_{600} was the same as those of *S. aureus* and *B. subtilis* (1.0 A.U.). Subsequent colony formation assays revealed that at an OD_{600} of 1.2, *S. aureus* RN4220 exhibited 187 colonies on TSB-Agar plates at a dilution factor of 10^6, while at the same dilution *L. plantarum* formed 49 colonies. This indicated that at the same OD_{600}, there were approximately 4x less viable cells of *L. plantarum* compared to *S. aureus* suggesting that the higher pellet weight of *L. plantarum* was not due to an increased number of cells. Instead, it was hypothesized that the increased weight resulted from buffer retention in the pellet during the washing stages of the experiment. Despite the removal of the buffer during centrifugation to recover the bacterial pellet, it was observed that the buffer solution was retained within the pellet, as evidenced by partial bacterial filaments and liquid solution in the pipette tip upon pipetting the pellet. This phenomenon was not observed in cells like RN4220 and explains why the weight of *L. plantarum* was not adjusted to fall within the 50-60 mg range of *S. aureus* and *B. subtilis*. Multiple trials were conducted for each organism, and bacterial pellet weights were adjusted between trials to maintain a pellet weight difference within a 5 mg range.

As shown in Table 1, the release of D-Ala from *S. aureus*, *B. subtilis*, and *L. plantarum* increased with the concentration of FmtA in the sample, although the error for *B. subtilis* was high. This confirmed that FmtA was able to release D-Ala from ribitol-phosphate WTAs bound to *S. aureus in vivo*. In addition, although FmtA is native to *S. aureus*, it was able to hydrolyze the bond between D-Ala and WTAs present in the envelope of *B. subtilis* and *L. plantarum in vivo*. *B. subtilis* and *L. plantarum* possess glycerol-phosphate WTAs. In this thesis, we define cell envelope as both the cell membrane and cell wall of the bacterial species.

Among the three organisms, *S. aureus* exhibited the lowest D-Ala release, with 20 μM FmtA releasing an average of 38 ± 3.0 μM D-Ala. *B. subtilis* showed an average D-Ala release of 148 ± 77 μM after incubation with 20 μM FmtA, while *L. plantarum* exhibited a substantial D-Ala removal of 1.6 ± 0.25 mM with 10 μM FmtA incubation and over 2 ± 0.023 mM after 20 μM FmtA treatment (Table 1). The *L. plantarum* D-Ala values mentioned were calculated based on the

comparison with the 150 μM standard. The accuracy of these measurements was later validated using a 1 mM D-Ala standard, which yielded *L. plantarum* D-Ala concentrations similar to those determined using the 150 μM standard, thereby ensuring the reliability of the data. The D-Ala concentrations derived from the 1 mM standard were 728 ± 132 μM in the absence of FmtA incubation, 1.4 ± 0.224 mM following incubation with 10 μM FmtA, and 1.8 ± 0.095 mM with 20 μM FmtA (Table 1). A negative control was conducted for *S. aureus* RN4220 confirming that without FmtA incubation, there was no D-Ala release detected (Figure 29 in Appendix C). A previous student in Dr. Golemi-Kotra's lab utilized Gram-negative *E. coli* as a negative control for D-Ala release concluding that the ^{1}H-NMR D-Ala peak is only observed for Gram-positive organisms. The results obtained here imply two possibilities. The first possibility is that glycerol-phosphate WTAs in *B. subtilis* and *L. plantarum* may have a higher substitution of D-Ala then the ribitol-phosphate WTAs of *S. aureus*. The second possibility is that there are higher amounts of WTAs in the cell envelopes of *L. plantarum* and *B. subtilis*.

Furthermore, *B. subtilis* and *L. plantarum* displayed D-Ala peaks even in the absence of FmtA, suggesting that these organisms might release D-Ala independently, possibly through mechanisms different from those in *S. aureus*. However, the addition of FmtA led to an increased release of D-Ala, which further intensified with higher FmtA concentrations. In *B. subtilis*, there was an average D-Ala release of 62 ± 57 μM without FmtA incubation. However, upon FmtA incubation, there was an additional release of 34.7 ± 14.7 μM D-Ala with 10 μM FmtA incubation, 52.6 ± 28 μM with 15 μM FmtA, and 85 ± 31 μM with 20 μM FmtA resulting in a total release of 97 ± 52 μM, 115 ± 56 μM, and 148 ± 77 μM D-Ala respectively. In addition, *L. plantarum* displayed an average D-Ala release of 791 ± 122 μM without FmtA incubation. However, upon FmtA incubation, there was an additional release of 762 ± 128 μM D-Ala with 10 μM FmtA incubation, and 1247 ± 99 μM with 20 μM FmtA resulting in a total release of 1553 ± 248 μM and 2037 ± 23 μM D-Ala respectively. Figures 3-5 illustrate typical ^{1}H-NMR spectra for each organism, showing the varying sizes of D-Ala peaks at different FmtA concentrations.

Table 1. Quantification of D-Ala release from *S. aureus* RN4220, *B. subtilis* 168, and *L. plantarum* NCIMB 8826 at varying concentrations of exogenous FmtA. Three independent trials were conducted to assess the impact of exogenous FmtA concentrations, ranging from 0 μM to 20 μM, on the release of D-Ala. Cells were incubated for 1 hour, and the corresponding bacterial weights for each trial, as well as the standard deviations across the three trials, are provided. The concentration of released D-Ala (μM) was calculated using D-Ala standard peaks established on the 700 series ^{1}H-NMR. The experimental D-Ala peaks were directly compared to these standard peaks for quantification.

***S. aureus* RN4220 D-Ala Release Relative to 40 μM D-Ala Standard (μM)**					
Trial	0μM FmtA	10μM FmtA	15μM FmtA	20μM FmtA	Bacterial Pellet Weights (mg)
1	0	22.1	33.4	37.6	55
2	0	24.2	36.5	41.0	53
3		20.6	31.1	35.0	58
Average	0	22.3 ± 1.8	33.6 ± 2.7	37.9 ± 3.0	
***B. subtilis* 168 D-Ala Release Relative to 80 μM D-Ala Standard (μM)**					
Trial	0μM FmtA	10μM FmtA	15μM FmtA	20μM FmtA	Bacterial Pellet Weights (mg)
1	28.5	54	59.4	78.3	55
2	128.4	155.2	170.9	231.3	55
3	30.1	81.8	114.5	133.2	59
Average	62 ± 57	97 ± 52	115 ± 56	148 ± 77	
***L. plantarum* NCIMB 8826 D-Ala Release Relative to 150 μM D-Ala Standard (μM)**					
Trial	0μM FmtA	10μM FmtA	15μM FmtA	20μM FmtA	Bacterial Pellet Weights (mg)
1	798.3	1601.5		2044.3	74
2	908.6	1772.6		2056.1	77
3	665.1	1284.1		2011.3	77
Average	791 ± 122	1553 ± 248		2037 ± 23	
Average (using 1 mM Standard)	728 ± 132	1369 ± 224		1825 ± 95	

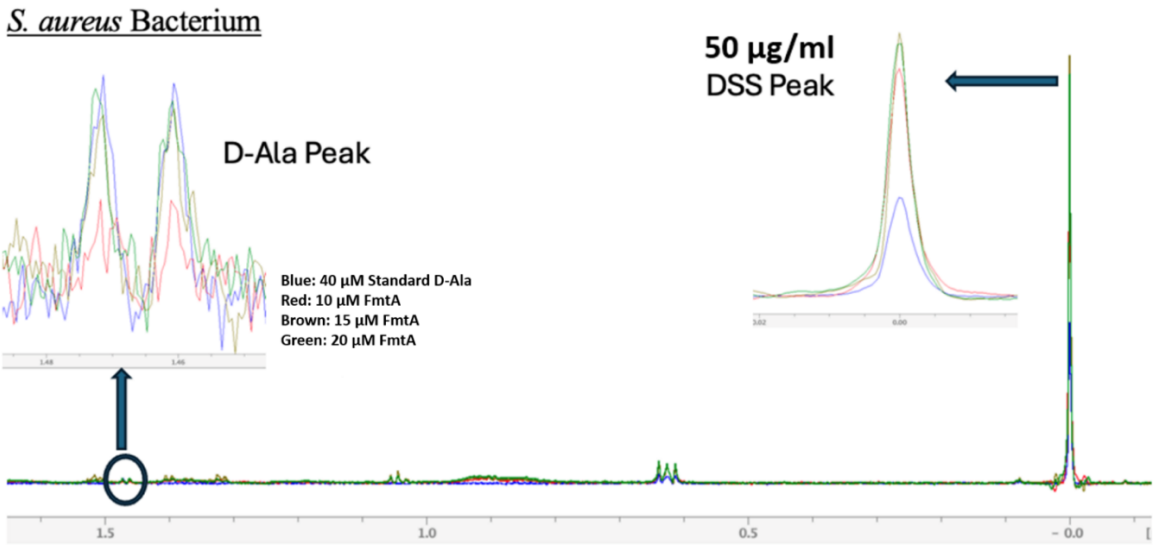

Figure 3. ^{1}H-NMR data depicting D-Ala release from RN4220 cells incubated with 10 µM, 15 µM, or 20 µM FmtA. This figure is a partial ^{1}H-NMR spectrum for RN4220 D-Ala release after FmtA incubation and portrays the first trial conducted. The D-Ala peak is located at 1.47 ppm, and the 40 µM D-Ala standard peak was used for quantification. Blue peak: 40 µM D-Ala standard, red peak: D-Ala released from 10 µM FmtA, brown peak: D-Ala released from 15 µM FmtA, green peak: D-Ala released from 20 µM FmtA.

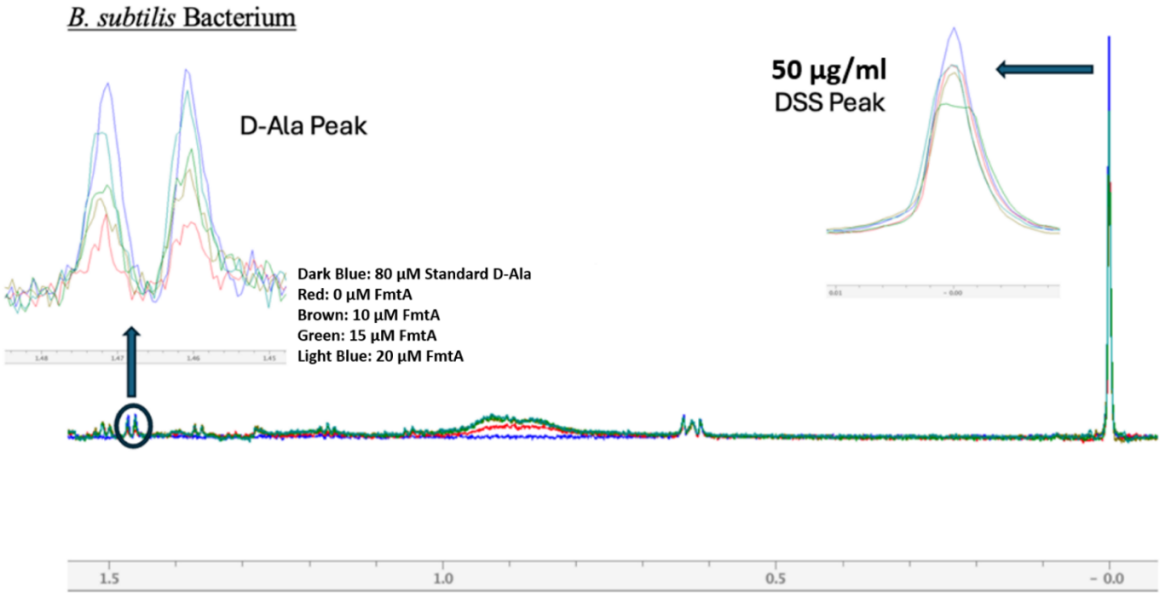

Figure 4. ^{1}H-NMR data depicting D-Ala release from *B. subtilis* 168 cells incubated with 0 µM, 10 µM, 15 µM, or 20 µM FmtA. This figure is a partial ^{1}H-NMR spectrum for *B. subtilis* D-Ala release after FmtA incubation and portrays the first trial conducted. The D-Ala peak is located at 1.47 ppm, and the 80 µM D-Ala standard peak was used for quantification. Dark blue peak: 80 µM D-Ala standard, red peak: D-Ala released from 0 µM FmtA, brown peak: D-Ala released from 10 µM FmtA, green peak: D-Ala released from 15 µM FmtA. blue peak: D-Ala released from 20 µM FmtA.

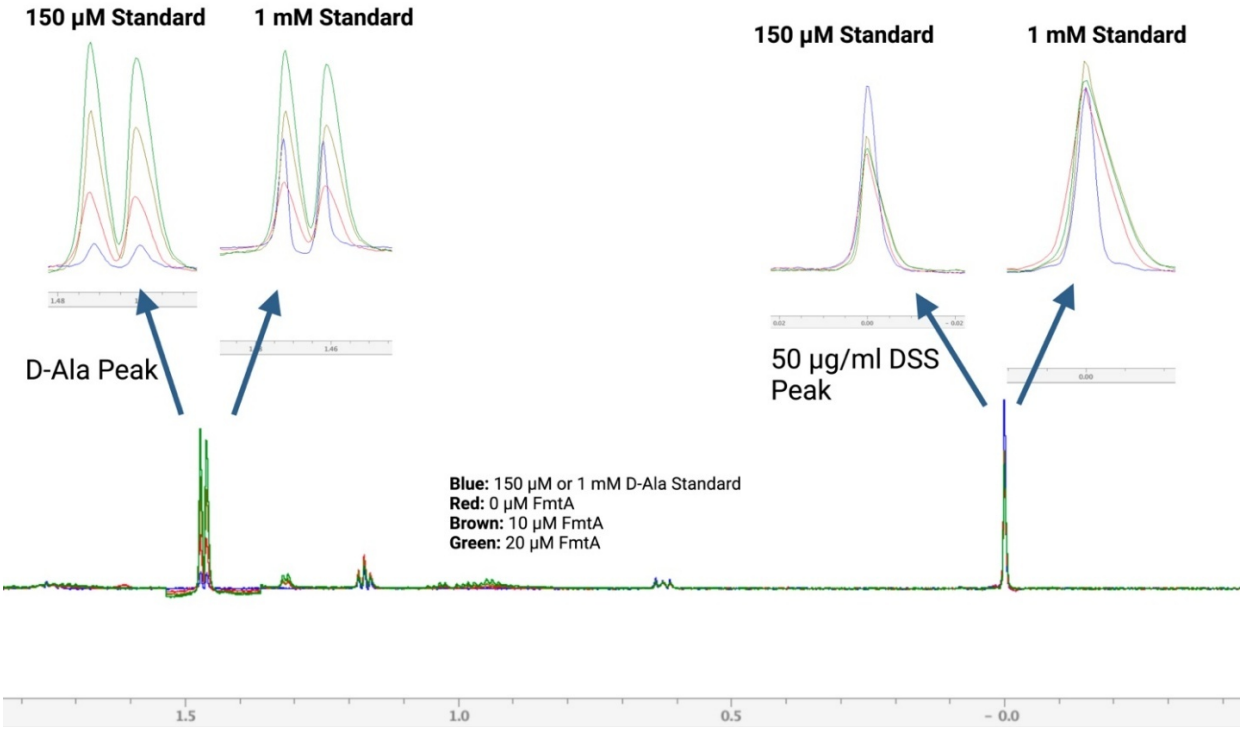

Figure 5. ^{1}H-NMR data depicting D-Ala release from *L. plantarum* NCIMB 8826 cells incubated with 0 µM, 10 µM, or 20 µM FmtA. This figure is a partial ^{1}H-NMR spectrum for *L. plantarum* D-Ala release after FmtA incubation and portrays the first trial conducted. The D-Ala peak is located at 1.47 ppm, and the 150 µM and 1 mM D-Ala standard peaks were used for quantification. Blue peak: 150 µM or 1 mM D-Ala standard, red peak: D-Ala released from 0 µM FmtA, brown peak: D-Ala released from 10 µM FmtA, green peak: D-Ala released from 20 µM FmtA.

Comparative Analysis of WTA and D-Ala Quantity Between *S. aureus*, *B. subtilis*, and *L. plantarum*

Experimental data revealed that 20 µM of FmtA facilitated a greater removal of D-Ala from the WTAs of *L. plantarum* compared to *B. subtilis and S. aureus in vivo.* Based on these observations, we hypothesized that either *L. plantarum* possesses a higher D-Ala content on its WTAs than the other two organisms, or there is a higher abundance of WTAs present on the surface of *L. plantarum*. To investigate these hypotheses, WTA was isolated from *L. plantarum* and *B. subtilis* using a standardized protocol previously employed for *S. aureus* WTA isolation. The WTA samples were subsequently compared based on total inorganic phosphate and D-Ala content present in the sample. Phosphate content, a direct indicator of WTA abundance, was measured using a colorimetric phosphate assay (QuantiChrom Phosphate Assay Kit). The D-Ala content was

quantified via ^{1}H-NMR utilizing a D-Ala to DSS standard curve. The isolated WTA samples were divided for phosphate and D-Ala quantification, and appropriate dilution factors were accounted for when calculating the values for D-Ala and phosphate in the original undiluted WTA sample.

The estimated WTA concentrations isolated from 1 L of culture for each organism are presented in Table 2, along with the corresponding total CFU/L quantified for each culture. Additionally, Table 2 outlines the final concentrations of D-Ala and phosphate in the WTA samples dissolved in 300 µl of solution, as well as the calculated D-Ala/phosphate ratios. For *S. aureus* RN4220, the CFU/L was determined to be 1.9×10^{12}. At an equivalent OD_{600}, the *B. subtilis* 168 culture exhibited a total of 1.1×10^{11} CFU/L, representing a 17-fold reduction compared to the *S. aureus* culture. Similarly, the *L. plantarum* NCIMB 8826 culture demonstrated a total of 4.9×10^{11} CFU/L, which was approximately 4-fold lower than that of *S. aureus*. From these cultures, varying concentrations of WTAs were isolated. The concentration of WTA isolated from *S. aureus* was 1.25 mg/ml, comparable to the 1.0 mg/ml obtained from *B. subtilis*. In contrast, a higher concentration of 2.8 mg/ml WTA was extracted from *L. plantarum*.

The *S. aureus* WTA sample was found to contain a total of 300 µM of D-Ala and 1.2 mM of phosphate. In contrast, the WTA samples isolated from *L. plantarum* and *B. subtilis* exhibited significantly higher concentrations of both D-Ala and phosphate. The *B. subtilis* WTA sample contained a D-Ala concentration of 1.4 mM, representing a 4.7-fold increase compared to *S. aureus*, and a phosphate concentration of 13.3 mM, which was 11-fold higher than that of *S. aureus*. Notably, *L. plantarum* exhibited both higher phosphate and D-Ala content compared to *S. aureus* and *B. subtilis.* The total phosphate concentration was 45.1 mM, and the D-Ala concentration was 20.9 mM. In terms of phosphate content, *L. plantarum* demonstrated a 38-fold increase relative to *S. aureus* and a 3.4-fold increase when compared to *B. subtilis.* Regarding D-Ala, *L. plantarum* demonstrated a 70-fold higher content than *S. aureus* and a near 15-fold higher content compared to *B. subtilis.* Based on these D-Ala and phosphate values, if the *L. plantarum* and *B. subtilis* CFU/L were normalized with that of the *S. aureus* CFU/L, it would be expected that the D-Ala and phosphate content in the 300 µl WTA sample isolated from *L. plantarum* and *B. subtilis* would increase 4-fold and 17-fold respectively.

Figure 6 displays a partial ^{1}H-NMR spectrum illustrating the D-Ala peaks corresponding to various WTA dilutions of *L. plantarum* and *B. subtilis*. Additionally, D-Ala peaks from 1 mM and 6 mM D-Ala standards were provided for comparison. The D-Ala concentrations were

calculated based on a D-Ala standard curve ranging from D-Ala concentrations of 200 µM to 10 mM, with the curve generated based on D-Ala and DSS peak integration. As evident in Figure 6, the DSS peaks in the D-Ala standards spectra were smaller than those of the *L. plantarum* and *B. subtilis* samples. This discrepancy likely resulted from improper preparation of the DSS stock solution. Since the initial DSS stock solution had been depleted, a new stock was prepared and used for the standards, which were analyzed after the *L. plantarum* and *B. subtilis* samples. To address this issue and ensure consistency in the standard curve, the integration of all standard D-Ala peaks was performed using the DSS peak from the 300 µg *L. plantarum* WTA spectrum. In this way, all standard values were based on the same DSS peak and the issue with DSS peak height was resolved. The variance between the 200 µg *B. subtilis* and the 300 µg *L. plantarum* DSS peak height integration was 10%.

Table 2. Quantification of the D-Ala and phosphate content present in the 300 µl solution of WTA isolated from a 1 L culture of three Gram-positive organisms: *S. aureus* RN4220, *B. subtilis* 168, and *L. plantarum* NCIMB 8826. The CFU (1 L) values for each organism are presented alongside the total estimated concentration of WTAs isolated from each respective 1 L culture. The entire isolated WTA sample was dissolved in 300 µl solution. The D-Ala/phosphate ratio is also provided. The protocol utilized for WTA isolation was the same in all species and the total phosphate and D-Ala content was calculated for the entire 300 µl sample. Phosphate quantity was determined using a colorimetric phosphate assay and total D-Ala was calculated in the presence of 0.1 M NaOH using ^{1}H-NMR. The values for RN4220 were graciously provided by lab colleague, Sai Sundararaman.

Bacterium	**CFU (1 L Culture)**	**Weight of Bacterial Pellet (g)**	**Concentration of WTA (mg/ml), 300 µl**	**D-Ala (mM), 300 µl**	**Phosphate (mM), 300 µl**	**D-Ala / Phosphate**
S. aureus RN4220	1.9×10^{12}	1.4	1.25	0.3	1.2	0.24
B. subtilis 168	1.1×10^{11}	2.9	1.0	1.41	13.3	0.1
L. plantarum NCIMB 8826	4.9×10^{11}	3.2	2.8	20.9	45.1	0.46

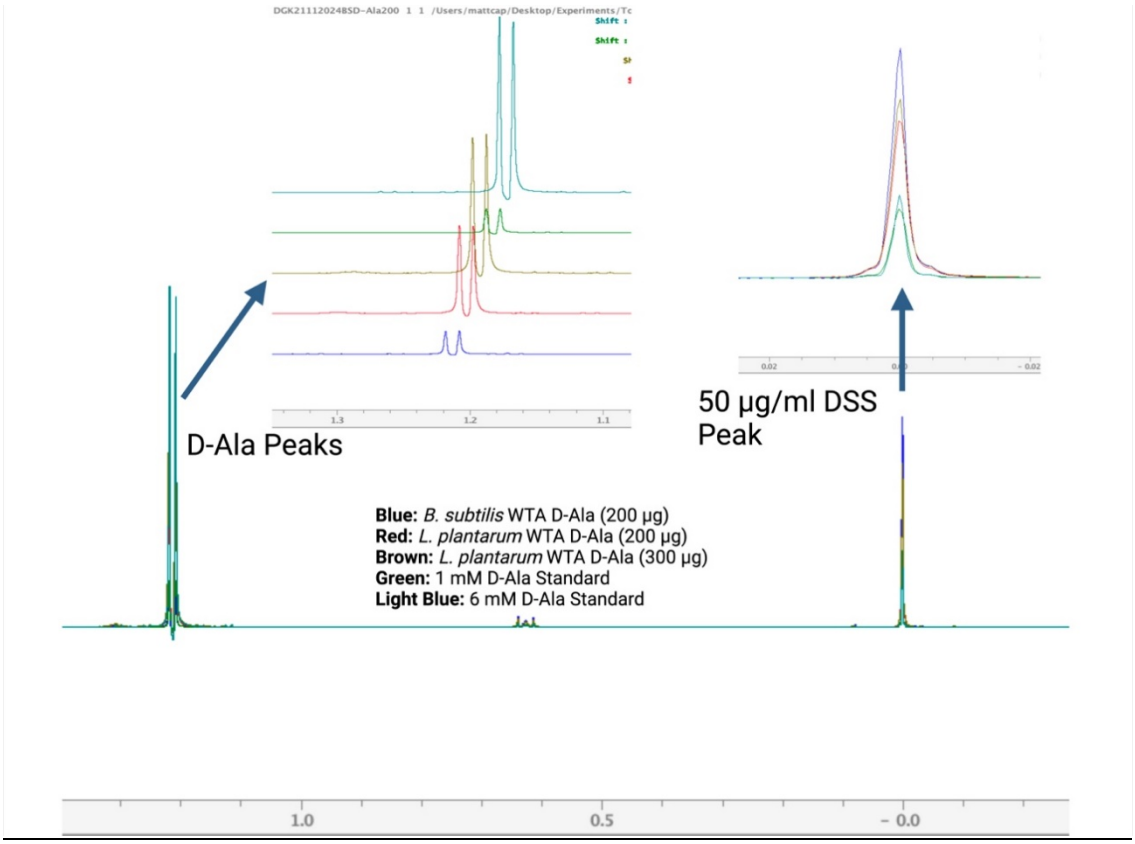

Figure 6. Partial ^{1}H-NMR spectra illustrating the quantification of D-Ala released from isolated WTAs of *B. subtilis* 168 and *L. plantarum* NCIMB 8826 after treatment with 0.1 M NaOH. Both 200 µg and 300 µg WTA samples were prepared and used to calculate total D-Ala present in the original isolated WTA sample. The D-Ala signal appears at approximately 1.2 ppm, attributed to the presence of NaOH. D-Ala concentrations were quantified using a standard D-Ala equation based on the integration of the D-Ala peak relative to the DSS reference peak. For visual comparison, the figure includes D-Ala standards at 1 mM and 6 mM. Peaks are color-coded as follows: blue (200 µg *B. subtilis* WTA), red (200 µg *L. plantarum* WTA), brown (300 µg *L. plantarum* WTA), green (1 mM D-Ala standard), and light blue (6 mM D-Ala standard). The variance between the 200 µg *B. subtilis* and the 300 µg *L. plantarum* DSS peak height integration was 10%.

Determining D-Ala to Phosphate Ratio from Isolated WTA

This study aimed to reveal the ratio of D-Ala to phosphate groups in the WTA of *S. aureus* RN4220, providing insights into the spatial distribution of D-Ala across the WTA structure. Specifically, it sought to determine whether D-Ala is present on every ribitol-phosphate subunit, or every second, third, etc. subunit. This information is also essential for accurately estimating the molecular weight of the WTA polymer. Phosphate concentration was quantified using the QuantiChrom Phosphate Assay Kit (DIPI-500) and compared to the amount of D-Ala released

following incubation with 10 μM FmtA, utilizing equivalent concentrations of isolated WTA. The data confirmed a proportional increase in both phosphate and D-Ala content with rising WTA concentrations (Table 3). Notably, the D-Ala to phosphate ratio for nearly all WTA concentrations ranged between 0.2 and 0.3, with an average ratio of 0.27. This implies that D-Ala is present on approximately every fourth ribitol-phosphate unit in the WTA (Table 3). Based on this ratio, the molecular weight of the WTA polymer was calculated to be 19,811.06 g/mol. The calculations performed to achieve this molecular weight are provided in Appendix D (Figure 30).

Table 3. Quantification of total inorganic phosphate and D-Ala on isolated WTA from *S. aureus* RN4220 cells. The concentrations of D-Ala and phosphate were determined from equivalent concentrations of isolated WTA to ensure comparability. The ratio of D-Ala to phosphate was calculated by dividing the D-Ala concentration by the phosphate concentration. Phosphate quantification was performed using the QuantiChrom Phosphate Assay Kit (DIPI-500), which employs a malachite green dye and molybdate reagent that fluoresces upon interaction with inorganic phosphate. D-Ala concentration was quantified using a fluorescent enzyme coupled assay employing FAD and DAO enzymes in the presence of Amplex Red and HRP.

Isolated WTA Concentration (μg/μl)	D-Ala Released (μM) using 10μM FmtA	Phosphate Content (μM)	D-Ala/Pi
0.05	26 ± 2	62 ± 7	0.42
0.1	37 ± 6	152 ± 6	0.24
0.15	54 ± 2	241 ± 5	0.22
0.2	79 ± 6	295 ± 27	0.27
0.25	81 ± 7	361 ± 30	0.22
D-Ala/Pi Average			0.27

Discussion

FmtA removal of D-Ala from WTA of *S. aureus*, *B. subtilis*, and *L. plantarum* was confirmed to occur *in vivo*. Quantification of the total D-Ala released from these three different Gram-positive bacterial strains was also performed. For *S. aureus* RN4220 cells, no D-Ala was detected in the control samples without FmtA. However, as the concentration of FmtA increased, the amount of D-Ala released, as measured by ^{1}H-NMR, also increased, seemingly reaching a saturation at 20 μM FmtA (Table 1). In contrast, *B. subtilis* 168 and *L. plantarum* NCIMB 8826 cells exhibited detectable D-Ala release even in the absence of FmtA incubation, suggesting an intrinsic mechanism for D-Ala release comparable to that mediated by FmtA in *S. aureus*. Consistent with RN4220, D-Ala release from *B. subtilis* and *L. plantarum* increased proportionally with FmtA concentration, supporting the capability of FmtA to remove D-Ala from both ribitol-phosphate WTAs in the cell envelope of *S. aureus*, and glycerol-phosphate WTAs in the cell envelope of *B. subtilis* and *L. plantarum in vivo*. D-Ala binds to glycerol-phosphate WTA in the same way it does to ribitol-phosphate WTA, using an ester linkage (Archibald et al., 1961). Previous data from our lab identified the capability of FmtA to release D-Ala *in vitro* from isolated ribitol-phosphate and glycerol-phosphate teichoic acids of *S. aureus* (Rahman et al. 2016). The data discussed in this thesis confirmed that FmtA is capable of hydrolyzing the bond between D-Ala and WTA from glycerol-phosphate WTAs and ribitol-phosphate WTAs *in vivo*, while the WTAs are attached to the cell surface of viable cells.

The D-Ala release from *B. subtilis* varied between trials, yielding high standard deviation, which could be partially attributed to the variability in D-Ala release from the control without FmtA (Table 1). Additionally, these higher error rates may be attributed to incorrect ^{1}H-NMR calibration as some of the trials performed for *B. subtilis* were run directly prior to ^{1}H-NMR repair interruption. The total D-Ala released from *B. subtilis* seemingly exceeded that from RN4220 cells, indicating a higher D-Ala release from *B. subtilis* utilizing FmtA. However, when the standard deviation and the D-Ala released independently of FmtA were accounted for, the values appeared to be comparable to those of *S. aureus* for the 10 μM and 15 μM FmtA concentrations. At 10 μM FmtA, *B. subtilis* experienced an additional D-Ala release of 34.7 ± 14.7 μM attributed solely to the FmtA, while *S. aureus* exhibited 22.3 ± 1.8 μM D-Ala release. At 15 μM FmtA, *B. subtilis* experienced an additional D-Ala release of 52.6 ± 28 μM attributed solely to the FmtA, while *S.*

aureus exhibited 33.6 ± 2.7 μM D-Ala release (Table 1). At 20 μM FmtA, the difference in D-Ala release became increasingly divergent. An additional 85 ± 31 μM D-Ala was released from the *B. subtilis* strain due to FmtA, which was greater when compared to the 37.9 ± 3 μM D-Ala released from *S. aureus*. In *L. plantarum* NCIMB 8826, D-Ala removal was also observed without FmtA incubation, similar to *B. subtilis*, and increased as FmtA was added. However, *L. plantarum* exhibited substantially higher D-Ala release compared to both *S. aureus* and *B. subtilis*. Without FmtA, *L. plantarum* released nearly 800 μM of D-Ala, with FmtA incubation elevating these levels into the 2 mM range at 20 μM FmtA. Although, if we account for the D-Ala release without FmtA, FmtA alone released a total of 1.25 ± 0.1 mM at 20 μM FmtA.

It was hypothesized that the WTAs of *L. plantarum* and *B. subtilis* exhibit a greater degree of D-Ala substitution relative to those of *S. aureus*. Alternatively, it was proposed that *L. plantarum* and *B. subtilis* possess a greater abundance of WTAs within their cell envelopes, thereby increasing the total D-Ala present in the cell envelope of these species. Experimental analyses revealed that the WTA sample isolated from 1.1 x 10^{11} CFU/L of *B. subtilis* exhibited 11-fold more phosphate and 4.7-fold more D-Ala than the WTA sample isolated from 1.9 x 10^{12} CFU/L of RN4220. Phosphate content was an indicator of WTA abundance. In contrast, the *L. plantarum* WTA sample isolated from a 4.9 x 10^{11} CFU/L culture exhibited 38-fold more phosphate and 70-fold more D-Ala than the WTA sample isolated from the same RN4220 culture. These results also suggested that the *L. plantarum* and *B. subtilis* cultures contained fewer cells for WTA isolation. Therefore, we concluded that *B. subtilis* WTAs are less substituted with D-Ala compared to RN4220 WTAs, as the D-Ala/phosphate ratio for *B. subtilis* was 0.1, while for *S. aureus* it was 0.21. However, due to *B. subtilis* having more WTAs, the quantity of D-Ala on the surface was greater than that of the RN4220 bacterium. In contrast, *L. plantarum* WTAs are more heavily substituted with D-Ala than *B. subtilis* and *S. aureus* WTAs, as the D-Ala/phosphate ratio for *L. plantarum* was 0.46. Additionally, the substantial phosphate content in the *L. plantarum* WTA sample resulted in a total D-Ala surface content greater than that of *B. subtilis* and *S. aureus*. This would likely explain the observed capacity for greater D-Ala release following FmtA incubation in *L. plantarum* compared to both *B. subtilis* and *S. aureus* (Figure 3-5). Also, when comparing the total D-Ala present in the isolated WTA samples of each organism to those released by 20 μM of FmtA *in vivo*, it became evident that the FmtA activity is consistent for all organisms.

A study by Lam et al. (2009) reported that certain bacteria including *S. aureus*, *B. subtilis*, and *Streptomyces lividans,* release D-amino acids, including D-Ala, into the extracellular medium upon reaching the stationary growth phase. This release of D-amino acids exerts a variable impact on peptidoglycan synthesis and organization, conceivably enhancing or reducing cell wall stability (Lam et al., 2009). As noted in this chapter, even without FmtA incubation, organisms such as *B. subtilis* and *L. plantarum* exhibited D-Ala release into the extracellular solution. Lam et al. (2009) confirmed that the organisms mentioned above can release D-amino acids, including D-Ala by some strains like *S. aureus*, for their benefit, during the stationary growth period. Although Lam et al. (2009) observed D-Ala release in *S. aureus* but not in *B. subtilis*, contrary to the findings in this chapter, several explanations are plausible. Firstly, the cells used to determine D-Ala release with FmtA were collected during the exponential phase, not the stationary phase. Secondly, strain-specific variations could impact D-Ala synthesis, attachment, and release differently from those observed by Lam et al. (2009). Nevertheless, the data from Lam et al. (2009) support the idea, similar to our findings, that certain organisms can release D-amino acids, including D-Ala, without FmtA incubation, and that these released D-amino acids play a role in certain aspects of cellular peptidoglycan processes and conformation.

Based on the observed D-Ala to phosphate ratio from isolated WTAs of RN4220, it appears that there are, on average, four times as many phosphate residues on the WTA as there are D-Ala modifications. Therefore, it was concluded that there is one D-Ala substitution present on every fourth ribitol-phosphate backbone, correlating with the approximate 0.27 ratio calculated. The structure of WTA from gram-positive organisms and its corresponding modifications have been studied since the late 20th century. Mirelman et al. (1970) analyzed the structure of WTA and concluded that D-Ala substitutions are highly likely to be positioned on the second carbon of the ribitol-phosphate subunit. The researchers of this study observed that D-Ala is not substituted at the third carbon position and, because N-Acetylglucosamine is located at the fourth carbon position, consequently hypothesized that D-Ala is not substituted at the fourth carbon position. If D-Ala can only be present at the second carbon of a single ribitol-phosphate subunit, the individual ribitol-phosphate subunits cannot be saturated with multiple D-Ala amino acids. However, not every ribitol-phosphate repeat contains a D-Ala bound to its second carbon as observed in our study. Therefore, understanding the distribution of D-Ala across the WTA is important, and by

analyzing the phosphate and D-Ala content from isolated WTA, a clearer picture of the WTA structure begins to emerge.

The total calculated number of phosphate molecules correlates with the total number of ribitol-phosphate repeats, as there is one phosphate molecule per subunit. The higher concentration of phosphate molecules in the RN4220 strain further confirms that not every ribitol-phosphate subunit is modified with D-Ala. Considering the results presented by Mirelman et al. (1970), suggesting that D-Ala is only situated on the second ribitol carbon, a D-Ala to phosphate ratio of 0.27 indicates that, on average, for every four ribitol-phosphate repeats, there is one D-Ala present. It is also critical to note that a study conducted by Jenni and Berger-Bächi (1998) identified that various *S. aureus* strains exhibited a consistent N-Acetylglucosamine-to-ribitol ratio of 1.0. This implies that each ribitol-phosphate subunit is modified by one N-Acetylglucosamine molecule. Assuming that the *S. aureus* strain RN4220 possesses a comparable N-Acetylglucosamine-to-ribitol ratio, it can be inferred that certain individual ribitol-phosphate subunits may undergo a modification with both N-Acetylglucosamine and D-Ala.

References

Archibald, A. R., Armstrong, J. J., Baddiley, J., & Hay, J. B. (1961). Teichoic acids and the structure of bacterial walls. *Nature*, *191*(4788), 570–572.

Bhavsar, A. P., Erdman, L. K., Schertzer, J. W., & Brown, E. D. (2004). Teichoic acid is an essential polymer in *Bacillus subtilis* that is functionally distinct from teichuronic acid. *Journal of Bacteriology*, *186*(23), 7865–7873.

Hurst, A., Hughes, A., Duckworth, M., & Baddiley, J. (1975). Loss of D-alanine during sublethal heating of *Staphylococcus aureus* S6 and magnesium binding during repair. *Journal of General Microbiology*, *89*(2), 277–284.

Jenni, R., & Berger-Bächi, B. (1998). Teichoic acid content in different lineages of Staphylococcus aureus NCTC8325. *Archives of Microbiology*, *170*(3), 171–178.

Koch, H. U., Döker, R., & Fischer, W. (1985). Maintenance of D-alanine ester substitution of lipoteichoic acid by reesterification in *Staphylococcus aureus*. *Journal of Bacteriology*, *164*(3), 1211–1217.

Kojima, N., Araki, Y., & Ito, E. (1985). Structure of the linkage units between ribitol teichoic acids and peptidoglycan. *Journal of Bacteriology*, *161*(1), 299–306.

Lam, H., Oh, D.-C., Cava, F., Takacs, C. N., Clardy, J., de Pedro, M. A., & Waldor, M. K. (2009). D-amino acids govern stationary phase cell wall remodeling in bacteria. *Science*, *325*(5947), 1552–1555.

MacArthur, A. E., & Archibald, A. R. (1984). Effect of culture pH on the D-alanine ester content of lipoteichoic acid in *Staphylococcus aureus*. *Journal of Bacteriology*, *160*(2), 792–793.

Mirelman, D., Beck, B. D., & Shaw, D. R. D. (1970). The location of the D-alanyl ester in the ribitol teichoic acid of staphylococcusaureus. *Biochemical and Biophysical Research Communications*, *39*(4), 712–717.

Rahman, M. M., Hunter, H. N., Prova, S., Verma, V., Qamar, A., & Golemi-Kotra, D. (2016). The *Staphylococcus aureus* methicillin resistance factor FmtA is a d-amino esterase that acts on teichoic acids. *mBio*, *7*(1).

Tomita, S., Irisawa, T., Tanaka, N., Nukada, T., Satoh, E., Uchimura, T., & Okada, S. (2010). Comparison of components and synthesis genes of cell wall teichoic acid among *Lactobacillus plantarum* strains. *Bioscience, Biotechnology, and Biochemistry*, *74*(5), 928–933.

Chapter Three:

Implications of D-Alanine Removal on *S. aureus* Viability Under Favourable and Non-Favourable Laboratory-Controlled Conditions

Introduction

We have, up to this point, documented that D-Ala bound to WTA on the surface of *S. aureus* is removed by the native enzyme FmtA, not only from isolated WTAs but also from live cells cultured under laboratory-optimized conditions. However, it remains unclear how this removal of D-Ala by FmtA impacts the physiology and growth dynamics of *S. aureus*. Early studies related to FmtA revealed that the gene encoding this protein, *fmtA*, maintains the resistance properties of MRSA in the presence of β-lactam antibiotics upon successful expression (Komatsuzawa et al., 1997). The loss of *fmtA* function due to an induced mutation leads to a decrease in observed antibiotic resistance, including resistance to oxacillin (Komatsuzawa et al., 1997). Consequently, it is safe to assume that FmtA contributes to the antibiotic resistance of *S. aureus*, potentially through its enzymatic activity on WTA, hydrolyzing the bond between WTA and D-Ala. Additionally, the WTA polymers, along with their glycosylation modifications, play a major role in the survival of MRSA *S. aureus* under antibiotic pressure (Brown et al., 2012). WTA D-Ala amino acids are implicated in physiological processes essential for maintaining *S. aureus* viability. For instance, the immune system that targets *S. aureus* for destruction acts as a harmful environmental stressor for this organism. Without the synthesis of D-Ala-substituted WTAs, *S. aureus* would struggle to survive and counteract the effects of this system. D-Ala provides an additional layer of protection, facilitating *S. aureus* invasion and growth within or on the host (Simanski et al., 2013; Collins et al., 2002). Given the association of WTA and its D-Ala modification with several *S. aureus* mechanisms, including antibiotic resistance and virulence, excision of D-Ala by exogenous FmtA may offer further insight into the functional significance of this amino acid, potentially associating D-Ala with cellular growth in non-stress environments. This would underscore its necessity for *S. aureus* viability.

Brown et al. (2012) demonstrated that for *S. aureus* cells to achieve the formation of symmetrical division septa, which leads to efficient cell division, the synthesis of WTA is vital.

However, following their deletion of the *dltA* gene, responsible for D-alanylation, along with the glycosylation genes, cell division and septum formation remained comparable to wild-type cells, maintaining optimal division. This would indicate that while the presence of WTA is essential for these processes to occur without complications, its modification with D-Ala is not crucial. Although normal *S. aureus* cell division proceeds in the absence of D-Ala (Brown et al., 2012), the removal of D-Ala using exogenous FmtA might influence the growth rate of this organism under laboratory-optimized stress-free conditions. It is conceivable that the release of D-Ala from the cell WTA adversely impacts the organism's growth capabilities. This chapter aims to elucidate this hypothesis.

Environmental adaptation is a unique trait of bacterial organisms (Haruta and Kanno, 2015). Unfavourable growth environments trigger various alterations to bacterial cellular processes, ensuring the organism remains alive and viable. Stressors in the environment can encompass a multitude of different factors, with common ones being temperature and the presence of antibiotics. Depending on the bacterium, these organisms adapt in various ways including mutations and changes to their cell envelope (Haruta and Kanno, 2015). WTAs extending from the surface of *S. aureus* cells have been shown to be highly involved in the viability of the organism, as their presence and modifications can help the *S. aureus* adapt and resist cellular compromise under excessive salt content or the absence of nutrients (Mistretta et al., 2019; Jorge et al., 2018). It is important to restate that the D-Ala bound to WTAs has also been proven to promote cell functionality by limiting the detrimental effects induced on the cell by antimicrobial molecules and the innate immune system (Peschel et al., 1999; Collins et al., 2002; Simanski et al., 2013). Hence, this chapter also seeks to further explore the function of D-Ala modification on WTA for cell viability by presenting data from various *S. aureus* strains in the presence of different stressors.

In this study, lysozyme was the first stressor the *S. aureus* RN4220 strain was subjected to for the purpose of growth and lysis assays. Lysozyme is endogenously synthesized across diverse organisms, spanning from humans and birds to small life forms, such as insects and crustaceans (Khorshidian et al. 2022). Originally observed in the early 1900s by Alexander Fleming, multiple variants of this protein have since been discovered and categorized based on conformation, organism of origin, and antimicrobial effectiveness. Due to its high accessibility, owing to its localization within milk, blood, and the albumen of eggs, lysozyme is employed in food production for the elimination of bacterial pathogens because of its identified bactericidal potential

(Khorshidian et al. 2022). Although human lysozyme achieved more than double the efficiency of lysozyme from chickens (Wu et al., 2015), the organism of origin is not the only variable that plays a role in the bacterial lysis potential of lysozyme. As with most other enzymatic proteins, lysozymes from each category also have an ideal pH and temperature-sensitive operation (Khorshidian et al. 2022). The covalently linked N-Acetylmuramic acid and N-Acetylglucosamine sugar molecules, which constitute Gram-positive peptidoglycan, are the primary targets of lysozyme. Lysozyme acts to break this bond (Nawaz et al. 2022). Figure 7 illustrates the specific site of lysozyme action on the peptidoglycan structure.

Lysostaphin is another such enzyme considered as a potential stressor for bacteria like *S. aureus*. Similar to lysozyme, it facilitates cell wall damage, consequently leading to disruption of the peptidoglycan layer and ensuing cell death. The structurally compromised cell wall stems from lysostaphin-mediated disruption of a single glycine-glycine peptide bond in the cross-linking bridges formed between N-Acetylmuramic acid residues throughout the peptidoglycan layer (Bastos et al., 2010). Figure 7 also illustrates the lysostaphin target site within the peptidoglycan matrix. The antibacterial activity of lysostaphin was first identified by Schindler and Schuhardt in the 1960s by exposing 86 bacterial organisms, including *S. aureus*, to this protein, of which nearly 70% were *Staphylococcus* species. Against these *Staphylococcus* organisms, particularly *S. aureus*, lysostaphin's enzymatic function resulted in cell death. Notably, lysostaphin is developed and released by an organism also from the genus *Staphylococcus,* namely *Staphylococcus simulans,* which appears to remain unaffected by this enzyme (Schindler and Schuhardt, 1964; Baba and Schneewind, 1996). Lysostaphin has been studied extensively over several decades as a potential addition to or replacement of conventional ineffective antibiotics. Although not fully confirmed, antibiotics like vancomycin, used against highly resistant *S. aureus*, achieve a lower degree of infection clearance compared to lysostaphin, which has shown promising results in reducing the viability of resistant *S. aureus* strains (Placencia et al. 2009).

The lysostaphin enzyme is not solely studied for its effectiveness against antibiotic resistant strains of *S. aureus.* Studies regarding *S. aureus* biofilms have confirmed that these cells, which attach to each other and remain stationary, exhibit enhanced defensive properties against antibiotics, such as β-lactams and vancomycin, thereby promoting their viability (Wu et al. 2003). The release of the extracellular matrix encompassing these cells, however, does not appear to limit the action of lysostaphin, as it is indeed able to lyse the colonies of cells attached to different

surfaces, unlike the antibiotics, resulting in the breakdown of the biofilm (Wu et al. 2003). Due to lysostaphin-induced bacterial stress, which leads to the death of the organism, lysostaphin continues to be studied for implementation in areas such as commercial and house-hold products (Zha et al. 2022). In particular, maintaining the quality of perishable foods is of utmost importance, and the testing of lysostaphin for this specific purpose began as early as the 1990s. Cavadini et al. (1998) observed the *S. aureus*-suppressing lysostaphin function in meats prone to bacterial contamination. Other examples include lysostaphin containing disinfectants, livestock diet, and solutions for healthy crop yields (Zha et al. 2022). It is undeniable that lysostaphin could be advantageous in healthcare applications and other industries for combating *S. aureus* infections. This chapter explores lysostaphin lysis efficiency against FmtA treated *S. aureus* RN4220.

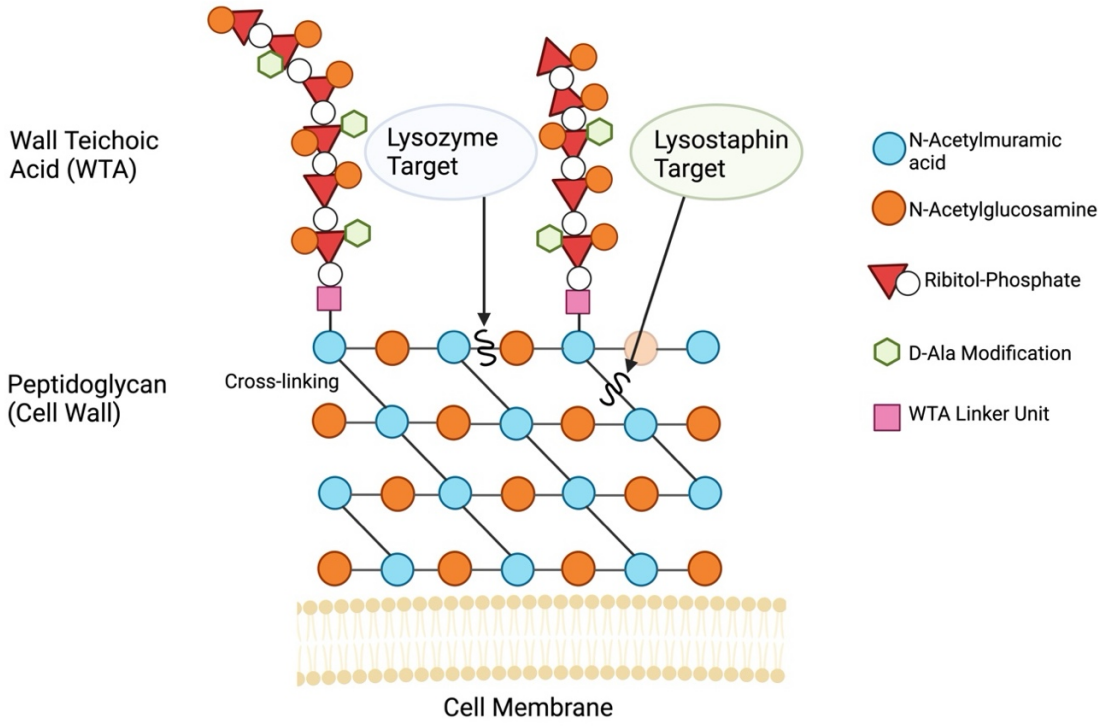

Figure 7. Depiction of the peptidoglycan structure of *S. aureus*, including cross-linking and partial visualizations of WTAs. The target sites of lysostaphin and lysozyme within the peptidoglycan are indicated by an arrow, and the cleavage of the corresponding peptidoglycan region is represented by a curved line. Created in BioRender.com

In addition to the studies performed using lysozyme and lysostaphin as stressors, we explored the alteration of FmtA-treated *S. aureus* viability in the presence of a β-lactam antibiotic.

Oxacillin was designed based on the original penicillin structure, with modifications to side chains to ensure endurance against β-lactamase degradation. Therefore, this antibiotic is categorized as a penicillin and serves to restrict access of the peptide substrate in the cell wall to the PBP active site (Bush and Bradford, 2016). We aimed to discover whether the absence of D-Ala on WTA would influence the survival of both MRSA and MSSA strains in the presence of oxacillin. MRSA antibiotic resistance properties is attributed to the success of several biological processes. These include the upkeep of adequately cross-linked peptidoglycan by PBP2a, the formation of glycosidic bonds between N-Acetylmuramic acid and N-Acetylglucosamine catalyzed by PBPs such as PBP2 (Pinho et al., 2001), and the synthesis and binding of WTA to PBP2a, which has been proposed to be a requisite for its catalytic function (Brown et al., 2012; Qamar and Golemi-Kotra, 2012). In addition, as cells divide, PBP4 localization is reliant on the generation of WTA, which leads to the formation of the characteristic and structurally interconnected net-like structure of the cell wall (Hill et al., 2019; Atilano et al., 2010; Łęski and Tomasz, 2005). This mesh-like architecture of the cell wall is indicative of cross-linking between peptidoglycan layers, which are naturally reduced in MRSA VISA strains to optimize vancomycin resistance (Hiramatsu et al., 2014). We hypothesized that the removal of D-Ala by FmtA may impact the ability of *S. aureus* to properly regulate PBPs, leading to altered antibiotic susceptibility.

WTAs are not solely involved in supporting PBP cross-linking function. They are also crucial for the precise intracellular spatial arrangement of AtlA, which leads to an efficient autolysis process at the site of cell division. The removal of WTA causes dysregulation of this process and AtlA activity, ultimately resulting in an increased number of cells prone to lysis (Schlag et al., 2010). Specifically, in the context of *S. aureus* autolysis, Boles et al. (2010) demonstrated that endogenously synthesized FmtA does in fact influence the regulation of autolysis. Furthermore, because FmtA enzymatically separates D-Ala from WTAs, as seen in our study, the D-Ala modification, therefore, appears to play a role in the regulation of this process. The subsequent sections of this chapter outline the results of Minimum Inhibitory Concentration (MIC) assays conducted on multiple *S. aureus* strains, encompassing both MSSA and MRSA phenotypes, in the presence and absence of FmtA. MIC assays are utilized to establish the smallest concentration of an antibiotic necessary to inhibit the growth of a specific bacterial strain like *S. aureus*. In our case, oxacillin was chosen as the antibiotic with which to perform this study.

Materials and Methods

S. aureus RN4220 Culture Preparation for Growth and Lysis Experiments

A 1 ml overnight culture of *S. aureus* RN4220, incubated at 37°C with agitation at 200 rpm, was inoculated into 99 mL of TSB media (Sigma-Aldrich). The culture was further incubated at 37°C with agitation at 170 rpm until the OD_{600} reached 1.0 A.U. Upon reaching an OD_{600} of 1.0 A.U., a 50 mL aliquot of the culture was collected and subjected to centrifugation at 5000 × g for 15 minutes at 22°C. The resulting bacterial cell pellets were washed thrice with 20 mL of 50 mM sodium phosphate buffer (pH 7.2). The buffer was created based on an established protocol with chemicals purchased from Fisher Chemical. The buffer was then filtered using Sarstedt Filtropur 0.2 μm syringe filters. Each washing step involved centrifugation at 5000 × g for 15 minutes at 22°C to remove the buffer. The washed cell pellets were weighed, and adjustments were made to ensure consistent mass across all experimental trials. The majority of RN4220 cell pellets were kept within 50-60 mg for these studies unless otherwise stated (Appendices E-I).

S. aureus RN4220 Growth After One Hour Incubation with Exogenous FmtA

Following the preparation of the cell culture, one bacterial pellet (≈ 50-60 mg) was resuspended in 1 ml of 50 mM sodium phosphate buffer (pH 7.2), while another pellet (≈ 50-60 mg) was resuspended in 1 ml of the designated concentration of FmtA, either 10 μM or 20 μM. The suspensions were incubated for 1 hour on a three-dimensional rotator at 22°C. After incubation, the samples were centrifuged at 10,200 RCF at 22°C for 10 minutes, and the supernatant, containing FmtA and D-Ala, was discarded. The resulting pellets were then resuspended in 1 ml of TSB and subsequently added to 49 ml of TSB. Following this, 2 ml from each of the two samples was used to inoculate 98 ml of TSB to achieve a 50-fold dilution. These samples were incubated at 37°C with shaking at 200 rpm. OD_{600} was measured for each culture every 40 minutes. Additionally, every 40 minutes, 5 μl of both 10^{-4} and 10^{-5} serial dilutions were plated onto Luria-Bertani agar (LB-Agar) plates and incubated at 37°C for 13 hours to determine the colony-forming units per milliliter (CFU/ml). The Luria-Bertani broth was purchased from Sigma-Aldrich and the agar was purchased from Fisher Bioreagents.

S. aureus RN4220 Growth in the Presence of Continuous FmtA Incubation

Upon completion of the bacterial cell preparation, the bacterial cell pellets (≈ 55mg) were resuspended in 1 ml TSB and subjected to a 50-fold dilution. This 50-fold dilution was further diluted by pipetting out a 2 ml aliquot and adding it to 98 ml of TSB media to create another 50-fold dilution. The final dilution factor was 2,500. Immediately following the dilution, 1 ml of 20 μM FmtA, yielding a final concentration of 0.2 μM, was added to one of the bacterial samples, while 1 ml of 50 mM sodium phosphate buffer (pH 7.2) was added to the second bacterial sample. The OD_{600} was measured and recorded at 40-minute intervals over a total duration of 240 minutes.

The concentration of FmtA was further elevated to assess the viability of *S. aureus* RN4220 over a continuous incubation period of 300 minutes using 20 μM FmtA. For this purpose, the cell culture was prepared as previously described, and after determining the mass of the bacteria accumulated (≈ 55 mg), the bacterial cells were resuspended in 1 ml of TSB and subjected to a subsequent 50-fold dilution in TSB. This diluted culture served as the bacterial stock, from which 3 μl was added to 110 μl of TSB in 96-well culture plates (SPL Life Sciences). The FmtA solution was introduced at the end to achieve a final FmtA concentration of 20 μM in the 96-well culture plate. Solutions containing 50 mM sodium phosphate buffer (pH 7.2) served as the control. OD_{600} was recorded every 40 minutes, and 5 μl aliquots of bacterial dilutions ranging from 10^{-3} to 10^{-5} were prepared and plated onto TSB-agar plates and incubated at 37°C for 13 hours, after which CFU/ml was determined for each time point.

FmtA Treated *S. aureus* RN4220 Cell Growth in the Presence of Lysozyme

The lysozyme enzyme (from chicken egg) was purchased from Sigma-Aldrich. Following the preparation of the bacterial cells, one of the bacterial pellets (≈ 56 mg) was resuspended in 1 mL of 20 μM FmtA solution, while another pellet (≈ 56 mg) was resuspended in 1 ml of 50 mM sodium phosphate buffer (pH 7.2). Both suspensions were incubated for 1 hour at 22°C on a three-dimensional rotator. After the incubation period, the suspensions were centrifuged at 10,200 RCF for 10 minutes at 22°C, and the supernatant was discarded. The pellets were subsequently resuspended in 1 ml of TSB broth, and each suspension was subjected to a 2,500-fold dilution in TSB. At the start of the reading, lysozyme was added to both cell cultures at a final concentration of 500 μg/ml to monitor initial changes. The bacterial suspensions were then incubated at 37°C with shaking at 170 rpm for a total duration of 360 minutes. OD_{600} was measured at 40-minute

intervals and concurrently, 5 µl aliquots of 10^{-4} and 10^{-5} dilutions were prepared and plated onto TSB agar plates at each time point. The plates were incubated at 37°C for 13 hours, and CFU/ml was calculated from the resulting colony counts.

FmtA Treated *S. aureus* RN4220 Cell Lysis in the Presence of Lysozyme

After the RN4220 cells were collected and weighed, one of the bacterial pellets (≈ 57 mg) was resuspended in 600 µl of 20 µM FmtA, and another pellet (≈ 57 mg) was resuspended in 600 µl of 50 mM sodium phosphate buffer (pH 7.2). The suspensions were incubated for 1 hour on a three-dimensional rotator at 22°C. Following the incubation, the samples were centrifuged at 10,200 RCF at 22°C for 10 minutes, and the supernatant was discarded. The cells were resuspended in 1 ml of 1× phosphate-buffered saline (PBS). The 1x PBS was created from a 10x stock purchased from BioShop Canada. A cell concentration of 2 mg/ml was prepared in 5 ml of 1× PBS for each suspension, and 193 µl of the 2 mg/ml bacterial concentration was transferred to the wells of a 96-well culture plate. Lysozyme at a concentration of 350 µg/ml was added at the 0-minute time point to both the control and the cell samples previously incubated with 20 µM FmtA, and measurements commenced. OD_{600} readings were taken every 40 minutes for a total duration of 240 minutes. Additionally, bacterial cultures were plated onto TSB-Agar plates after serial dilutions of 10^{-4} and 10^{-5}. The TSB-Agar plates were incubated at 37°C for 13 hours following the completion of the 240-minute lysis assay. CFU/ml was calculated from the colonies grown on the TSB-Agar plates for each time point.

FmtA Treated *S. aureus* RN4220 Cell Lysis in the Presence of Lysostaphin

The lysostaphin enzyme was purchased from Cedarlane Labs (Canada). Following the preparation of the bacterial cells, one bacterial pellet (≈ 57 mg) was resuspended in 600 µl of 20 µM FmtA, serving as the experimental variable, while another pellet (≈ 57 mg) was resuspended in 600 µl of 50 mM sodium phosphate buffer (pH 7.2), serving as the control variable. Both suspensions were incubated for 1 hour at 22°C on a three-dimensional rotator. After the incubation period, the suspensions were centrifuged at 10,200 RCF for 10 minutes at 22°C, and the supernatant was discarded. The cell pellets were resuspended in 1 ml of 50 mM Tris–HCl buffer (pH 7.5), followed by adjustment to a final concentration of 2 mg/ml in 5 ml of 50 mM Tris–HCl buffer (pH 7.5). The 50 mM Tris-HCl buffer was created from a Tris crystalline powder and HCl

solution both purchased from Fisher Scientific. Using the 2 mg/ml bacterial solutions, 200 µl was aliquoted into the wells of a 96-well culture plate. Lysostaphin was added to both the control and experimental samples at a final concentration of 0.25 µg/ml. The lysis of cells was monitored at 40-minute intervals over a total period of 240 minutes by measuring the OD_{600}, while the 96-well plate was incubated at 37°C with agitation at 200 rpm. Concurrently, bacterial colony growth was assessed by plating 5 µl of the diluted bacterial culture, after serial dilutions were performed ranging from 10^{-5} to undiluted, onto TSB-Agar plates at each time point. The plates were incubated at 37°C for 13 hours after which colony growth was enumerated to determine CFU/ml.

Determining Change in Antibiotic Susceptibility of FmtA Incubated *S. aureus* Strains

The SA 113 and SA 113 *Δfmta* strains were graciously provided by Friedrich Gotz (IMIT, Germany). The N315 strain was graciously provided by Vijay Pancholi (Ohio State). The MSSA 1112 strain was graciously provided by Guoqing Xia (IMIT, Germany). Lastly, the MU50 strain was obtained from the American Type Culture Collection (ATCC).

An overnight culture of MSSA or MRSA, incubated at 37°C with shaking at 200 rpm for 16 hours, was prepared. The SA 113 *Δfmta* culture was grown in 2.5 µg/ml erythromycin (Sigma-Aldrich) to ensure *Δfmta* mutant growth exclusively. A 1 mL aliquot of the overnight culture was inoculated into 99 mL of TSB and incubated at 37°C with agitation at 170 rpm until the OD_{600} reached 0.6 A.U. At this point, a 1 mL sample, corresponding to a concentration of 1.2 x 10^8 CFU/ml, was withdrawn and subjected to a 10-fold dilution in TSB to obtain a final concentration of 1.2 x 10^7 CFU/ml. The solution was kept on ice until ready to be used.

To the wells of a 96-well culture plate, 100 µl of TSB was first added, followed by 100 µl of an oxacillin solution, a β-lactam antibiotic, to the first well. Oxacillin was purchased from Cayman Chemical. Serial dilutions were performed by transferring 100 µl from the first well to the second well with subsequent wells receiving 100 µl of solution from the previous well. These dilutions reduced the concentration of oxacillin by half each time. For wells containing FmtA, a 43.5 µM stock solution of purified FmtA was used; thus, 92 µl of this stock was added to achieve a final concentration of 20 µM in a 200 µl final volume. The FmtA protein was filtered using Millipore Millex 0.2 µm PVDF membrane filters to ensure sterility. For the control, 92 µl of 50 mM sodium phosphate buffer (pH 7.2) was added instead of FmtA.

The final step consisted of adding 8 µl of the bacterial culture to each well, achieving a total volume of 200 µl per well and a final bacterial concentration of approximately 5 x 10^5 CFU/ml. The 96-well plates were incubated at 37°C for 22 hours. Please note, following the bacterial and FmtA (or buffer) solution additions, the antibiotic concentrations were further diluted. After the 22-hour incubation period, the wells were inspected visually for growth. Bacterial samples from the wells were extracted and plated onto TSB-Agar to further assess the presence of viable cells and determine the MIC.

Statistical Analysis

The statistical analysis performed for the data presented was a 2-way ANOVA test. The results were displayed as graphs constructed based on results from GraphPad Prism 10 software. A p value of <0.05 was considered as a significant difference.

Results

***S. aureus* RN4220 Growth After One Hour Incubation with Exogenous FmtA**

The removal of D-Ala from WTA by FmtA may result in distinct growth patterns when compared to cells retaining D-Ala. This study was conducted under optimal 37ºC nutrient-rich TSB growth conditions, with data from three independent trials involving *S. aureus* RN4220 incubated with and without 10 µM FmtA. The data was averaged and used to plot OD_{600} and CFU/ml graphs (Figure 8, 9). The same methodology was subsequently applied to analyze RN4220 growth following incubation with 20 µM FmtA (Figure 10, 11). The study utilizing 10 µM FmtA consisted of bacterial pellet weights with an average of 10 mg variance between trials. The study utilizing 20 µM FmtA consisted of bacterial pellet weights with an average of 14 mg variance between trials. The bacterial cells were treated with either 10 µM or 20 µM FmtA for 1 hour, after which FmtA was removed, and the cells were allowed to grow in TSB media, with LB-Agar plating performed at 40-minute intervals. The OD_{600} and CFU/ml values for each trial, along with the averages for the 10 and 20 µM FmtA incubations, are presented in the Appendix E (Table 5, Table 6).

As evidenced by the CFU/ml and the OD_{600} values for the 10 μM FmtA incubation, the growth kinetics of FmtA-treated RN4220 and non-treated cells did not exhibit significant differences (Figure 8, 9). Both cultures demonstrated exponential growth over a 360-minute interval, achieving peak values of approximately $8x10^8$ CFU/ml and 4.0 A.U. The overlapping standard deviation bars at nearly every time point on both the CFU/ml and OD_{600} graphs further substantiate the absence of significant variation in growth dynamics between the control and experimental groups following D-Ala removal. A comparable trend was observed when the FmtA concentration was increased to 20 μM. Comparison between the control and RN4220 cells pre-incubated with 20 μM FmtA again revealed exponential bacterial growth throughout the 360-minute period, with maximum values similarly reaching $8x10^8$ CFU/ml and 4.0 A.U. The overlapping standard deviation bars at all growth intervals suggest that the two conditions are not different (Figure 10, 11). Statistical analysis was performed for OD_{600} and CFU/ml data comparing both the 10 μM and 20 μM FmtA samples directly to the FmtA-absent samples for each time point. These analyses did not reveal a statistically significant difference in growth rates for FmtA-treated cultures. The findings conclude that the removal of D-Ala from the initial bacterial cultures did not impact cellular growth under optimal growth conditions, with no observable changes even during the early stages of growth.

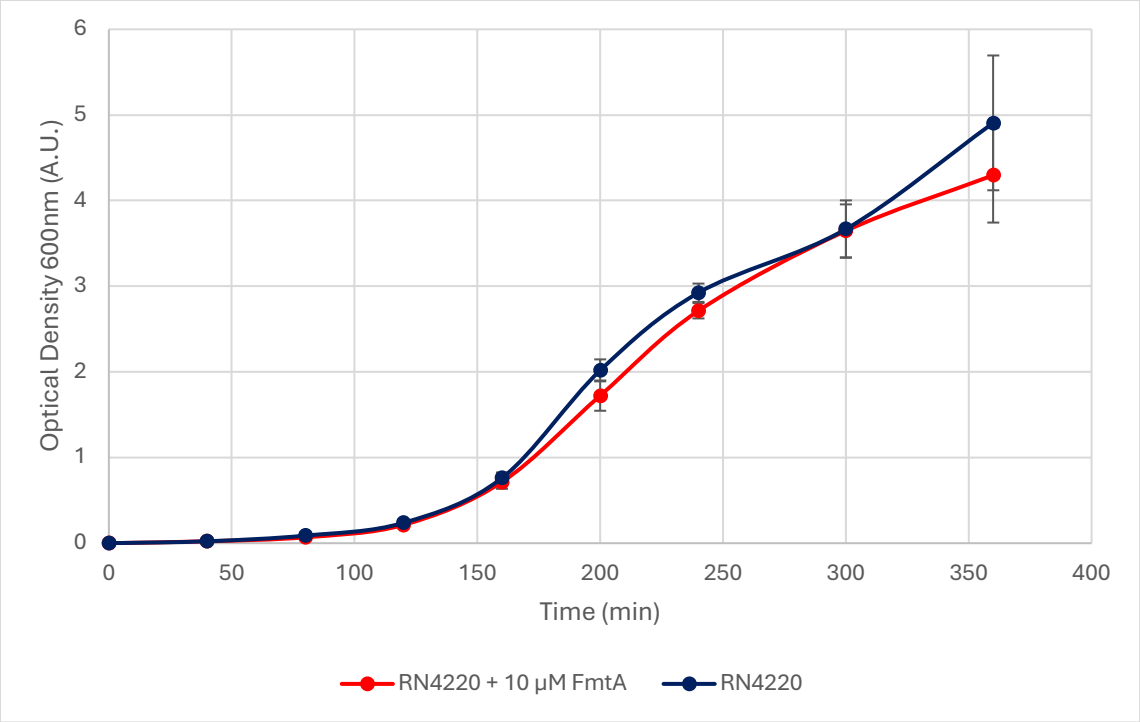

Figure 8. OD_{600} measurements for the growth cultures of *S. aureus* RN4220 following a 1-hour incubation with 10 µM FmtA compared to RN4220 cultures without D-Ala release. The RN4220 cells were washed and subjected to either FmtA or 50 mM sodium phosphate buffer (pH 7.2). Growth kinetics were monitored every 40 minutes over a 360-minute period in TSB media. The graph represents the mean values from three independent experimental trials, with ± standard deviation error bars calculated from these trials. A 2-way ANOVA test was performed for statistical analysis using GraphPad Prism 10.

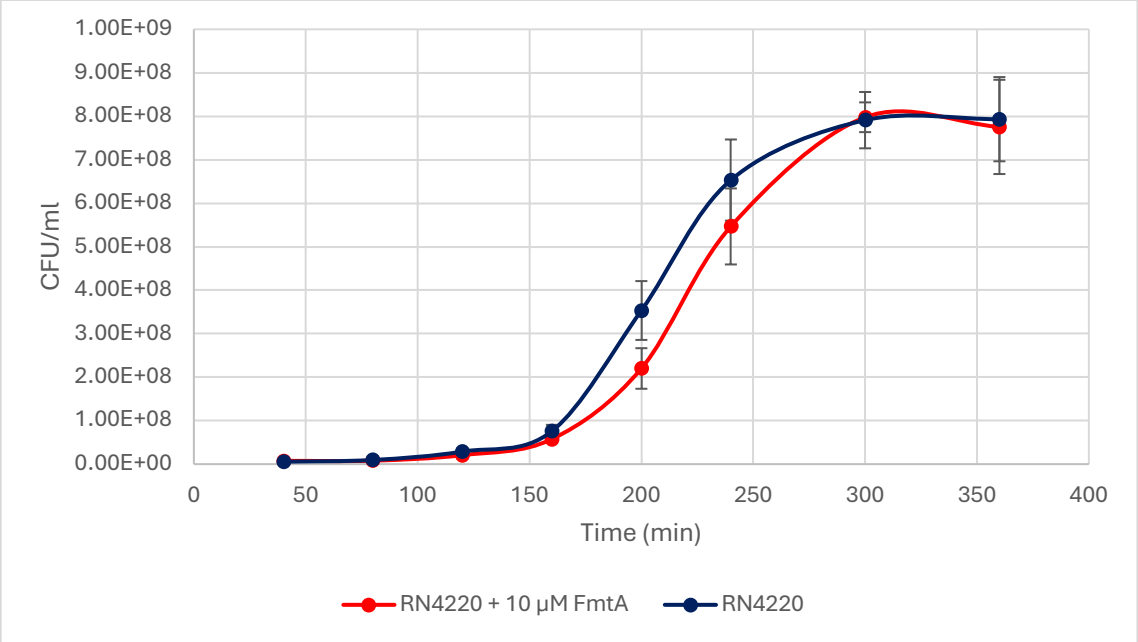

Figure 9. Graphical representation of CFU/ml of RN4220 cells grown on LB-Agar plates following a 1-hour incubation with and without 10 µM FmtA. The RN4220 cells were washed and incubated with either FmtA or 50 mM sodium phosphate buffer (pH 7.2). Growth was monitored every 40 minutes, and 5 µl of either a 10^{-4} or 10^{-5} dilution was plated in triplicates to obtain a more precise average of colony formation for each time point. Plates were incubated at 37°C for 13 hours to allow for colony development. The graph illustrates the average results from three independent trials, with ± standard deviation error bars calculated from these trials. A 2-way ANOVA test was performed for statistical analysis using GraphPad Prism 10.

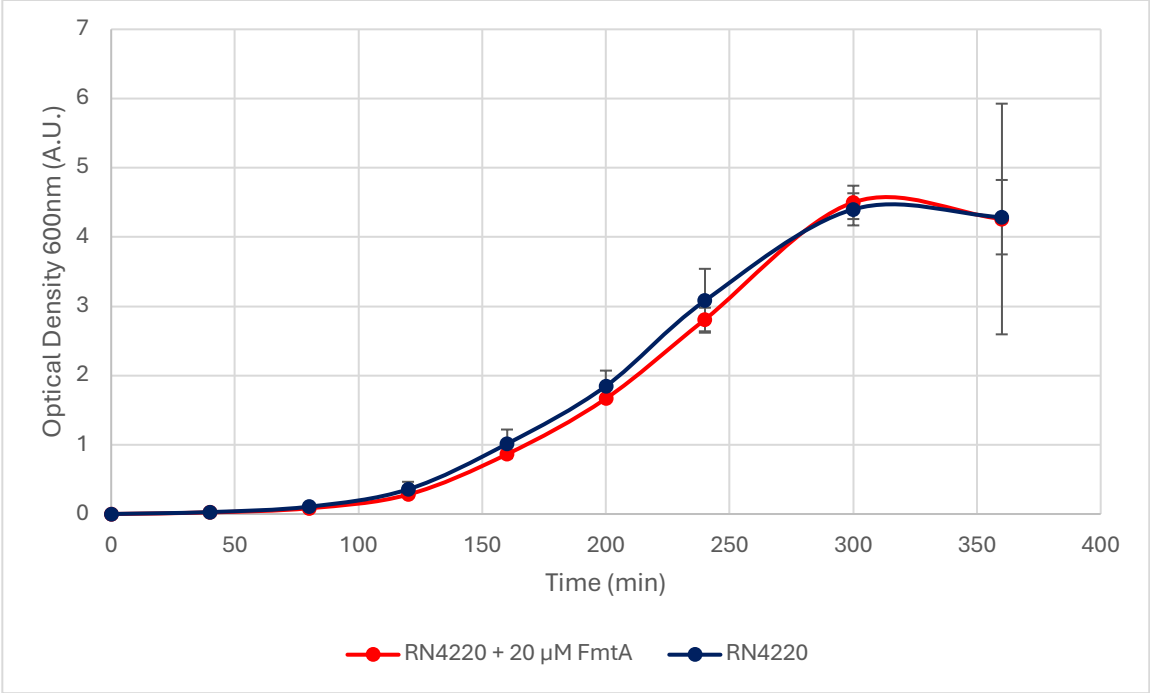

Figure 10. OD_{600} measurements for the growth cultures of *S. aureus* RN4220 following a 1-hour incubation with 20 µM FmtA compared to RN4220 cultures without D-Ala release. The RN4220 cells were washed and subjected to either FmtA or 50 mM sodium phosphate buffer (pH 7.2). Growth kinetics were monitored every 40 minutes over a 360-minute period in TSB media. The graph represents the mean values from three independent experimental trials, with ± standard deviation error bars calculated from these trials. A 2-way ANOVA test was performed for statistical analysis using GraphPad Prism 10.

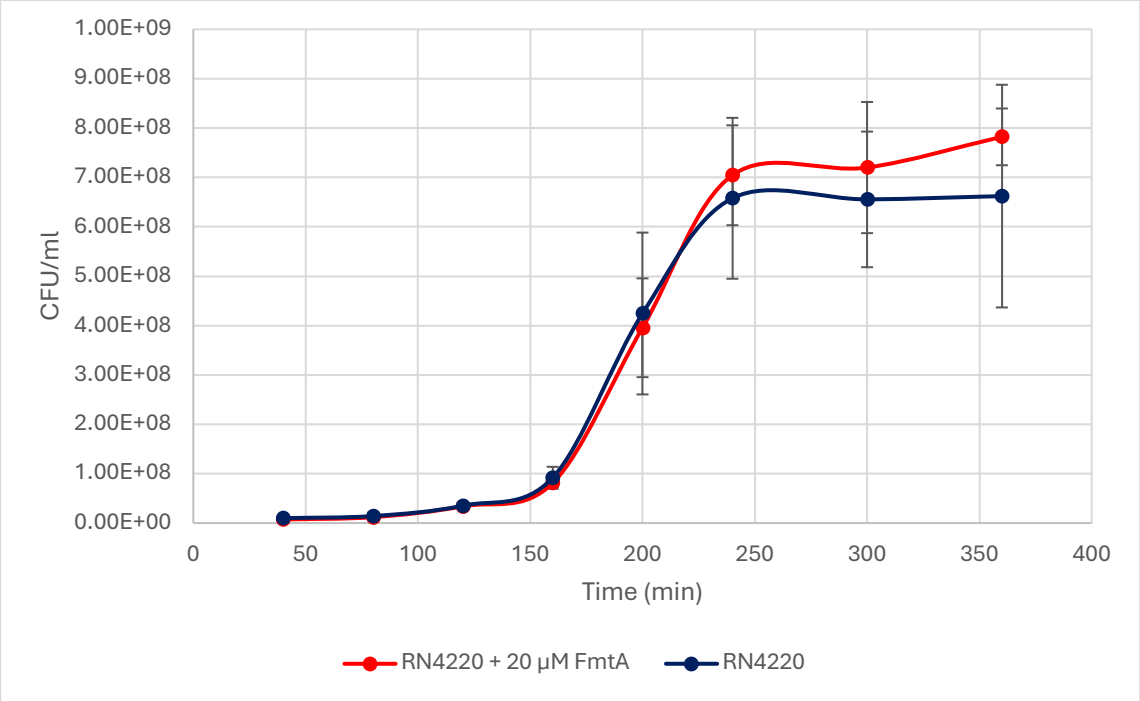

Figure 11. Graphical representation of CFU/ml of RN4220 cells grown on LB-Agar plates following a 1-hour incubation with and without 20 µM FmtA. The RN4220 cells were washed and incubated with either FmtA or 50 mM sodium phosphate buffer (pH 7.2). Growth was monitored every 40 minutes, and 5 µl of either a 10^{-4} or 10^{-5} dilution was plated in triplicates to obtain a more precise average of colony formation for each time point. Plates were incubated at 37°C for 13 hours to allow for colony development. The graph illustrates the average results from three independent trials, with ± standard deviation error bars calculated from these trials. A 2-way ANOVA test was performed for statistical analysis using GraphPad Prism 10.

S. aureus RN4220 Growth in the Presence of Continuous FmtA Incubation

In the previous section, RN4220 cells were incubated with 10 µM or 20 µM exogenous FmtA for 1 hour to facilitate the hydrolysis of the bond between D-Ala and WTA. Following this incubation, FmtA was removed, and the cells were allowed to multiply in TSB. Based on the results recorded from this section, a hypothesis was formulated suggesting that the absence of growth differences between cells with and without D-Ala might be attributed to the fact that only the initial parental cells experienced D-Ala removal, while the newly formed daughter cells retained normal D-Ala levels, leading to growth patterns comparable to the control. This hypothesis suggests that a more optimized way to investigate the potential difference in RN4220 cell growth without D-Ala would be to subject the culture to continuous FmtA incubation.

The change performed for this growth analysis was that 1 ml of 20 µM FmtA was added directly to the experimental cultures resulting in a final concentration of 0.2 µM FmtA. Figure 12

illustrates the average growth of the cell cultures, as determined by OD_{600} absorbance values. The data indicate no significant difference in growth between cells maintained with a constant 0.2 μM FmtA and those without FmtA. Both cultures exhibited exponential growth over a 240-minute period, with measurements taken every 40 minutes. The growth was near identical for the two variables. These findings suggest that exogenous FmtA concentrations of 0.2 μM or lower, which facilitate D-Ala removal from RN4220, do not affect the growth rate of RN4220 cells under environmentally favourable conditions.

An FmtA concentration of 0.2 μM may have been insufficient to elicit observable alterations in the growth patterns of RN4220. Consequently, the FmtA concentration was increased tenfold, with the cells now being cultured in the presence of 20 μM FmtA. The growth of RN4220 was monitored every 40 minutes via OD_{600} measurements. Additionally, colony growth characteristics were assessed at each time point by plating aliquots of the bacterial culture onto TSB-Agar plates. As depicted in Figure 13, the OD_{600} measurements suggest a potential difference in the growth characteristics between cells incubated with 20 μM FmtA and those without. The FmtA-incubated culture exhibited higher OD_{600} values at each time point throughout the experiment and both the FmtA-absent and the FmtA-incubated culture demonstrated exponential growth. This indicated that the culture with D-Ala removed had a faster growth rate than the cells retaining original levels of D-Ala attached to their WTAs. However, this pattern was not observed in the CFU/ml data (Figure 14, Figure 32). Plating the cultures on TSB-Agar plates at each time point revealed no difference in the total number of colonies between the FmtA-containing culture and the control culture. This finding, in contrast to the OD_{600} data, suggested that RN4220 cells devoid of D-Ala grew at a rate comparable to those with original levels of D-Ala. Given that the CFU/ml assay provides a more accurate representation of the total number of viable cells in a sample, this data was deemed more reliable than the OD_{600} measurements for assessing the growth rate of RN4220 cells with D-Ala removal. Therefore, it became apparent that at FmtA concentrations as high as 20 μM, the growth rate of RN4220 *S. aureus* remained similar to that of the control. This study was repeated twice to ensure reproducibility of the results, with the second trial yielding similar findings, again showing no discernable change in CFU/ml at each time point (Figure 31 and Figure 32 in Appendix F). Table 7 and 8 in the Appendix F provide the data for all three replicates in trial 1, including ± standard deviations and bacterial pellet weights.

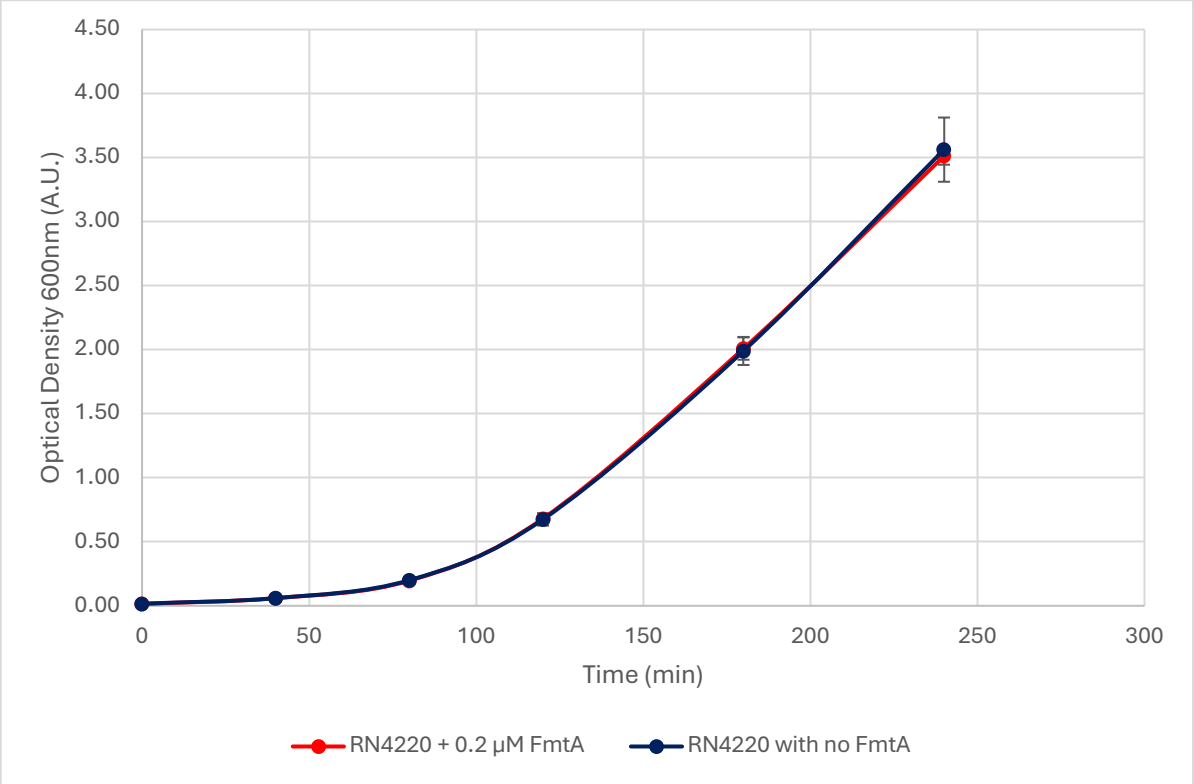

Figure 12. The average OD_{600} of an experimental RN4220 bacterial culture containing 0.2 µM FmtA compared to a control culture without FmtA incubation for the entirety of growth. Both cultures exhibited exponential growth over a 240-minute period. The plotted values represent the average results from three independent trials.

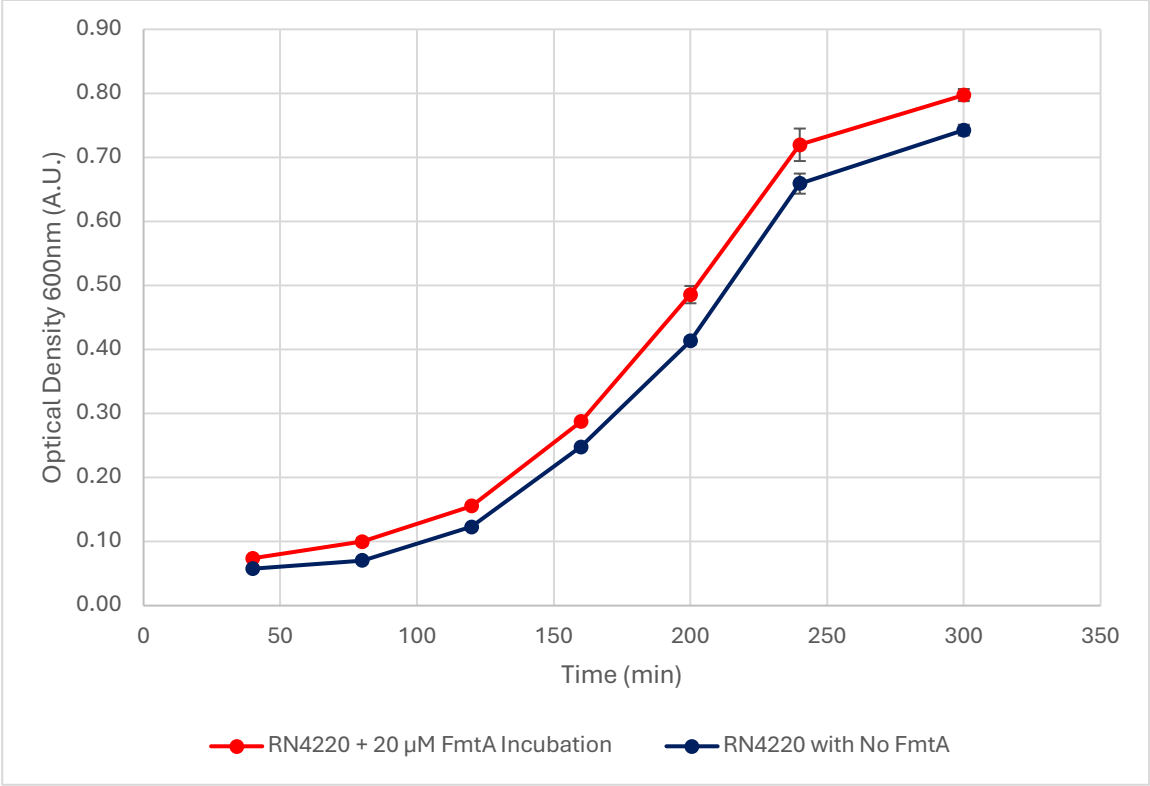

Figure 13. The mean OD_{600} values of RN4220 bacterial cultures incubated with 20 µM FmtA compared to control cultures without FmtA for the entirety of growth. Following an initial wash with 50 mM sodium phosphate buffer (pH 7.2), the cells were resuspended in TSB medium. Absorbance measurements were recorded every 40 minutes, with both cultures displaying exponential growth over a 300-minute period at 37°C. The plotted values represent the average results from a single trial (three replicates of the same trial), with ± standard deviation error bars calculated from these replicates.

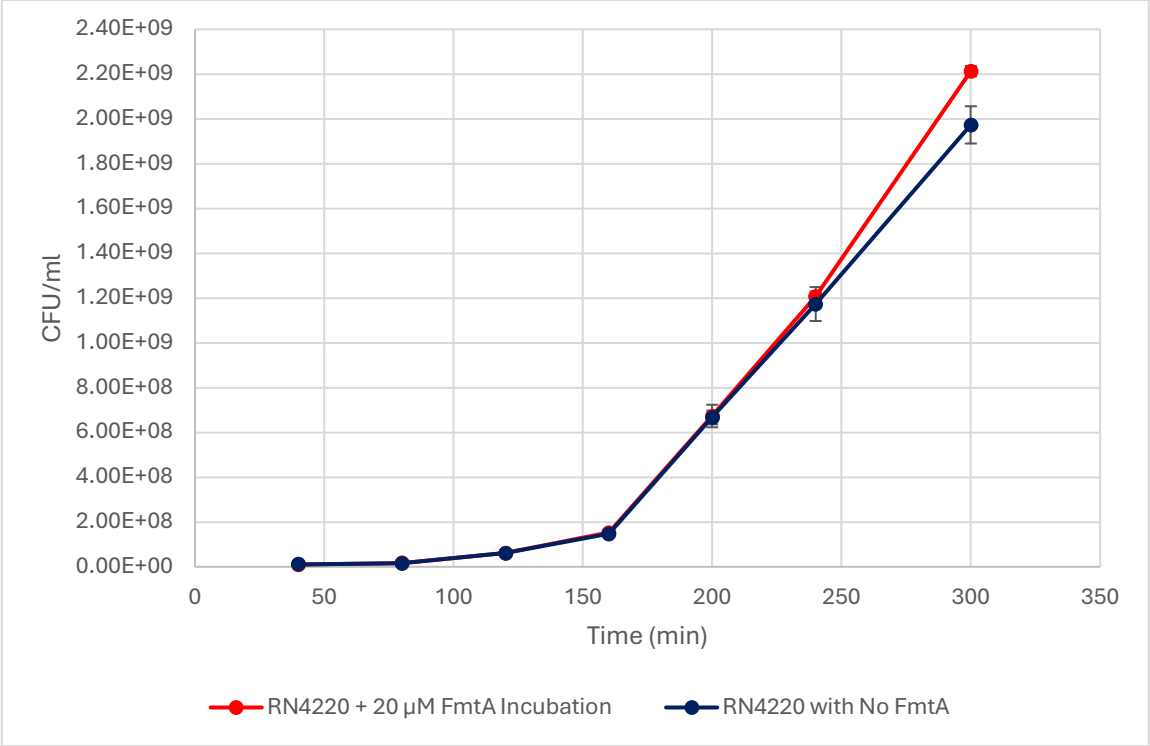

Figure 14. Average CFU/ml of RN4220 cells plated onto TSB-Agar plates at 40-minute intervals over a 300-minute period from bacterial cultures incubated with or without 20 µM FmtA at 37°C. The cells were initially washed with 50 mM sodium phosphate buffer (pH 7.2) and resuspended in TSB medium. Aliquots of 5 µl from dilutions ranging from 10^{-3} to 10^{-5} were plated in triplicate to obtain a precise average of colony formation at each time point. Plates were incubated at 37°C for 13 hours to facilitate colony development. The graph presents the mean results from a single trial (three separate colony formations of the same trial), with ± standard deviation error bars calculated from these three replicates for each time point.

FmtA Incubated *S. aureus* RN4220 Cell Growth in the Presence of Lysozyme

Figure 15 presents the mean OD_{600} data for both experimental, cells incubated with FmtA to hydrolyze the bond between D-Ala and WTA, and control, FmtA-absent, *S. aureus* RN4220 cell cultures. The OD_{600} measurements indicate that both experimental and control cells exhibited exponential growth over time in TSB media supplemented with 500 µg/ml lysozyme. Notably, the difference in growth between cells with D-Ala released and the control cells was not discernable, as both demonstrated similar growth trajectories. The standard deviation error bars also overlap for each time point providing further reason to conclude that the growth patterns did not change. This observation is corroborated by the data in Figure 16, which shows the average CFU/ml for both experimental and control cells at each measured time point. Colony growth data indicated the viability of *S. aureus* under lysozyme incubation over increasing induction periods. The number

of colonies formed by the experimental and control groups did not show a significant difference in growth patterns. A 2-way ANOVA statistical analysis was run on both the OD_{600} and CFU/ml data indicating nonsignificant alterations in growth for each time point. Consequently, in the presence of 500 µg/ml lysozyme, the enzymatic removal of D-Ala by exogenous FmtA did not significantly alter the growth rate of strain RN4220. Detailed raw data, including bacterial pellet weights and ± standard deviations for all trials, is provided in Table 9 and 10 in the Appendix G.

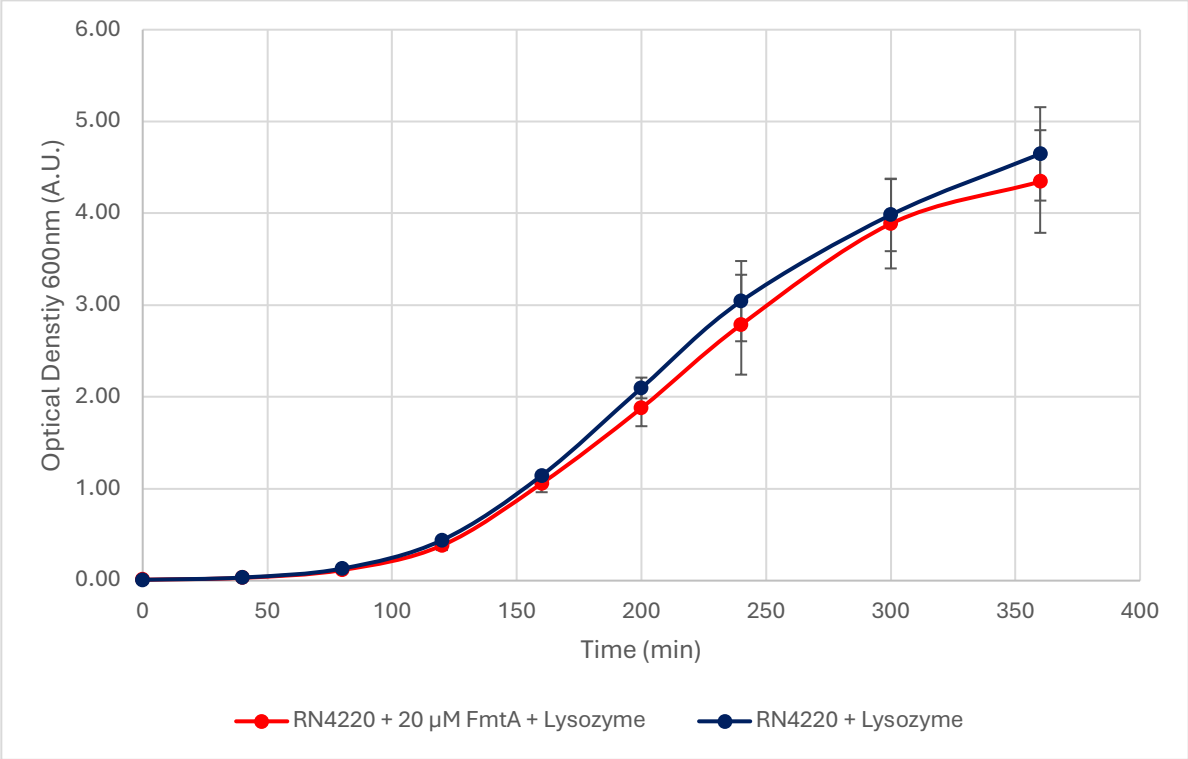

Figure 15. Mean optical density at 600 nm for *S. aureus* RN4220 cells, incubated either with or without 20 µM FmtA prior to growth in the presence of 500 µg/ml lysozyme in TSB. Measurements were recorded every 40 minutes over a period of 360 minutes. The plotted values represent the average of three independent trials, each conducted with identical bacterial pellet weights. A 2-way ANOVA test was performed for statistical analysis using GraphPad Prism 10.

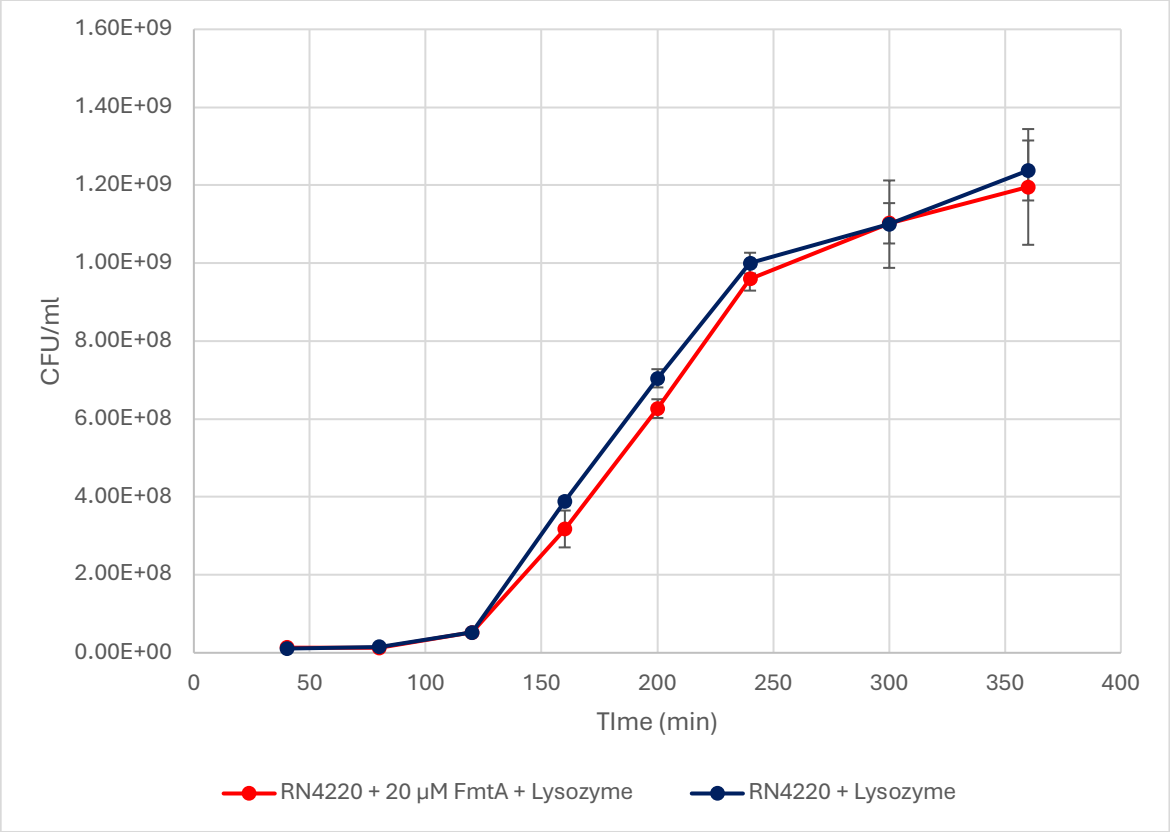

Figure 16. Mean CFU/ml for *S. aureus* RN4220 cells, incubated either with or without 20 µM FmtA prior to growth in the presence of 500 µg/ml lysozyme in TSB. Bacterial suspensions were diluted 10,000-fold and 100,000-fold at 40-minute intervals over a total duration of 360 minutes and subsequently plated on TSB-Agar plates in triplicates. The plates were incubated at 37°C for 13 hours, after which colony counts were performed. The plotted values represent the average of three independent trials, each conducted with identical bacterial pellet weights. Both cultures demonstrated exponential growth. A 2-way ANOVA test was performed for statistical analysis using GraphPad Prism 10.

FmtA Incubated *S. aureus* RN4220 Cell Lysis in the Presence of Lysozyme

In Figures 15 and 16, the data indicated that cellular growth of FmtA-treated RN4220, in the presence of 500 µg/ml lysozyme, was not affected; it exhibited a comparable growth rate to non-treated RN4220. Although the growth rate remained unaffected, it was hypothesized that an optimized approach to investigate lysozyme's mechanism of action on RN4220 viability, when co-incubated with FmtA, was to perform a lysis assay (Figure 17, Figure 18). The RN4220 cells were initially suspended in either 20 µM FmtA or 50 mM sodium phosphate buffer (pH 7.2), followed by collection and resuspension in 1x PBS to prohibit potential growth in nutrient-rich media. Cell

culture viability was assessed through OD_{600} measurements and bacterial colony enumeration on TSB-Agar plates.

The mean values from three independent trials for the OD_{600} and CFU/ml were calculated and graphically represented in Figures 17 and 18 respectively. When comparing these data with the lysis of RN4220 in the presence of lysostaphin (Figure 20), it was observed that 350 µg/ml lysozyme was not as effective in lysing the cells. The initial OD_{600} value was approximately 0.4 A.U., which only decreased by 0.1-0.2 A.U. after a full 240 minutes. Although this indicated that some lysis occurred, a remaining OD_{600} reading exceeding 0.2 A.U. suggested a substantial number of viable bacterial cells persisted. Notably, the culture exposed to FmtA lysed at a rate similar to the culture without FmtA exposure. This was evident as both cultures started with comparable OD_{600} values and concluded with nearly the same OD_{600} value of 0.2 A.U. Standard deviation error bars were also overlapping for both cultures at each time point signifying no alteration in lysis patterns.

The CFU/ml data further clarified the lytic potential of lysozyme on RN4220 cells. The results suggested that the efficacy of lysozyme in lysing RN4220 cells was minimal, evidenced by an initial decline in viable cell counts from the 0-minute to the 40-minute time point. However, post the initial 40 minutes, no further lysis was observed, indicated by a plateau in colony formation. Comparative analysis between the FmtA-incubated culture and the non-FmtA-incubated culture revealed no difference in the number of colony-forming units. Both cultures exhibited consistent and comparable colony growth over the 240-minute duration, culminating in approximately 8.1-8.2 x 10^7 CFU/ml. These findings imply that the removal of D-Ala does not affect lysozyme's ability to reach its target, as cells with D-Ala removal exhibited survival rates similar to those without D-Ala removal by FmtA. The raw data for each trial, indicating OD_{600} measurements, CFU/ml calculations, and bacterial cell pellet weights, is reported in the Appendix H (Table 11 and 12).

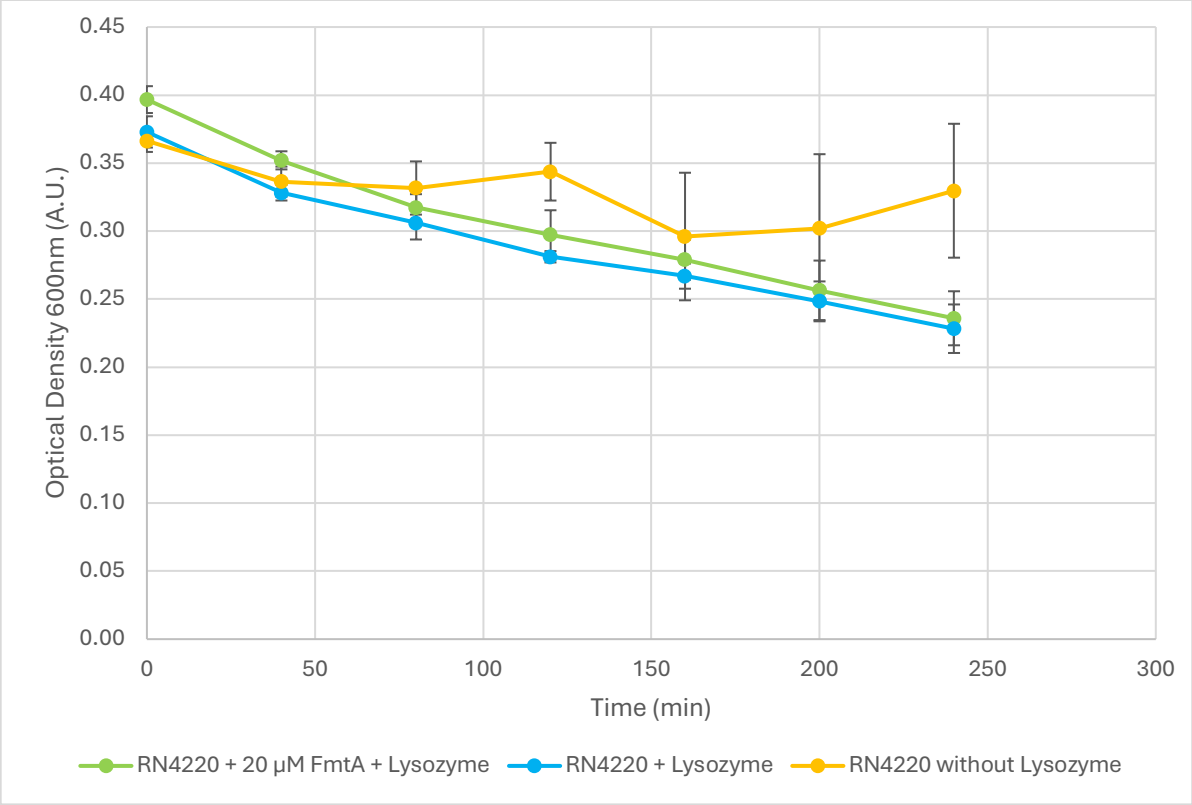

Figure 17. The mean OD_{600} of *S. aureus* RN4220 cell cultures in the presence of 350 µg/ml lysozyme, with and without prior incubation with 20 µM FmtA. The cells were initially washed with 50 mM sodium phosphate buffer (pH 7.2) and subsequently resuspended in nutrient-deficient 1x PBS buffer to facilitate accurate lysis observation. Absorbance readings were recorded at 40-minute intervals over a total duration of 240 minutes. The mean OD_{600} values represent data from three independent trials, each conducted with normalized bacterial pellet weights. An RN4220 control devoid of lysozyme was also incorporated as a standard to elucidate the presence or absence of cellular lysis.

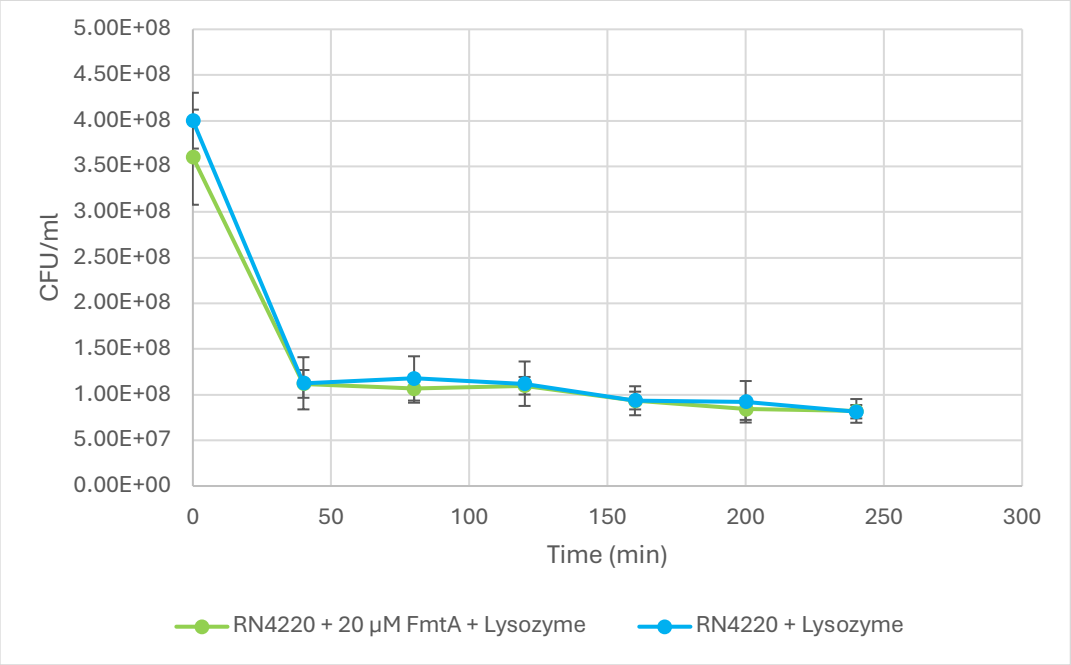

Figure 18. The mean CFU/ml of *S. aureus* RN4220 cell cultures exposed to 350 µg/ml lysozyme following pre-incubation with 20 µM FmtA, compared to cultures without FmtA pre-incubation. Prior to lysis observation, cells were washed with 50 mM sodium phosphate buffer (pH 7.2) and resuspended in nutrient-deficient 1x PBS buffer. A 5 µl aliquot of each bacterial culture was plated in triplicate on TSB-Agar every 40 minutes over a period of 240 minutes. Plates were then incubated at 37°C for 13 hours to facilitate colony growth, followed by enumeration of colonies at each time point. The reported mean values are derived from three independent experimental trials, with bacterial pellet weights normalized for each.

FmtA Incubated *S. aureus* RN4220 Cell Lysis in the Presence of Lysostaphin

Figure 19 illustrates the differences in the mean OD_{600} values across three independent trials, comparing *S. aureus* cells incubated with FmtA and 0.25 µg/ml lysostaphin (experimental variable), control cells without prior FmtA incubation, and a secondary control deficient of both lysostaphin and FmtA incubation. Figure 20 displays the average CFU/ml for all three trials, contrasting *S. aureus* cells incubated with FmtA and lysostaphin against control cells without prior FmtA incubation. Tables 13 and 14 in Appendix I present the raw data, including bacterial pellet weights and ± standard deviations for the OD_{600} values, as well as the CFU/ml for the three independent trials of both the experimental and control variables.

The OD_{600} results for both the control and FmtA incubated cultures demonstrated a similar lysis trend, with both starting at the same OD_{600} and reaching a constant, near-background level OD_{600} after approximately 100 minutes. This data indicated no significant difference based on the

pattern of RN4220 lysis in the presence of lysostaphin, regardless of D-Ala removal. The graph depicted a plateau in the lysis following the 120-minute time point at OD_{600} of 0.05 A.U. This plateau may have resulted from the possibility that the spectrophotometer is limited in its measurement capabilities, with changes below 0.05 A.U. being too low for the machine to detect. The secondary control, which lacked lysostaphin, exhibited no growth or lysis, maintaining a steady OD_{600}. This control differed from the FmtA-treated cells with lysostaphin, and from the control with lysostaphin incubation (Figure 19).

Colony growth observations revealed that the control variable produced more colonies than the experimental condition with prior FmtA incubation across all time points, except at the 0-minute time where no lysostaphin was added (Figure 20). To highlight the most significant differences observed, at the 80-minute time point, there was an approximately 6-fold reduction in CFU/ml for the cells incubated with FmtA compared to the control cells. Notably, at the 160-minute time point, the greatest variance was observed, with a 40-fold decrease in CFU/ml for the cells incubated with FmtA relative to the control. At the conclusion of the experiment, the 240-minute time point exhibited a 6.5-fold reduction in CFU/ml for the FmtA-incubated cells compared to the control (Figure 20). Therefore, the CFU/ml experiment concluded that D-Ala removal impacted RN4220 susceptibility to lysostaphin. The removal of D-Ala from the WTA led to fewer viable cells, resulting in increased cell lysis, and therefore, fewer colonies were developed. The OD_{600} and CFU/ml values were used to perform a 2-way ANOVA statistical analysis test. While the OD_{600} values did not display any statistical significance between lysis rates, the CFU/ml depicted statistical significance for two time points: the 40-minute and 200-minute. This confirmed that FmtA-treated RN4220 had statistical variance in lysis rates compared to non-FmtA treated cells in the presence of lysostaphin. As a negative control for the CFU/ml experiments, colony growth was tested without lysostaphin incubation or D-Ala removal at each time point to ensure colony numbers remained stable in 50 mM Tris-HCl (Figure 33 in the Appendix I). The total colony count for this control remained within $1.6x10^8$-$2.0x10^8$ CFU/ml across all time points, indicating no lysis or growth.

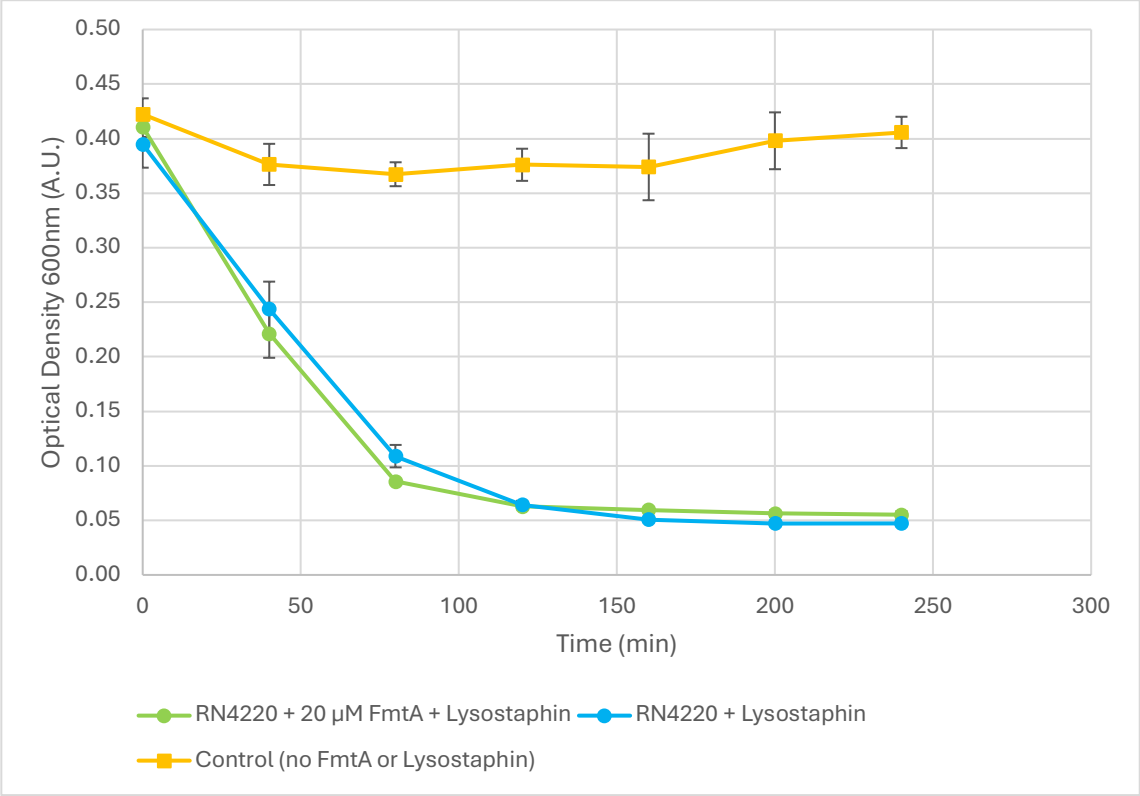

Figure 19. The mean OD_{600} for the lysis of RN4220 cells incubated with or without 20 µM FmtA. Lysis was induced by incubating both cultures in Tris–HCl buffer (pH 7.5) with 0.25 µg/ml lysostaphin and measured for a total of 240 minutes. The data shows a decrease in OD_{600} until 100-150 minutes, after which the values plateau. A secondary control was included, lacking both prior FmtA incubation and lysostaphin treatment over time. The secondary control (yellow), without lysostaphin and FmtA, exhibited no lysis or growth compared to the other two conditions. Lysis was conducted at 37°C and 200 rpm. The plotted values represent the average of three independent trials, each with consistent bacterial pellet weights. A 2-way ANOVA test was performed for statistical analysis using GraphPad Prism 10.

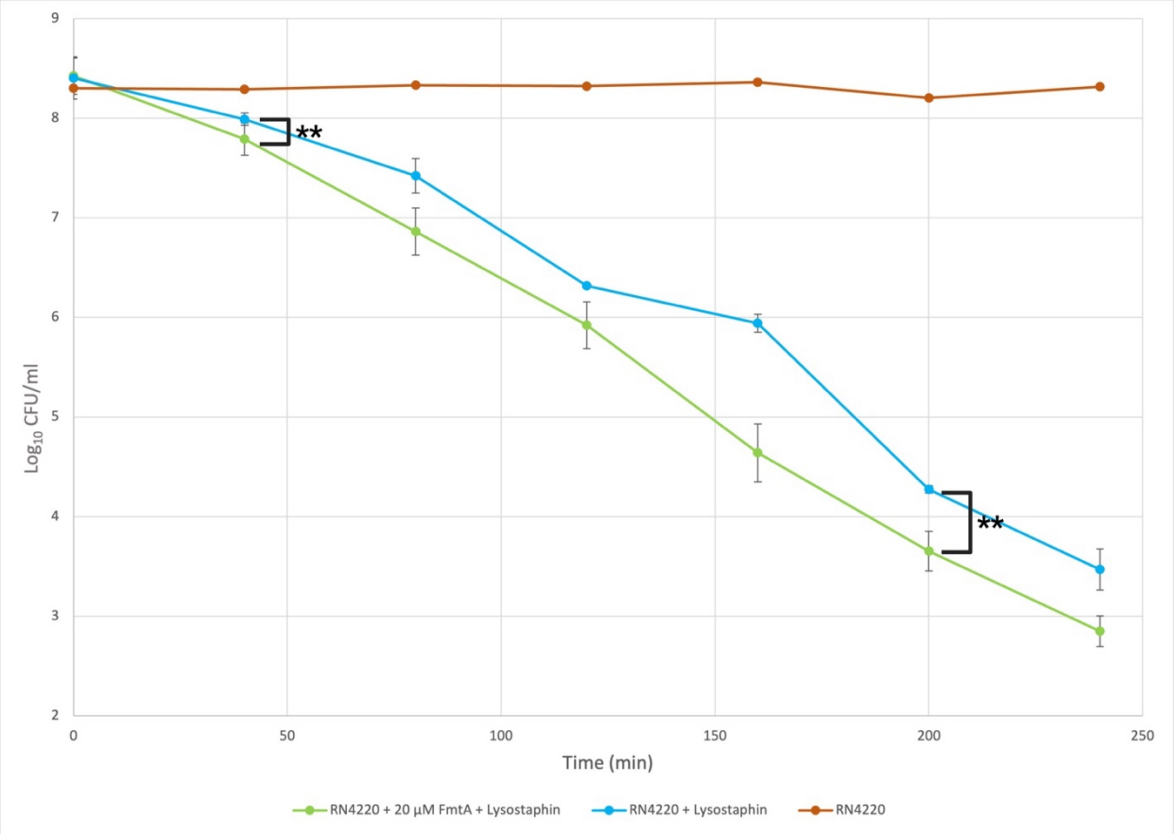

Figure 20. The average $\log_{10}$ CFU/ml of RN4220 cells incubated with 20 µM FmtA compared to RN4220 cells without prior FmtA incubation. Both cultures were subjected to lysis with 0.25 µg/ml lysostaphin in Tris–HCl buffer (pH 7.5) over a 240-minute period. A negative control was included comprising of RN4220 in Tris-HCl (pH 7.5) without FmtA or lysostaphin. Colony growth was assessed every 40 minutes by plating 5 µl of bacterial culture on TSB-Agar plates in triplicates, followed by incubation at 37°C for 13 hours. Colony counts were performed after. The plotted values represent the average of three independent trials, each with consistent bacterial pellet weights. A 2-way ANOVA test was performed for statistical analysis using GraphPad Prism 10 (*$p<0.05$, **$p<0.01$).

Determining Change in Antibiotic Susceptibility of FmtA incubated *S. aureus* strains

MIC broth microdilution assays are an effective method for assessing the antibiotic susceptibility of bacterial organisms. Our study was designed to evaluate whether the removal of D-Ala can impact the susceptibility of various clinical *S. aureus* methicillin-susceptible strains, such as MSSA 1112, SA 113, and SA 113 *ΔfmtA*, or methicillin-resistant strains, such as N315 and MU50, when exposed to oxacillin, a β-lactam antibiotic. Bacterial growth was assessed by visually inspecting the 96-well plates for depositions at the bottom of the wells and/or turbidity. Additionally, to further confirm bacterial viability in the presence of varying oxacillin

concentrations, cultures were removed and plated on TSB-Agar plates, and colony formation was observed after incubation.

As illustrated in Table 4, the MIC of oxacillin for both MSSA 1112 and SA 113 was established at 0.125 μg/ml in the absence of FmtA incubation. Upon the addition of 20 μM exogenous FmtA, the oxacillin MIC increased to 0.25 μg/ml, suggesting that the removal of D-Ala from WTA enhanced bacterial survival in the presence of oxacillin and FmtA. Figure 21 and Figure 22 display the 96-well plates for SA 113 and MSSA 1112 respectively. For control cultures without FmtA, both plates depicted clear bacterial growth and turbidity in solutions containing oxacillin concentrations lower than 0.125 μg/ml. At 0.125 μg/ml, the solutions were clear. However, with the addition of 20 μM FmtA, the wells containing 0.125 μg/ml oxacillin depicted bacterial growth at the bottom, which appeared to cease in wells containing 0.25 μg/ml oxacillin. Colony formation on TSB-Agar plates further confirmed the MIC of both strains as no growth was observed at 0.125 μg/ml oxacillin in solutions devoid of FmtA, while solutions containing FmtA ceased colony growth at 0.25 μg/ml oxacillin (Figure 34 and Figure 35 in Appendix J).

The same MIC assay was conducted with a mutant strain of SA 113, wherein the gene encoding FmtA was deleted. Consequently, this strain possessed a larger number of D-Ala on WTAs when compared to the wildtype SA 113. Figure 23 displays the growth of SA 113 *ΔfmtA* in the presence and absence of exogenous FmtA. Both FmtA-treated and non-FmtA treated cultures were able to grow at 0.125 μg/ml oxacillin as evident by the bacterial deposition at the bottom of the wells. At 0.25 μg/ml and 0.5 μg/ml oxacillin, the solutions appeared to have no growth inside of the wells. However, the colony formations on TSB-Agar plates confirmed that the SA 113 *ΔfmtA* strain remained viable at 0.25 μg/ml oxacillin as colonies were present for both FmtA-treated and non-FmtA treated cultures. At 0.5 μg/ml oxacillin, no colony formation was detected (Figure 36 in Appendix J). Therefore, we concluded that the oxacillin MIC for SA 113 *ΔfmtA* was 0.5 μg/ml for both FmtA-treated and non-FmtA treated samples (Table 4). When compared to the non-FmtA treated samples of the SA 113 wildtype, an MIC of 0.5 μg/ml oxacillin corresponded to a 4-fold increase in resistance to oxacillin over the wildtype strain. It was visually apparent from the agar plates containing colony growth from 0.5 μg/ml oxacillin cultures (Figure 36) that SA 113 *ΔfmtA* incubated with FmtA exhibited susceptibility characteristics similar to the control cultures, as there was no observed change in the oxacillin MIC.

In contrast to the MSSA data, the oxacillin MIC for the MRSA N315 strain decreased significantly following FmtA incubation. FmtA-absent cultures depicted an MIC of 8 μg/ml oxacillin, which was reduced to 2 μg/ml oxacillin following the addition of FmtA. Hence, the data indicates a 4-fold reduction in oxacillin resistance (Table 4). Upon observation of the wells in Figure 24, FmtA-absent cultures showed evidence of growth at oxacillin concentrations ranging between 0.25 – 2 μg/ml. Furthermore, the FmtA-absent solutions appeared to be clear inside of the 4 and 8 μg/ml oxacillin-containing wells. However, although no visible growth was seen at these concentrations in the wells, colony growth confirmed that N315 was indeed viable at 4 μg/ml oxacillin, as over 30 colonies were observed on the agar plate, and did not survive at 8 μg/ml oxacillin (Figure 37 in Appendix J). Conversely, FmtA-treated cultures did not depict growth at 2 μg/ml oxacillin in the wells, with only three small depositions appearing at 1 μg/ml oxacillin. This was indeed confirmed by colony formation on TSB-Agar plates, as FmtA-treated N315 cells were not able to survive at an oxacillin concentration of 2 μg/ml. The data suggests that the removal of D-Ala from WTA compromises the viability of MRSA in the presence of oxacillin.

The second MRSA strain, MU50, exhibited the highest resistance to oxacillin among all tested strains (Figure 25). Considering the colony formations of MU50 on TSB-Agar plates (Figure 38 in Appendix J), along with the results from the 96-well plates (Figure 25), MU50 was determined to possess an oxacillin MIC of 512 μg/ml whether FmtA was present in solution or not (Table 4). Both FmtA-treated and non-FmtA treated cultures depicted growth at the bottom of the 96-well plate ranging from 32 – 128 μg/ml oxacillin. At 256 μg/ml oxacillin, only FmtA-treated cells appeared to show growth, while at 512 μg/ml oxacillin, both cultures appeared to be clear. Colony formations provided further insight into the survivability of these cultures after an aliquot was extracted from the wells and plated. For both FmtA-treated and non-FmtA treated cultures, MU50 was not able to survive at an oxacillin concentration of 512 μg/ml. Although non-FmtA treated cultures grew at 256 μg/ml oxacillin on the agar plates, the growth of the colonies was smaller than those of the FmtA-treated culture. This was repeated and a similar observation was recorded. The viability of the highly resistant MU50 strain appears unaffected by the removal of D-Ala from WTA.

Analysis of the data from the 96-well plates containing the various strains revealed that the wells containing FmtA exhibited solution turbidity at every oxacillin concentration. A notable issue that was encountered was that, even after FmtA filtration using a Millipore PVDF membrane

protein filter, the negative control containing only FmtA and TSB (NC) displayed turbidity, while the negative control without FmtA did not. To verify the accuracy of growth observations in the 96-well plates and establish the purity of FmtA, solutions from several wells, including the NC, were plated on TSB-Agar plates (Figure 34-38 in Appendix J). The absence of growth on the TSB-Agar plates cultured with the NC confirmed the purity of FmtA, indicating no contamination. The increased turbidity observed in the FmtA-containing wells was credited to the presence of FmtA aggregation rather than bacterial growth.

Table 4. MIC of MSSA and MRSA strains of *S. aureus* with and without incubation with exogenous FmtA in the presence of oxacillin. Cells were exposed to varying concentrations of oxacillin to establish the minimum concentration required to inhibit bacterial growth, both with and without the addition of exogenous FmtA. Cultures were incubated for 22 hours at 37°C, starting with an initial inoculum of approximately $5x10^5$ CFU/ml. Growth determination was based on absorbance readings at 600 nm, visual inspection of wells, and subsequent culture on TSB-Agar plates followed by incubation at 37°C for 16 hours. The MIC is defined as the lowest concentration of oxacillin that resulted in no observable growth.

Strain	MIC with Oxacillin (-) FmtA Incubation (µg/ml)	MIC with Oxacillin (+) 20µM FmtA (µg/ml)
MSSA 1112	0.125	0.25
SA 113	0.125	0.25
SA 113 *Δfmta*	0.5	0.5
MRSA N315	8	2
MRSA MU50	512	512

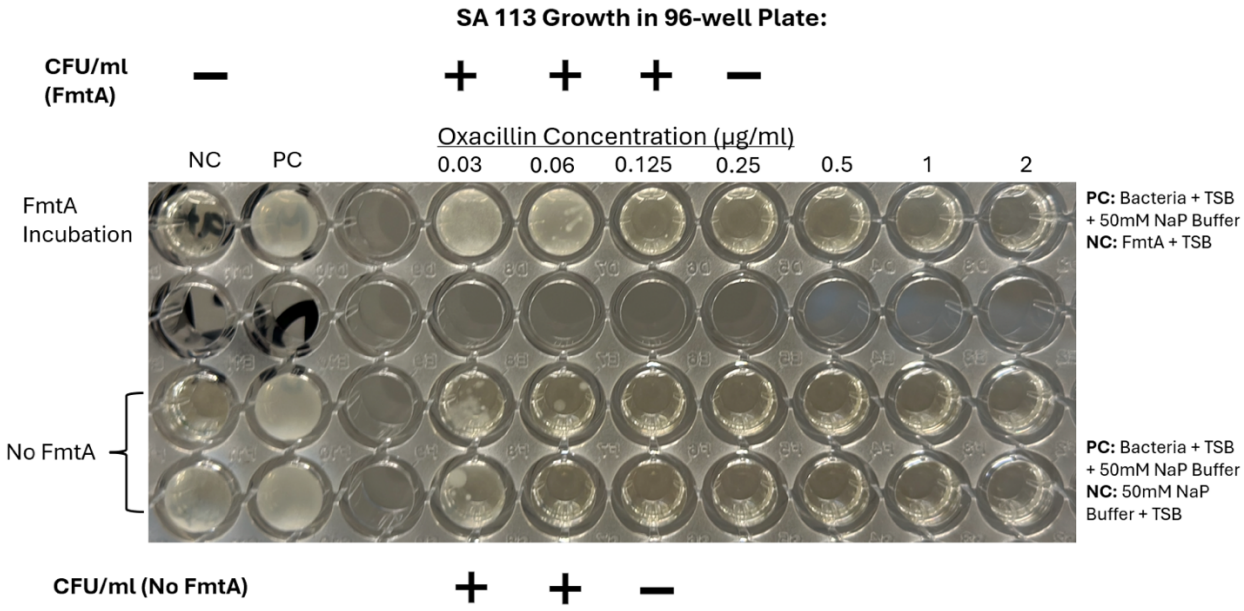

Figure 21. Visual representation of wells containing varying concentrations of oxacillin antibiotic, in which SA 113 organisms were cultured. Subsequent growth on TSB-Agar plates (CFU/ml) was depicted using the symbols "+" indicating growth and "-" indicating no growth (TSB-Agar growth plates can be found in Appendix J Figure 34). The bacterial cultures, with an initial density of approximately $5x10^5$ CFU/ml, were incubated inside the wells at 37°C for 22 hours with or without exogenous FmtA. Bacterial growth was assessed through a visual inspection of the wells and CFU/ml enumeration. Wells exhibiting visible growth at the bottom were considered positive for bacterial growth prior to inoculation onto TSB-Agar plates to confirm growth. The MIC was defined as the lowest concentration of oxacillin at which no bacterial growth was observed. A positive control (no antibiotic) and two negative controls (50 mM NaP buffer, pH 7.2, or FmtA solution) were included for comparison.

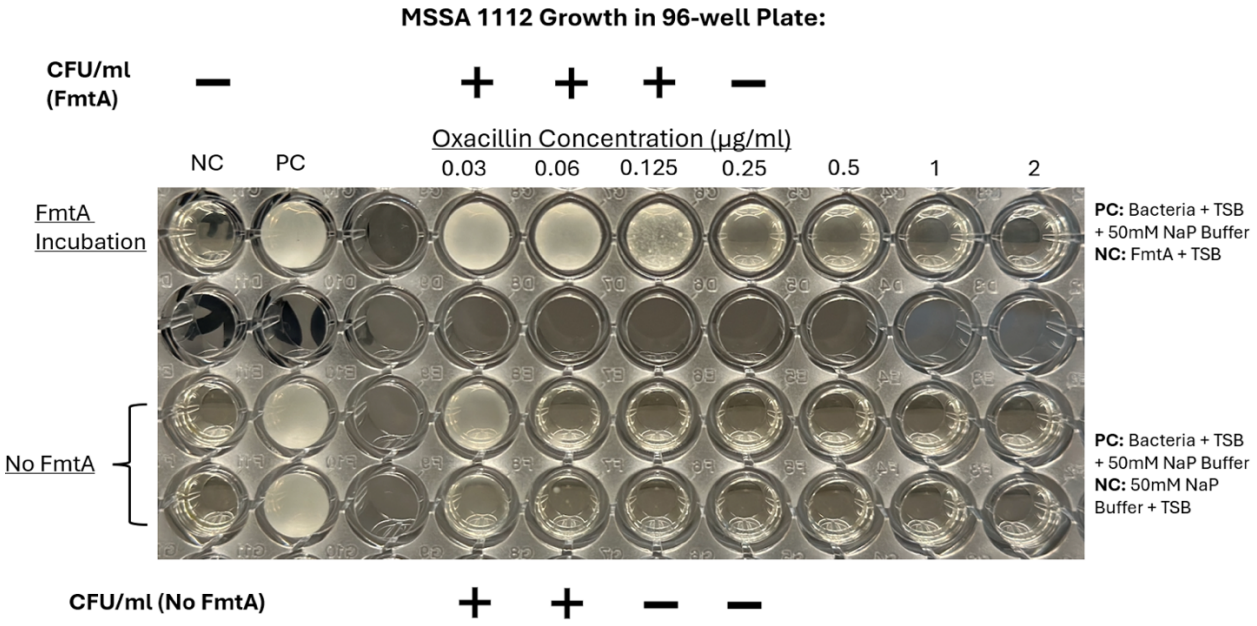

Figure 22. Visual representation of wells containing varying concentrations of oxacillin antibiotic, in which MSSA 1112 organisms were cultured. Subsequent growth on TSB-Agar plates (CFU/ml) was depicted using the symbols "+" indicating growth and "-" indicating no growth (TSB-Agar growth plates can be found in Appendix J Figure 35). The bacterial cultures, with an initial density of approximately $5x10^5$ CFU/ml, were incubated inside the wells at 37°C for 22 hours with or without exogenous FmtA. Bacterial growth was assessed through a visual inspection of the wells and CFU/ml enumeration. Wells exhibiting visible growth at the bottom were considered positive for bacterial growth prior to inoculation onto TSB-Agar plates to confirm growth. The MIC was defined as the lowest concentration of oxacillin at which no bacterial growth was observed. A positive control (no antibiotic) and two negative controls (50 mM NaP buffer, pH 7.2, or FmtA solution) were included for comparison.

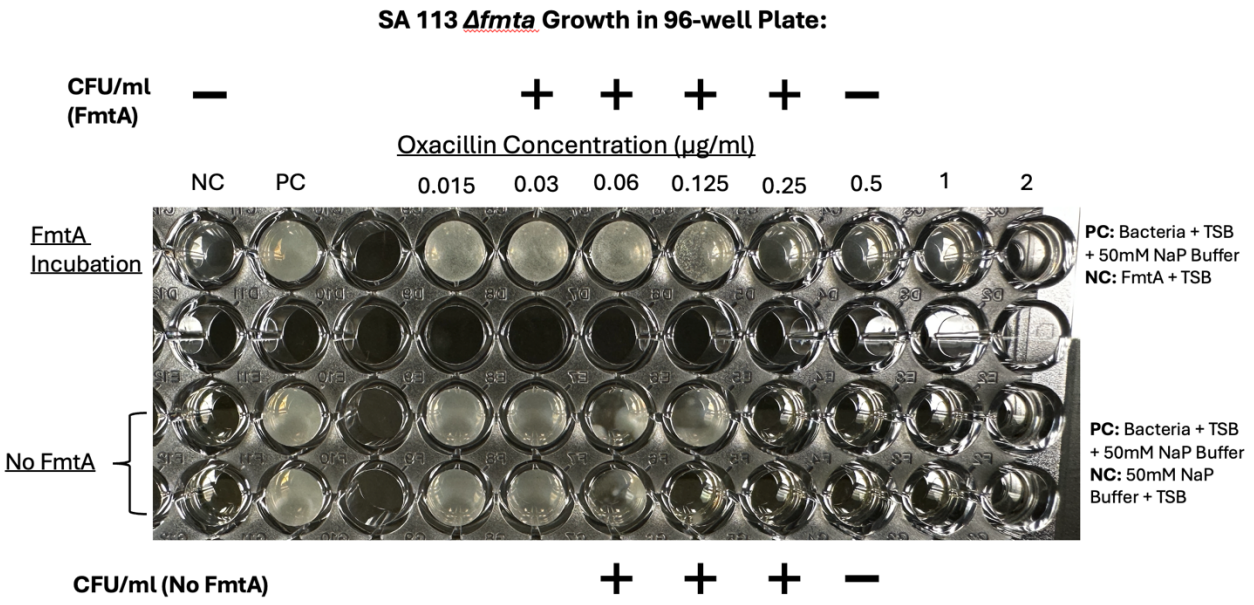

Figure 23. Visual representation of wells containing varying concentrations of oxacillin antibiotic, in which SA 113 *Δfmta* organisms were cultured. Subsequent growth on TSB-Agar plates (CFU/ml) was depicted using the symbols "+" indicating growth and "-" indicating no growth (TSB-Agar growth plates can be found in Appendix J Figure 36). The bacterial cultures, with an initial density of approximately $5x10^5$ CFU/ml, were incubated inside the wells at 37°C for 22 hours with or without exogenous FmtA. Bacterial growth was assessed through visual inspection of the wells and CFU/ml enumeration. Wells exhibiting visible growth at the bottom were considered positive for bacterial growth prior to inoculation onto TSB-Agar plates to confirm growth. The MIC was defined as the lowest concentration of oxacillin at which no bacterial growth was observed. A positive control (no antibiotic) and two negative controls (50 mM NaP buffer, pH 7.2, or FmtA solution) were included for comparison.

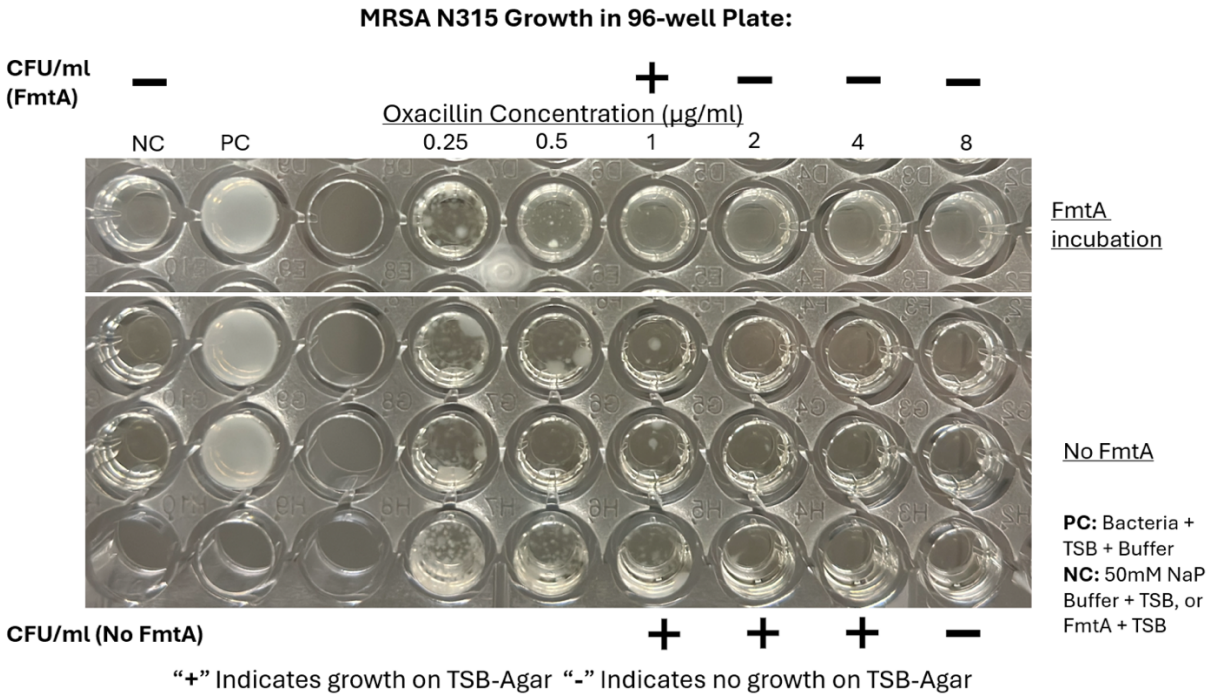

Figure 24. Visual representation of wells containing varying concentrations of oxacillin antibiotic, in which MRSA N315 organisms were cultured. Subsequent growth on TSB-Agar plates (CFU/ml) was depicted using the symbols "+" indicating growth and "-" indicating no growth (TSB-Agar growth plates can be found in Appendix J Figure 37). The bacterial cultures, with an initial density of approximately $5x10^5$ CFU/ml, were incubated inside the wells at 37°C for 22 hours with or without exogenous FmtA. Bacterial growth was assessed through a visual inspection of the wells and CFU/ml enumeration. Wells exhibiting visible growth at the bottom were considered positive for bacterial growth prior to inoculation onto TSB-Agar plates to confirm growth. The MIC was defined as the lowest concentration of oxacillin at which no bacterial growth was observed. A positive control (no antibiotic) and two negative controls (50 mM NaP buffer, pH 7.2, or FmtA solution) were included for comparison.

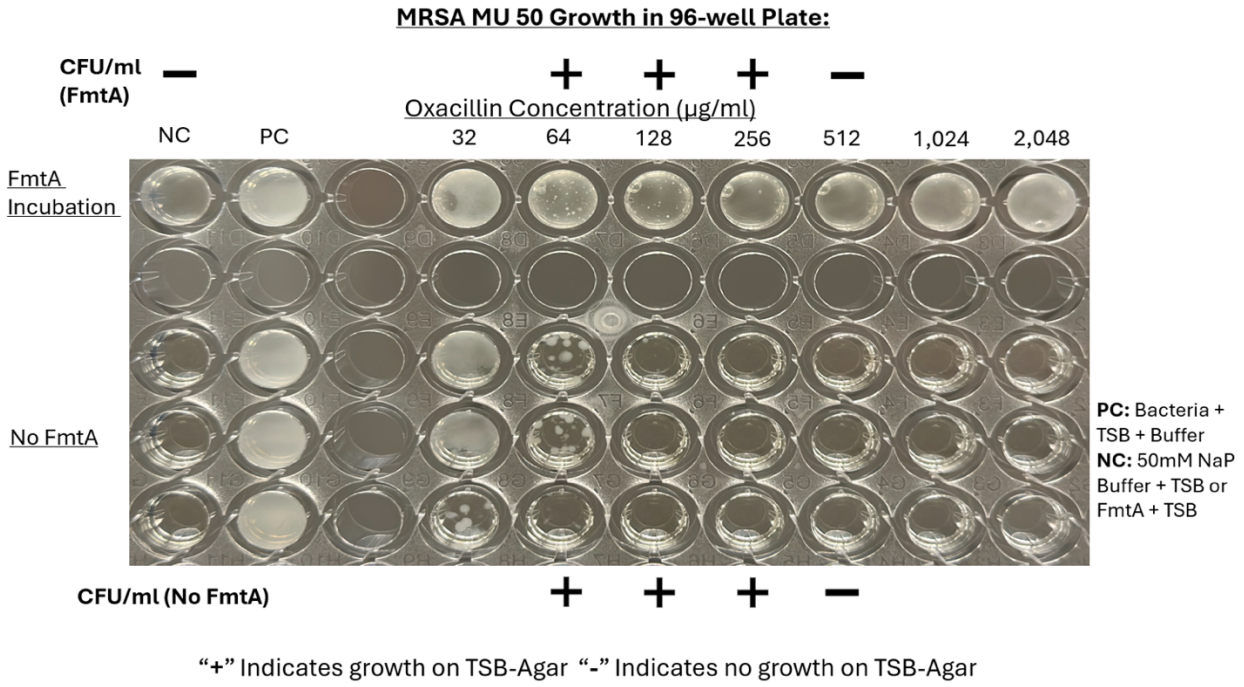

Figure 25. Visual representation of wells containing varying concentrations of oxacillin antibiotic, in which MRSA MU50 organisms were cultured. Subsequent growth on TSB-Agar plates (CFU/ml) was depicted using the symbols "+" indicating growth and "-" indicating no growth (TSB-Agar growth plates can be found in Appendix J Figure 38). The bacterial cultures, with an initial density of approximately $5x10^5$ CFU/ml, were incubated inside the wells at 37°C for 22 hours with or without exogenous FmtA. Bacterial growth was assessed through a visual inspection of the wells and CFU/ml enumeration. Wells exhibiting visible growth at the bottom were considered positive for bacterial growth prior to inoculation onto TSB-Agar plates to confirm growth. The MIC was defined as the lowest concentration of oxacillin at which no bacterial growth was observed. A positive control (no antibiotic) and two negative controls (50 mM NaP buffer, pH 7.2, or FmtA solution) were included for comparison.

Discussion

The growth rate of *S. aureus* RN4220, when incubated with and without FmtA, remained unaltered under favourable laboratory conditions in TSB media at 37ºC. The potential explanation for these growth patterns suggests that the D-Ala modification on WTA does not play a vital role in the growth of *S. aureus* under optimal laboratory conditions.

S. aureus synthesizes WTA, which significantly enhances various physiological characteristics of the organism. For example, the degree to which *S. aureus* cell walls are decorated with WTAs plays a critical role in shaping one of these characteristics, namely its virulence property (Wanner et al., 2017). WTAs contribute, in part, to other cellular processes beyond virulence, including antimicrobial resistance and the synthesis of the intricate, structurally stable peptidoglycan in daughter cells (Campbell et al., 2010). However, several studies have demonstrated that *S. aureus* cells remain active and undergo minimal adverse changes to their physiology in the absence of WTAs under laboratory conditions without stress stimulation. In particular, the subsequent and sustained growth of the organism was evident in the context of WTA deficiency (Campbell et al., 2010; D'Elia et al., 2006). Interestingly, Campbell et al. (2010, 2012) further noted that the growth rate of *S. aureus* underwent only a minimal decrease when WTA synthesis was impeded by a mutation or the use of tunicamycin. Given that *S. aureus* cells do not require WTA for growth in a laboratory-controlled setting, we predicted that merely removing the D-Ala from the synthesized WTA would likely not alter the rate of growth of these cells. This hypothesis aligns with the results we recorded when incubating RN4220 with FmtA in TSB at 37ºC. Our study focused solely on the growth rate, and the data supports the conclusion that removing D-Ala does not significantly impact the growth rate of *S. aureus* RN4220 under favorable growth conditions.

LTA might be the plausible explanation behind the continued growth of the *S. aureus* cells even in the absence of WTA. Although WTAs are not essential for *S. aureus* to maintain efficient growth rates (Campbell et al., 2010), studies indicate that LTAs also play a role in certain physiological processes regulated by WTAs. These include efficient cell septum formation for division, resistance to stressors such as antibiotics, autolysis regulation, and peptidoglycan synthesis (Karinou et al., 2019; Bæk et al., 2016; Oku et al., 2009; Hesser et al., 2020; Santa Maria et al., 2014). Similar to the absence of WTA, the lack of LTA negatively impacts the physiology

of *S. aureus*. As shown by Oku et al. (2009), at 37°C, a temperature at which *S. aureus* cells are expected to grow optimally, strain development in nutrient-rich media lacking LTA synthesis was inhibited. However, growth was restored under cooler conditions. In a separate study, it was shown that *S. aureus* cells devoid of LTA fail to adequately maintain the peptidoglycan synthesis process, ultimately resulting in an incomplete and structurally impaired cell wall. The *S. aureus* has the potential to overcome the loss of LTA through certain mutations that confer a selective advantage, thereby promoting viability (Karinou et al., 2019). Researchers have proposed that, due to the seemingly parallel functions of LTA and WTA, when one teichoic acid is impaired, the function of the other alleviates the resulting cellular impact (Oku et al., 2009; Santa Maria et al., 2014; Hesser et al., 2020). Even if WTAs were entirely essential for growth, the effects of removing D-Ala from WTA by FmtA could be mitigated, as D-Ala-modified LTA potentially compensates for the loss of D-Ala in WTA. To conclude, D-Ala release by FmtA in RN4220 cells grown under laboratory favourable conditions did not alter the rate of cell growth in these environments. Therefore, it is speculated that WTAs are not strictly required for growth under such conditions. It is conceivable that the addition of stressors might reveal a differential impact on *S. aureus* survivability when D-Ala is excised.

This chapter also investigates the impact of D-Ala removal from WTA in *S. aureus*, facilitated by exogenous FmtA, on the survival and growth of *S. aureus* cells in the presence of stressors. Analysis of RN4220 growth data in the presence of lysozyme revealed no significant differences in growth patterns between cells pre-incubated with FmtA and control cells. Both OD_{600} and CFU/ml data were examined. As evident here, *S. aureus* lysis by lysozyme is not affected by the content of D-Ala on WTA. Cell wall charge is dependent on D-Ala (Neuhaus and Baddiley, 2003; Brown et al., 2013), and D-Ala removal reduces the possibility of any steric hindrance that it could exert on lysozyme. However, our data indicates that the alteration in the charge of WTA and the possible reduction in steric hinderance has no impact on the accessibility of lysozyme to its peptidoglycan target. Under the experimental conditions, only the initial parental cells underwent D-Ala removal. As daughter cells with unaltered D-Ala levels grew, their growth behavior was comparable to that of the control group. Notably, no significant deviations in growth patterns were observed during the early growth stages, where parental cells lacking D-Ala would presumably exhibit effects. The lysozyme concentration of 500 μg/ml was selected based on prior

growth assays of various *S. aureus* strains and mutants in lysozyme presence, as reported by G C et al. (2019).

The experimental protocol was modified to include a lysis assay, given that RN4220 cell growth exhibited no significant variation in the presence of lysozyme. It was hypothesized that evaluating cell lysis might better clarify lysozyme's ability to reach its target under conditions with and without D-Ala. Previous lysis studies on *S. aureus* strains MU50 and USA300 conducted by G C et al. (2019) demonstrated that lysozyme at a concentration of 350 μg/ml effectively reduced cell survivability over time. Accordingly, a lysozyme concentration of 350 μg/ml was selected for our investigation to assess its impact. The *S. aureus* RN4220 cells incubated with lysozyme, when suspended in a nutrient-depleted solution, exhibited similar trends to those observed in TSB containing lysozyme, although this time, lytic potential rather than growth was observed. Both cultures, with and without prior incubation with FmtA, demonstrated a nearly identical rate of lysis. This indicates that lysozyme was effective in targeting and hydrolyzing the peptidoglycan bonds, leading to cell lysis at comparable rates in both D-Ala deficient cells and those with unaltered D-Ala modifications. This observation was corroborated by both OD_{600} measurements and CFU assays. It appears that D-Ala WTA substitutions do not play a role in protecting the *S. aureus* from enzymes like lysozyme, and D-Ala removal does not alter the structure of the peptidoglycan in a way that impacts the bond between N-Acetylmuramic acid and N-Acetylglucosamine.

We confirmed that 20 μM of FmtA was indeed able to release D-Ala from RN4220 WTAs as discussed in Chapter 2. Therefore, there was no doubt that the FmtA was indeed removing the D-Ala from the RN4220 cells prior to incubation with lysozyme. Studies have revealed that antibacterial stressors, such as β-lactams, can cause enhanced detrimental effects against cells with no D-Ala present on WTA, as the organism becomes more susceptible to these agents. This trend is observed for *S. aureus*, as well as other Gram-positive microbials like *B. subtilis* (Bernal et al., 2009; Wecke et al., 1997; Coupri et al., 2021). However, lysozyme has a different mechanism of action compared to these antibiotics (Nawaz et al. 2022), which may explain the lack of a significant difference in cell viability observed here. Secondly, studies with D-Ala deficiency typically involve the deletion or mutation of the *dlt* operon that codes for proteins involved in the modification of WTA with D-Ala (Peschel et al., 1999; Wecke et al., 1997; Collins et al., 2002; Brown et al., 2012; Simanski et al., 2013). In our lysis assay, the native FmtA protein was used to

remove D-Ala from the WTA, which provided an alternative to the deletion of the *dlt* operon. Deletion of genes and modifications of genetic material may impact the physiology of an organism in ways that remain unknown. Also, FmtA may not completely remove the D-Ala on the WTA, whereas deleting the *dlt* gene produces D-Ala deficient WTAs. Deletion may not be an optimal approach, as it was discovered that *S. aureus* allocates 12% or more of its D-Ala to WTA modification to ensure cell wall integrity (Singh et al., 2017). Because the lysis assay did not promote growth, as the *S. aureus* cells were suspended in buffer and not in a growth medium, the experiment was not bound by the same limitations that the growth assay was, i.e. cell division could not occur. The cells at the 0-minute time point all had the majority of D-Ala removed, and it was these same cells that were lysed over the complete 240-minute time period. There were no daughter cells being formed with regular levels of D-Ala substitutions.

The lysis data for RN4220 *S. aureus* revealed significant alterations in cell viability in the presence of lysostaphin. CFU/ml assays demonstrated a reduction in viable cells for FmtA-incubated cultures compared to controls at all tested time points. This was evident by the fewer number of colonies grown from FmtA-incubated cultures. The reduction in colony growth on TSB plates was consistent across all trials. OD_{600} measurements, while presented, were insufficient to accurately reveal cell viability due to the inability to distinguish between live and dead cells. Consequently, no discernible difference was observed in lysis rates between FmtA-incubated and non-incubated cells based on OD_{600} readings. However, the CFU/ml data clearly indicated a significant impact of D-Ala removal on lysostaphin's ability to reach its target. The removal of D-Ala from WTA facilitates increased cell lysis by lysostaphin, suggesting a consequential alteration to the cell wall, which enhances access to cell wall crosslinking regions.

One plausible explanation for this enhanced accessibility of lysostaphin to the peptidoglycan is the electrostatic attraction between lysostaphin and the cell wall. The abundance of lysine and arginine amino acids in lysostaphin confers a net positive charge on the enzyme at a neutral pH (Walsh et al., 2003). Therefore, lysostaphin would exhibit greater attraction to the cell surface following D-Ala removal, as the source of the positive charge on the WTA, the D-Ala, is no longer attached. The prevalent phosphate molecules on the WTA backbone contribute highly to the negative charge of the cell wall, and D-Ala mitigate this charge (Neuhaus and Baddiley, 2003; Brown et al., 2013). The removal of D-Ala amplifies the negative charge, potentially limiting electrostatic repulsions and enhancing lysostaphin attraction and interaction with the cell wall.

This hypothesis is supported by Peschel et al. (2000), who speculated that electrostatic interactions between lysostaphin and WTA increases in the absence of D-Ala. Their knockout of the *dltA* gene resulted in a faster rate of cell lysis in the presence of lysostaphin, mirroring the effects observed in this study with FmtA and lysostaphin incubation. Additionally, the removal of D-Ala from the WTA may assist lysostaphin in reaching its target, as the presence of D-Ala alone could block the pathway to the cell surface peptidoglycan. Removing D-Ala partially eliminates the clutter present on the surface of the cell and provides an unobstructed path for the lysostaphin to reach the cross-linking units.

The oxacillin MIC results support the notion that for MSSA strains, hydrolysis of the bond between D-Ala and WTA via exogenous FmtA, in conjunction with endogenously synthesized FmtA, facilitates the enhancement of resistance phenotypes against β-lactam antibiotics. However, for both MSSA 1112 and SA 113, the increase in resistance was a marginal 2-fold shift going from 0.125 μg/ml to 0.25 μg/ml. The data denotes that excision of D-Ala from the surface of the cell wall promotes survival in the presence of oxacillin to a minor extent, prompting the development of a theory to explain the underlying mechanism. To our knowledge, most research addressing antibiotic resistance of *S. aureus* is conducted using MRSA strains and not MSSA strains. Therefore, we were not able to locate any published literature that reports on the increase or decrease in antibiotic susceptibility of MSSA strains as WTA D-Ala levels diminish.

For the MIC studies conducted, we employed 20 μM of FmtA. Previous work in our lab has revealed that FmtA is pivotal for cellular autolysis regulation. The 20 μM concentration of FmtA used was well above the threshold discovered to suppress autolysis in the cells (Qamar and Golemi-Kotra, 2012). Corroborating these findings, data from other research groups using alternative methods have demonstrated that inhibition of endogenous FmtA synthesis leads to elevated lysis rates in growing cultures (Boles et al., 2010). Given that FmtA is primarily used to separate D-Ala from WTAs by cleaving the ester bond between them (Rahman et al., 2016), a study by Peschel et al. (2000) aligns with the observations reported by Boles et al. (2010). Peschel's group identified that the SA 113 strain has greater difficulty undergoing autolysis when WTAs are devoid of D-Ala. They achieved this by deleting the *dltA* gene (Peschel et al., 2000). Therefore, it appears that elevated levels of D-Ala in WTAs correlate with an increase in autolysis, whereas the absence or reduction of D-Ala in WTAs is associated with a decrease in autolytic activity.

Alteration in the regulation of autolysis likely explains the outcomes observed in our experiments with FmtA-treated SA 113 and MSSA 1112 in the presence of oxacillin. The reduced susceptibility of these strains is perhaps attributable to the reduction in autolysis. As 20 μM of FmtA removes D-Ala from WTAs, autolysin proteins may no longer be properly localized to the peptidoglycan. As previously noted, the proper location of autolysin activity within the cell is occupied by AtlA only when WTAs with normal D-Ala modifications are present on the cell wall (Schlag et al., 2010). Consequently, we propose that with diminished regulation of autolysis following D-Ala removal, there is a corresponding increase in the maintenance of cell wall integrity, thereby enhancing growth and survivability in the presence of oxacillin. The increase in oxacillin MIC observed may reflect this phenomenon in SA 113 and MSSA 1112 (Table 4). The reduction in autolysis likely does not considerably enhance cell viability in the presence of oxacillin, which could account for the moderate 2-fold increase in the MIC that we observed. Our hypothesis is further supported by findings from a study by G C et al. (2019), which reported that the effectiveness of the antibiotic oxacillin was enhanced against MRSA due to impaired cell wall assembly. This physiological alteration was a consequence of upregulated autolytic enzyme synthesis, resulting in amplified autolysis (G C et al., 2019). Therefore, it is reasonable to infer that a reduction in autolysis could produce the opposite effect, decreasing susceptibility. We believe that this reasoning can be extended to MSSA strains, further validating our proposed theory. As FmtA removes D-Ala from WTAs, the ensuing reduction in autolysis due to improper localization of autolytic enzymes likely results in enhanced cell wall integrity and decreased cell lysis. This would be associated with a marginally reduced susceptibility to oxacillin.

The deletion of the *fmtA* gene in *S. aureus* results in the loss of FmtA protein synthesis, leading to the over modification of WTAs with D-Ala and the absence of a corresponding hydrolysis mechanism (Rahman et al., 2016; Komatsuzawa et al., 1997). Our findings indicated that the SA 113 Δ*fmtA* mutant remained viable at oxacillin concentrations of 0.25 μg/ml, which represented a 4-fold susceptibility decrease compared to the wild-type strain. This finding suggested that inhibiting FmtA synthesis confers reduced susceptibility to oxacillin. Formulating a plausible explanation for this unexpected outcome proved challenging, particularly as we were not able to find any published reports implicated in a similar study. However, the observed increase in WTA-bound D-Ala appears to hinder the ability of oxacillin to perform its function, possibly due to its inability to access its target, peptidoglycan. Gautam et al. (2015) observed that WTAs

can inhibit the interaction of antibodies with peptidoglycan, functioning as a defense mechanism for the organism. They speculated that this inhibition likely occurs due to two possibilities, one of which was steric hindrance that traps the antibodies above the peptidoglycan (Gautam et al., 2015). In light of this, an increase in D-Ala on WTAs may similarly obstruct antibiotics from reaching their targets. Consequently, we speculate that the over-modification of WTAs with D-Ala may impede oxacillin from effectively reaching its target within the peptidoglycan, likely due to increased steric hindrance imposed by the D-Ala. This hindrance would only marginally impact oxacillin efficacy, as some oxacillin would still reach the peptidoglycan layer, thus explaining why the change in MIC was a 4-fold increase rather than a more pronounced change. Figure 26 provides a visualization of this theory and was inspired based on the study by Gautam et al., (2015).

The SA 113 Δ*fmtA* culture treated with exogenous FmtA exhibited a susceptibility pattern comparable to that observed in the untreated culture. The introduction of exogenous FmtA into the culture removed the D-Ala from the WTAs, thereby reducing the predicted steric hindrance that impeded oxacillin activity. This reduction should have enhanced the susceptibility of the culture compared to the FmtA-untreated control. However, consistent with observations made in the SA 113 and MSSA 1112 strains, the reduction in D-Ala concentration likely correlates with a decrease in cell autolysis. In the SA 113 Δ*fmtA* strain, similar to other *S. aureus* strains, both an elevated accumulation of D-Ala on WTAs (Rahman et al., 2016) and elevated autolysis rates (Boles et al., 2010) were observed upon removal of the *fmtA* gene. The introduction of exogenous FmtA into the cultures successfully reduced the elevated D-Ala levels, potentially prompting a decrease in cell lysis. We hypothesize that the reduction in D-Ala steric hindrance could enhance *S. aureus* oxacillin susceptibility, while a decrease in autolysis simultaneously leads to promotion of bacterial cell survival. Therefore, the occurrence of these two mechanisms happening at once may account for the observed lack of change in susceptibility of the SA 113 Δ*fmtA* strain in the presence of exogenous FmtA.

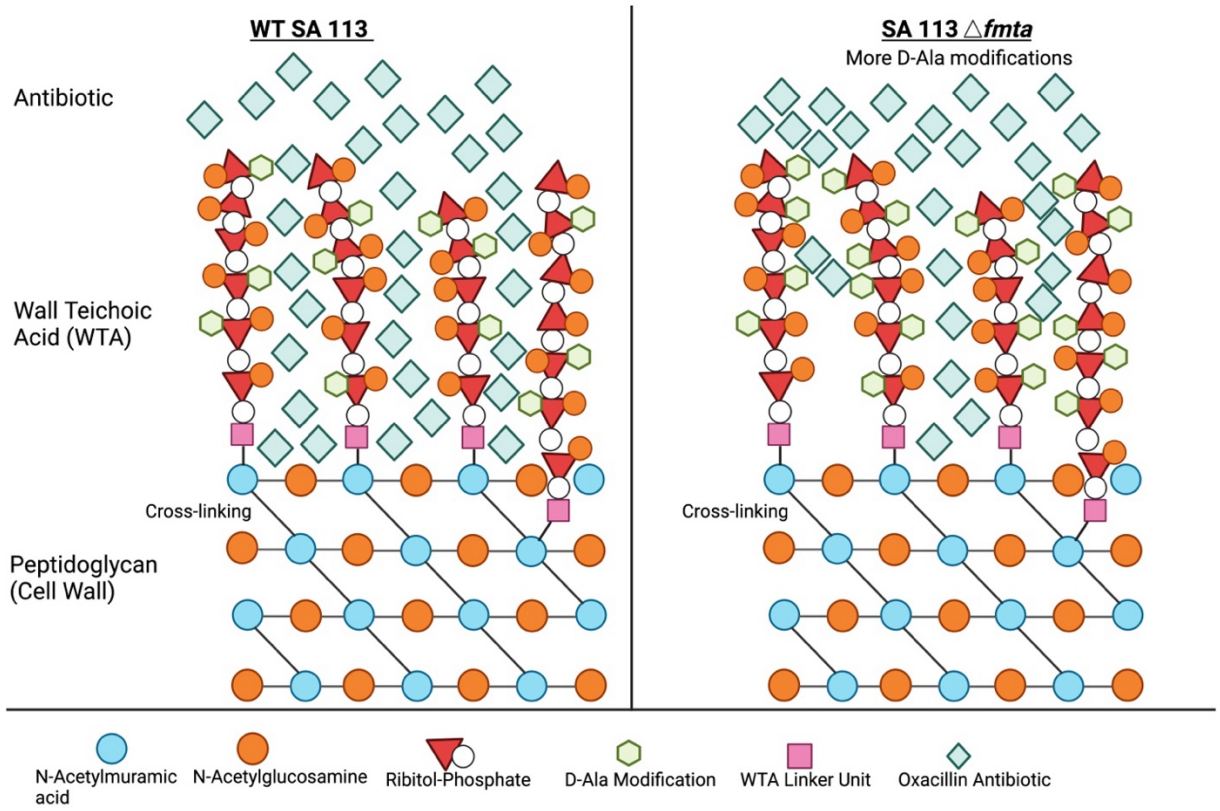

Figure 26. Schematic representation of the proposed mechanism by which *fmta* gene knockout in SA 113 prevents D-Ala removal from WTA, potentially causing steric hindrance to oxacillin. In WT SA 113 (left), the FmtA enzyme facilitates the removal of D-Ala from WTAs, allowing access of oxacillin to the peptidoglycan layer with little resistance. In contrast, in the *fmta* knockout mutant (right), the persistence of D-Ala modifications on WTAs is hypothesized to increase resistance, thereby reducing the number of oxacillin molecules reaching the bacterial cell wall, marginally impairing antibiotic efficacy.

In parallel to the potential autolysis alterations of the *S. aureus* cells induced by FmtA incubation, the modifications in the glycosylation patterns of WTAs in *S. aureus* SA 113 and MSSA 1112 could be directly associated with the observed increase in MIC. D-Ala and N-Acetylglucosamine (GlcNAc) are bound to mature WTA polymers, with the orientation of GlcNAc assuming either an α or β conformation depending on gene expression. The phenotypic antimicrobial resistance of MRSA to β-lactams and of VISA to vancomycin, along with the apparent ability of *S. aureus* to reduce immune activation by avoiding detection, are all exclusively associated with the β-GlcNAc WTA variant. (Brown et al., 2012; Hort et al., 2021; Gerlach et al., 2018). Although, to our knowledge, the exact mechanisms continue to be under investigation.

Mistretta et al. (2019) reported that the same strain utilized in our study, the SA 113, undergoes predominant *tarM* gene expression under conditions devoid of stressors. Conversely, a targeted downregulation of *tarM* and an elevated expression of *tarS*, which encodes β-GlcNAc, occur when SA 113 is cultured under conditions that prevent the organism from modifying WTAs with D-Ala (Mistretta et al., 2019). *S. aureus* is capable of growing under circumstances characterized by elevated salt content; however, these conditions suppress the synthesis of WTA D-Ala-modifying proteins (Koprivnjak et al., 2006). These same stress conditions were employed by Mistretta et al. (2019) in their studies on SA 113. Additionally, the *in vitro* conformational shift in GlcNAc orientation from the α to the β variant in MSSA strains is also confirmed by *in vivo* infection studies using the Newman strain. The presence of the immune system presents the organism with alternative stress factors (Mistretta et al., 2019).

In our study, exogenous FmtA was employed to remove D-Ala from WTAs. When SA 113 was incubated with oxacillin and FmtA, this created a stress condition that likely triggered a similar shift to β-GlcNAc synthesis. To our knowledge, the β orientation is not associated with antibiotic resistance potential in MSSA strains, as these strains lack similar resistance properties to those of MRSA (Dien Bard et al., 2014). Brown et al. (2012) predicted that the MRSA PBP2a enzyme favours the β-GlcNAc WTA for localization, rather than α-GlcNAc WTA. However, due to the data presented by Mistretta et al. (2019), which indicated that MSSA strains shift their GlcNAc orientation to the β configuration under D-Ala substitution inhibition and host infection, we cannot ignore the possibility of an adaptive response. This shift may enhance the viability of MSSA in stress-inducing environments. Nonetheless, it remains uncertain whether the shift is associated with a decrease in MSSA susceptibility to oxacillin under FmtA incubation, which may account for the observed increase in oxacillin MIC. If GlcNAc orientation is involved, it is reasonable to suggest that a similar physiological response occurred in MSSA 1112, given the similarities shared with SA 113. Both are MSSA strains, exhibited the same baseline MIC prior to FmtA incubation, and showed comparable increases in MIC following FmtA treatment. However, the role of glycosylation orientation in antibiotic resistance may be limited, which would further explain the modest 2-fold increase in oxacillin MIC reported.

D-Ala release from WTA of MRSA strains did produce significant survivability distinctions in the presence of oxacillin. MRSA N315 *S. aureus* experienced a 4-fold decrease in the MIC of oxacillin attributable to their incubation with FmtA to remove D-Ala. The efficiency

of oxacillin increased, signifying that D-Ala does contribute to the antibiotic resistance properties of MRSA strains. Bernal et al. (2009) and Coupri et al. (2021) reached similar conclusions when observing susceptibility of MRSA strains to a variety of β-lactams including oxacillin. They employed different techniques to prevent D-Ala attachment to WTA, confirming diminished β-lactam resistance properties in these strains. Granted, FmtA does not prevent D-Ala attachment, but hydrolysis of the bond between D-Ala and WTA post-synthesis will produce a similar outcome, as evidenced by our supporting data. MRSA strains exhibit significant resistance, attributable in part to their capability to synthesize β-lactam-elusive PBP2a in conjunction with native PBPs (Dien Bard et al., 2014). Notably, PBP4 and PBP2a are the only PBPs demonstrated to be directly reliant on the peptidoglycan-bound WTA (Qamar and Golemi-Kotra, 2012; Atilano et al., 2010; Lu et al., 2023).

We formulated a theory to explain the reduction in MIC of oxacillin against MRSA N315 based on a similar concept proposed by Coupri et al. (2021). It is safe to speculate that D-Ala modifications on WTA contribute to the localization of PBP4 and PBP2a, as WTAs in their entirety have been shown to either exhibit affinity for or directly impact localization of these proteins (Qamar and Golemi-Kotra, 2012; Lu et al., 2023; Lam et al., 2018; Hill et al., 2019). We believe that when D-Ala undergoes deesterification from the WTA, the PBP4 and the PBP2a enzymes are partially delocalized, contributing to their diminished activity. The removal of D-Ala may influence the localization of these enzymes. However, it may not be sufficient to fully delocalize all synthesized PBP2a and PBP4 proteins, as WTAs, with their remaining glycosylation modifications, persist on the cell surface. A similar hypothesis was introduced by Coupri et al. (2021); however, they did not discuss the possibility of only partial delocalization of PBPs. Hence, a partial reduction in PBP2a localization would presumably decrease the antibiotic resistance properties of the MRSA cells without leading to a reduction comparable to those of MSSA strains. This phenomenon may account for the 4-fold decrease of oxacillin concentration observed in the N315 strain, which nonetheless exhibits higher resistance compared to MSSA strains. Oxacillin likely targets the remaining susceptible PBP enzymes, leading to a reduction in cell viability.

Contrary to the reduction in oxacillin MIC of the N315 MRSA strain, the MU50 MRSA strain demonstrated no alteration in the MIC of oxacillin when D-Ala was removed from the WTA. The MIC remained at 512 μg/ml oxacillin with and without FmtA incubation. Comparison of the oxacillin MIC of MU50 with that of N315 reveals that the MU50 strain is exceedingly more

resistant to oxacillin than N315. This heightened resistance is attributed to MU50's classification as a Vancomycin-Intermediate *Staphylococcus aureus* (VISA), a subgroup of resistant *S. aureus* strains that typically exhibit greater resistance than MRSA (Sun et al., 2021). The main features of VISA strains that set them apart from MRSA are their partial vancomycin resistance and their morphological alterations, particularly at the cell wall. In MU50 and VC40, compared to non-VISA strains, these peptidoglycan alterations include a significant augmentation and reduction in thickness and cross-links, respectively, along with a confirmed elevation in WTA synthesis and nearly 50% more D-Ala modifications in VC40 (Cui et al., 2000; Hort et al., 2021). Consequently, these VISA-specific alterations influence their antimicrobial resistance phenotypes. Specifically, we predict that the reduced number of cross-linking regions observed throughout the peptidoglycan matrix may indicate a targeted downregulation or delocalization of PBPs by the organism. If this is the case, oxacillin and other β-lactam antibiotics would have a diminished activity resulting from fewer PBPs active in the peptidoglycan to target (Bush and Bradford, 2016). Accordingly, antibiotic resistance increases, which supports the higher oxacillin MIC of MU50. This could further explain why even after removing the D-Ala from the WTA using FmtA, there was no alteration in the MIC of oxacillin.

An alternative explanation for why the MIC of the MU50 strain remained unchanged even after D-Ala removal is also plausible. If we assume that MU50 has a similar level of D-Ala and WTA surge that the VC40 VISA strain exhibited (Hort et al., 2021), this increase in D-Ala and WTA synthesis could mitigate the effect of the D-Ala that is lost as a result of FmtA incubation. The 20 μM of FmtA will release the same amount of D-Ala in a set period of time. Assuming that 20 μM FmtA does not completely eliminate D-Ala residues from the WTAs, the increase in D-Ala levels in the VISA strain may exceed the threshold required to detect changes in the MIC of oxacillin after a 22-hour incubation period. In other words, the residual D-Ala levels following FmtA treatment are anticipated to be higher compared to those in other strains, such as MRSA N315. Consequently, the remaining D-Ala may sufficiently compensate for the loss of D-Ala due to FmtA, thereby providing the necessary protection against oxacillin. This results in no significant alteration in its MIC in the presence versus the absence of FmtA.

In contrast to the MSSA strain SA 113, MRSA strains such as N315 and MU50 harbor only the *tarS* gene, with no presence of the *tarM* gene. Therefore, the WTAs of N315 and MU50 are exclusively modified with β-GlcNAc, lacking the ability to alter the orientation of this sugar

(Winstel et al., 2014). The glycosylation pattern of N315 and MU50 is unlikely to influence the oxacillin MIC we observed, as evidenced by the fact that only N315 exhibited a change despite both strains sharing this β-GlcNAc modification. Notably, a previously unidentified protein, TarP, was discovered in MRSA strains such as N315, leading to the observation that strains synthesizing TarP exhibited weak activation of immune system factors (Gerlach et al., 2018). In particular, the TarP protein shares similarities with the TarS protein, with a key distinction between them being their influence on the final localization of the β-GlcNAc molecule on the backbone of WTA. Specifically, when the TarP protein is active, the third carbon position of ribitol experiences β-GlcNAc binding, in contrast to the conventional fourth carbon position (Gerlach et al., 2018). However, it remains unknown whether this specific substitution alteration impacts oxacillin MIC in media containing exogenous FmtA, or if this substitution even occurs under these conditions.

Akin to the *S. aureus* WTAs devoid of D-Ala upon incubation with exogenous FmtA in our study, D-Ala-absent WTAs are also detected during salt-triggered microbial stress (Koprivnjak et al., 2006). In several *S. aureus* strains, this same salt-stress response leads to deviations in the WTA GlcNAc synthesis profile, which differs from the norm seen in growth environments lacking stressors. In particular, two distinct types of WTAs are present on the cell wall: one with β-GlcNAc bound to the third carbon and the other with β-GlcNAc bound to the fourth carbon, resulting from a change in the location on the ribitol-phosphate backbone where β-GlcNAc binds (Mistretta et al., 2019). It remains uncertain whether N315 exhibits this glycosylation adjustment in our studies or whether such a modification would reduce oxacillin MIC. The only discernible pattern is that β-GlcNAc substitution at the third ribitol carbon increases the viability of N315, allowing for continued persistence inside the host (Gerlach et al., 2018). We believe it is conceivable that this substitution confers increased resistance through an unknown mechanism. Since N315 possesses the capability to synthesize β-GlcNAc at this position on the WTA backbone, it is probable that under stress conditions induced by FmtA and oxacillin, which inhibit WTA D-Ala incorporation during antibiotic exposure, N315 no longer restricts GlcNAc attachment to a single carbon position. Instead, it may incorporate β-GlcNAc at the fourth backbone carbon repeat while also maintaining incorporation at the third position (Mistretta et al., 2019), as a consequence of FmtA presence. This modification possibly relates to a decrease in antimicrobial resistance, which would otherwise be maintained by glycosylation entirely at the 3rd carbon position. Consequently, this could explain the observed reduction in oxacillin MIC in our studies.

References

Atilano, M. L., Pereira, P. M., Yates, J., Reed, P., Veiga, H., Pinho, M. G., & Filipe, S. R. (2010). Teichoic acids are temporal and spatial regulators of peptidoglycan cross-linking in *Staphylococcus aureus*. *Proceedings of the National Academy of Sciences*, *107*(44), 18991–18996.

Bæk, K. T., Bowman, L., Millership, C., Dupont Søgaard, M., Kaever, V., Siljamäki, P., Savijoki, K., Varmanen, P., Nyman, T. A., Gründling, A., & Frees, D. (2016). The cell wall polymer lipoteichoic acid becomes nonessential in *Staphylococcus aureus* cells lacking the ClpX chaperone. *mBio*, *7*(4).

Baba, T., & Schneewind, O. (1996). Target cell specificity of a bacteriocin molecule: A C-terminal signal directs lysostaphin to the cell wall of *Staphylococcus aureus*. *The EMBO Journal*, *15*(18), 4789–4797.

Bastos, M. do, Coutinho, B. G., & Coelho, M. L. (2010). Lysostaphin: A Staphylococcal bacteriolysin with potential clinical applications. *Pharmaceuticals*, *3*(4), 1139–1161.

Bernal, P., Zloh, M., & Taylor, P. W. (2009). Disruption of D-alanyl esterification of *Staphylococcus aureus* cell wall teichoic acid by the β-lactam resistance modifier (−)-epicatechin gallate. *Journal of Antimicrobial Chemotherapy*, *63*(6), 1156–1162.

Boles, B. R., Thoendel, M., Roth, A. J., & Horswill, A. R. (2010). Identification of genes involved in polysaccharide-independent *Staphylococcus aureus* biofilm formation. *PLoS ONE*, *5*(4).

Brown, S., Santa Maria, J. P., & Walker, S. (2013). Wall teichoic acids of gram-positive bacteria. *Annual Review of Microbiology*, *67*(1), 313–336.

Brown, S., Xia, G., Luhachack, L. G., Campbell, J., Meredith, T. C., Chen, C., Winstel, V., Gekeler, C., Irazoqui, J. E., Peschel, A., & Walker, S. (2012). Methicillin resistance in *Staphylococcus aureus* requires glycosylated wall teichoic acids. *Proceedings of the National Academy of Sciences*, *109*(46), 18909–18914.

Bush, K., & Bradford, P. A. (2016). B-lactams and β-lactamase inhibitors: An overview. *Cold Spring Harbor Perspectives in Medicine*, *6*(8).

Campbell, J., Singh, A. K., Santa Maria, J. P., Kim, Y., Brown, S., Swoboda, J. G., Mylonakis, E., Wilkinson, B. J., & Walker, S. (2010). Synthetic lethal compound combinations reveal

a fundamental connection between wall teichoic acid and peptidoglycan biosyntheses in *Staphylococcus aureus*. *ACS Chemical Biology*, *6*(1), 106–116.

Campbell, J., Singh, A. K., Swoboda, J. G., Gilmore, M. S., Wilkinson, B. J., & Walker, S. (2012). An antibiotic that inhibits a late step in wall teichoic acid biosynthesis induces the cell wall stress stimulon in *Staphylococcus aureus*. *Antimicrobial Agents and Chemotherapy*, *56*(4), 1810–1820.

Cavadini, C., Hertel, C., & Hammes, W. P. (1998). Application of lysostaphin-producing lactobacilli to control staphylococcal food poisoning in meat products. *Journal of Food Protection*, *61*(4), 419–424.

Collins, L. V., Kristian, S. A., Weidenmaier, C., Faigle, M., van Kessel, K. P. M., van Strijp, J. A. G., Götz, F., Neumeister, B., & Peschel, A. (2002). *Staphylococcus aureus* strains lacking d-alanine modifications of teichoic acids are highly susceptible to human neutrophil killing and are virulence attenuated in mice. *The Journal of Infectious Diseases*, *186*(2), 214–219.

Coupri, D., Verneuil, N., Hartke, A., Liebaut, A., Lequeux, T., Pfund, E., & Budin-Verneuil, A. (2021). Inhibition of d-alanylation of teichoic acids overcomes resistance of methicillin-resistant *Staphylococcus aureus*. *Journal of Antimicrobial Chemotherapy*, *76*(11), 2778–2786.

Cui, L., Murakami, H., Kuwahara-Arai, K., Hanaki, H., & Hiramatsu, K. (2000). Contribution of a thickened cell wall and its glutamine nonamidated component to the vancomycin resistance expressed by *Staphylococcus aureus* MU50. *Antimicrobial Agents and Chemotherapy*, *44*(9), 2276–2285.

D'Elia, M. A., Pereira, M. P., Chung, Y. S., Zhao, W., Chau, A., Kenney, T. J., Sulavik, M. C., Black, T. A., & Brown, E. D. (2006). Lesions in teichoic acid biosynthesis in *Staphylococcus aureus* lead to a lethal gain of function in the otherwise dispensable pathway. *Journal of Bacteriology*, *188*(12), 4183–4189.

Dien Bard, J., Hindler, J. A., Gold, H. S., & Limbago, B. (2014). Rationale for eliminating *Staphylococcus* breakpoints for β-lactam agents other than penicillin, oxacillin or cefoxitin, and ceftaroline. *Clinical Infectious Diseases*, *58*(9), 1287–1296.

Gautam, S., Kim, T., Lester, E., Deep, D., & Spiegel, D. A. (2015). Wall teichoic acids prevent antibody binding to epitopes within the cell wall of *Staphylococcus aureus*. *ACS Chemical Biology*, *11*(1), 25–30.

G C, B., Sahukhal, G. S., & Elasri, M. O. (2019). Role of the *msaABCR* operon in cell wall biosynthesis, autolysis, integrity, and antibiotic resistance in *Staphylococcus aureus*. *Antimicrobial Agents and Chemotherapy*, *63*(10).

Gerlach, D., Guo, Y., De Castro, C., Kim, S.-H., Schlatterer, K., Xu, F.-F., Pereira, C., Seeberger, P. H., Ali, S., Codée, J., Sirisarn, W., Schulte, B., Wolz, C., Larsen, J., Molinaro, A., Lee, B. L., Xia, G., Stehle, T., & Peschel, A. (2018). Methicillin-resistant *Staphylococcus aureus* alters cell wall glycosylation to evade immunity. *Nature*, *563*, 705–709.

Haruta, S., & Kanno, N. (2015). Survivability of microbes in natural environments and their ecological impacts. *Microbes and Environments*, *30*(2), 123–125.

Hesser, A. R., Matano, L. M., Vickery, C. R., Wood, B. M., Santiago, A. G., Morris, H. G., Do, T., Losick, R., & Walker, S. (2020). The length of lipoteichoic acid polymers controls *Staphylococcus aureus* cell size and envelope integrity. *Journal of Bacteriology*, *202*(16).

Hill, M. A., Lam, A. K., Reed, P., Harney, M. C., Wilson, B. A., Moen, E. L., Wright, S. N., Pinho, M. G., & Rice, C. V. (2019). BPEI-induced delocalization of PBP4 potentiates β-lactams against MRSA. *Biochemistry*, *58*(36), 3813–3822.

Hiramatsu, K., Kayayama, Y., Matsuo, M., Aiba, Y., Saito, M., Hishinuma, T., & Iwamoto, A. (2014). Vancomycin-intermediate resistance in *Staphylococcus aureus*. *Journal of Global Antimicrobial Resistance*, *2*(4), 213–224.

Hort, M., Bertsche, U., Nozinovic, S., Dietrich, A., Schrötter, A. S., Mildenberger, L., Axtmann, K., Berscheid, A., & Bierbaum, G. (2021). The role of β-glycosylated wall teichoic acids in the reduction of vancomycin susceptibility in vancomycin-intermediate *Staphylococcus aureus*. *Microbiology Spectrum*, *9*(2).

Jorge, A. M., Schneider, J., Unsleber, S., Xia, G., Mayer, C., & Peschel, A. (2018). *Staphylococcus aureus* counters phosphate limitation by scavenging wall teichoic acids from other staphylococci via the teichoicase GlpQ. *Journal of Biological Chemistry*, *293*(38), 14916–14924.

Karinou, E., Schuster, C. F., Pazos, M., Vollmer, W., & Gründling, A. (2019). Inactivation of the monofunctional peptidoglycan glycosyltransferase SgtB allows *Staphylococcus aureus* to survive in the absence of lipoteichoic acid. *Journal of Bacteriology*, *201*(1).

Khorshidian, N., Khanniri, E., Koushki, M. R., Sohrabvandi, S., & Yousefi, M. (2022). An overview of antimicrobial activity of lysozyme and its functionality in cheese. *Frontiers in Nutrition*, *9*, 833618.

Komatsuzawa, H., Sugai, M., Ohta, K., Fujiwara, T., Nakashima, S., Suzuki, J., Lee, C. Y., & Suginaka, H. (1997). Cloning and characterization of the *fmt* gene which affects the methicillin resistance level and autolysis in the presence of Triton X-100 in methicillin-resistant *Staphylococcus aureus*. *Antimicrobial Agents and Chemotherapy*, *41*(11), 2355–2361.

Koprivnjak, T., Mlakar, V., Swanson, L., Fournier, B., Peschel, A., & Weiss, J. P. (2006). Cation-induced transcriptional regulation of the *dlt* operon of *Staphylococcus aureus*. *Journal of Bacteriology*, *188*(10), 3622–3630.

Lam, A. K., Hill, M. A., Moen, E. L., Pusavat, J., Wouters, C. L., & Rice, C. V. (2018). Cationic branched polyethylenimine (BPEI) disables antibiotic resistance in methicillin-resistant *Staphylococcus epidermidis* (MRSE). *ChemMedChem*, *13*(20), 2240–2248.

Lu, Y., Chen, F., Zhao, Q., Cao, Q., Chen, R., Pan, H., Wang, Y., Huang, H., Huang, R., Liu, Q., Li, M., Bae, T., Liang, H., & Lan, L. (2023). Modulation of MRSA virulence gene expression by the wall teichoic acid enzyme TarO. *Nature Communications*, *14*(1), 1594.

Mistretta, N., Brossaud, M., Telles, F., Sanchez, V., Talaga, P., & Rokbi, B. (2019). Glycosylation of *Staphylococcus aureus* cell wall teichoic acid is influenced by environmental conditions. *Scientific Reports*, *9*(1).

Nawaz, N., Wen, S., Wang, F., Nawaz, S., Raza, J., Iftikhar, M., & Usman, M. (2022). Lysozyme and its application as antibacterial agent in food industry. *Molecules*, *27*(19), 6305.

Neuhaus, F. C., & Baddiley, J. (2003). A continuum of anionic charge: structures and functions of d-alanyl-teichoic acids in gram-positive bacteria. *Microbiology and Molecular Biology Reviews*, *67*(4), 686–723.

Oku, Y., Kurokawa, K., Matsuo, M., Yamada, S., Lee, B.-L., & Sekimizu, K. (2009). Pleiotropic roles of polyglycerolphosphate synthase of lipoteichoic acid in growth of *Staphylococcus aureus* cells. *Journal of Bacteriology*, *191*(1), 141–151.

Peschel, A., Otto, M., Jack, R., Kalbacher, H., Jung, G., & Götz, F. (1999). Inactivation of the *dlt* operon in *Staphylococcus aureus* confers sensitivity to Defensins, Protegrins, and other antimicrobial peptides. *Journal of Biological Chemistry*, *274*(13), 8405–8410.

Peschel, A., Vuong, C., Otto, M., & Götz, F. (2000). The D-alanine residues of *Staphylococcus aureus* teichoic acids alter the susceptibility to vancomycin and the activity of autolytic enzymes. *Antimicrobial Agents and Chemotherapy*, *44*(10), 2845–2847.

Pinho, M. G., de Lencastre, H., & Tomasz, A. (2001). An acquired and a native penicillin-binding protein cooperate in building the cell wall of drug-resistant staphylococci. *Proceedings of the National Academy of Sciences*, *98*(19), 10886–10891.

Placencia, F. X., Kong, L., & Weisman, L. E. (2009). Treatment of methicillin-resistant *Staphylococcus aureus* in neonatal mice: Lysostaphin versus vancomycin. *Pediatric Research*, *65*(4), 420–424.

Qamar, A., & Golemi-Kotra, D. (2012). Dual roles of FmtA in *Staphylococcus aureus* cell wall biosynthesis and autolysis. *Antimicrobial Agents and Chemotherapy*, *56*(7), 3797–3805.

Rahman, M. M., Hunter, H. N., Prova, S., Verma, V., Qamar, A., & Golemi-Kotra, D. (2016). The *Staphylococcus aureus* methicillin resistance factor FmtA is a d-amino esterase that acts on teichoic acids. *mBio*, *7*(1).

Santa Maria, J. P., Sadaka, A., Moussa, S. H., Brown, S., Zhang, Y. J., Rubin, E. J., Gilmore, M. S., & Walker, S. (2014). Compound-gene interaction mapping reveals distinct roles for *Staphylococcus aureus* teichoic acids. *Proceedings of the National Academy of Sciences*, *111*(34), 12510–12515.

Schindler, C. A., & Schuhardt, V. T. (1964). Lysostaphin: A new bacteriolytic agent for the Staphylococcus. *Proceedings of the National Academy of Sciences*, *51*(3), 414–421.

Schlag, M., Biswas, R., Krismer, B., Kohler, T., Zoll, S., Yu, W., Schwarz, H., Peschel, A., & Götz, F. (2010). Role of staphylococcal wall teichoic acid in targeting the major autolysin Atl. *Molecular Microbiology*, *75*(4), 864–873.

Scientific Image and Illustration Software. BioRender. (n.d.). https://www.biorender.com

Simanski, M., Gläser, R., Köten, B., Meyer-Hoffert, U., Wanner, S., Weidenmaier, C., Peschel, A., & Harder, J. (2013). *Staphylococcus aureus* subverts cutaneous defense by D-alanylation of teichoic acids. *Experimental Dermatology*, *22*(4), 294–296.

Singh, M., Chang, J., Coffman, L., & Kim, S. J. (2017). Hidden mode of action of glycopeptide antibiotics: Inhibition of wall teichoic acid biosynthesis. *The Journal of Physical Chemistry B*, *121*(16), 3925–3932.

Sun, Y., Liu, M., Niu, M., & Zhao, X. (2021). Phenotypic switching of *Staphylococcus aureus* MU50 into a large colony variant enhances heritable resistance against β-lactam antibiotics. *Frontiers in Microbiology*, *12*.

Walsh, S., Shah, A., & Mond, J. (2003). Improved pharmacokinetics and reduced antibody reactivity of lysostaphin conjugated to polyethylene glycol. *Antimicrobial Agents and Chemotherapy*, *47*(2), 554–558.

Wanner, S., Schade, J., Keinhörster, D., Weller, N., George, S. E., Kull, L., Bauer, J., Grau, T., Winstel, V., Stoy, H., Kretschmer, D., Kolata, J., Wolz, C., Bröker, B. M., & Weidenmaier, C. (2017). Wall teichoic acids mediate increased virulence in *Staphylococcus aureus*. *Nature Microbiology*, *2*(4), 16257.

Wecke, J., Madela, K., & Fischer, W. (1997). The absence of D-alanine from lipoteichoic acid and wall teichoic acid alters surface charge, enhances autolysis and increases susceptibility to methicillin in Bacillus subtilis. *Microbiology*, *143*(9), 2953–2960.

Winstel, V., Xia, G., & Peschel, A. (2014). Pathways and roles of wall teichoic acid glycosylation in *Staphylococcus aureus*. *International Journal of Medical Microbiology*, *304*(3–4), 215–221.

Wu, J. A., Kusuma, C., Mond, J. J., & Kokai-Kun, J. F. (2003). Lysostaphin disrupts *Staphylococcus aureus* and *Staphylococcus epidermidis* biofilms on artificial surfaces. *Antimicrobial Agents and Chemotherapy*, *47*(11), 3407–3414.

Wu, H., Cao, D., Liu, T., Zhao, J., Hu, X., & Li, N. (2015). Purification and characterization of recombinant human lysozyme from eggs of transgenic chickens. *PLOS ONE*, *10*(12).

Zha, J., Li, J., Su, Z., Akimbekov, N., & Wu, X. (2022). Lysostaphin: Engineering and potentiation toward better applications. *Journal of Agricultural and Food Chemistry*, *70*(37), 11441–11457.

Łęski, T. A., & Tomasz, A. (2005). Role of penicillin-binding protein 2 (PBP2) in the antibiotic susceptibility and cell wall cross-linking of *Staphylococcus aureus*: Evidence for the cooperative functioning of PBP2, PBP4, and PBP2A. *Journal of Bacteriology*, *187*(5), 1815–1824.

Chapter Four:

Summary and Future Directions

This study primarily focused on the D-Ala modification of WTAs in *S. aureus*, with the specific objective of elucidating the physiological changes in these microorganisms following the removal of D-Ala using exogenous FmtA. Previous research in this field has extensively documented the role and synthesis of WTAs on the surface of *S. aureus*, identifying them as potential therapeutic targets in our ever-present battle against bacterial antibiotic resistance. Studies have gone further and also highlighted the role of WTA D-Ala. Based on these findings, we hypothesized that the utilization of native FmtA, which severs the bond between D-Ala and WTAs (Rahman et al., 2016), would induce significant changes in *S. aureus* viability and growth under various laboratory conditions.

In the first chapter, we demonstrated that the enzymatic activity of FmtA successfully catalyzed the removal of D-Ala from WTAs *in vivo*, and we quantified the amount of released D-Ala in both *in vivo* and *in vitro* conditions. Our findings showed that FmtA effectively cleaved D-Ala from WTAs within the cell envelope, with higher concentrations of FmtA correlating with increased levels of unbound D-Ala. This phenomenon was observed not only in *S. aureus* but also in other Gram-positive strains, including *B. subtilis* and *L. plantarum*. Notably, the *L. plantarum* and *B. subtilis* exhibited greater levels of unbound D-Ala compared to *S. aureus*, suggesting that FmtA was able to remove a larger number of D-Ala from the glycerol-phosphate WTAs in these strains. The rationale for this was confirmed as our data depicted the *L. plantarum* and *B. subtilis* strains possessing a higher abundance of WTA in their envelope relative to *S. aureus,* therefore also increasing the relative abundance of D-Ala. Interestingly, both *B. subtilis* and *L. plantarum* exclusively released D-Ala even in the absence of FmtA, indicating the presence of an alternative, yet unidentified, mechanism for D-Ala release in these strains. This mechanism may confer an advantage by facilitating the removal of D-Ala. For clarification, upon the introduction of FmtA, the amount of unbound D-Ala rose considerably in these two strains. Furthermore, under optimal conditions (37°C in TSB media), RN4220 *S. aureus* cells displayed an average D-Ala/phosphate ratio of 0.27, implying that approximately one D-Ala modification occurs for every four ribitol-phosphate residues. Investigating the spatial distribution of D-Ala on WTAs in *S. aureus* strains

provides deeper insights into the structural organization of WTAs and allows for more accurate determination of their molecular weight, which was calculated to be 19,811.06 g/mol for RN4220 *S. aureus* under these favorable conditions.

The growth rate of *S. aureus* was investigated to determine whether the removal of D-Ala from WTA by exogenous FmtA would affect the organism's viability. *S. aureus* RN4220 cells were initially cultured under optimal laboratory conditions at 37°C in TSB media, free from external stressors. The experimental design included two approaches: pre-incubation of cells with FmtA prior to growth measurements, and continuous FmtA incubation during the growth in TSB. In the pre-incubation study, cultures treated with 10 μM and 20 μM FmtA yielded growth patterns similar to those of untreated controls. Likewise, when cells were continuously exposed to 0.2 μM or 20 μM FmtA, the results remained unchanged. Hence, we concluded that under stress-free conditions, the D-Ala modification on WTA is not crucial for normal cell growth, indicating that cell viability remains unaffected by the removal of D-Ala from WTA.

Upon *S. aureus* exposure to stressors, deviations in cell lysis rates were observed. When the cells were treated with the antimicrobial agent lysozyme, the lysis patterns were comparable between cells incubated with and without FmtA. This indicated that the accessibility of the peptidoglycan to lysozyme was not affected, regardless of the presence or absence of D-Ala. However, a notable change in cell viability was detected when the cells were exposed to lysostaphin. The cell culture that underwent D-Ala removal exhibited a significantly faster lysis rate compared to those not incubated with FmtA. This increased susceptibility to lysostaphin suggests that D-Ala removal enhances the ability of lysostaphin to reach its target, thereby reducing cell viability. We hypothesize that this effect is a result of electrostatic alterations on the cell surface resulting from D-Ala removal. The loss of the positive charge contributed by D-Ala led to a highly negative cell surface, which likely increased the attraction of the positively charged lysostaphin (Walsh et al., 2003) to the cell wall, accelerating the lysis process and ultimately decreasing cell viability. A similar observation was observed by Peschel et al. (2000).

In the latter part of the third chapter, we report on the alteration in the MIC of oxacillin for multiple MSSA and MRSA strains following the enzymatic hydrolysis of the bond between D-Ala and WTAs via FmtA. This investigation was conducted to elucidate the contribution of D-Ala on WTA to antibiotic susceptibility and to determine whether its removal influences the susceptibility of both β-lactam-sensitive and β-lactam-resistant *S. aureus* strains.

Beginning with the two MSSA strains, MSSA 1112 and SA 113, the removal of D-Ala resulted in a 2-fold increase in oxacillin MIC, as indicated by the observable cell survival at an oxacillin concentration of 0.125 μg/ml. In contrast, no surviving cells were detected in cultures not subjected to FmtA treatment at the same oxacillin concentration. This phenomenon may be attributed to an alteration in autolytic activity occurring at the bacterial cell wall; the removal of D-Ala using FmtA resulted in autolysis impediment, consistent with results obtained from other studies (Qamar and Golemi-Kotra, 2012; Peschel et al., 2000). This led to increased peptidoglycan integrity and bacterial viability. In conjunction with this alteration, the bacterial cells may be switching their GlcNAc modifications from the α-variant to the β-configuration (Mistretta et al., 2019). These mechanisms may collectively contribute to the heightened antibiotic resistance observed in MSSA strains upon D-Ala depletion. Notably, the SA 113 *Δfmta* mutant strain exhibited a 4-fold decrease in susceptibility compared to its wild-type counterpart, a phenotype that was consistently observed regardless of the presence or absence of exogenous FmtA. We hypothesize that the observed phenomenon was likely due to an increase in steric hinderance of oxacillin caused by elevated levels of D-Ala. This mutant strain, which lacks the ability to endogenously synthesize FmtA, is expected to experience an elevated quantity of D-Ala attached to WTA compared to the wild-type SA 113 (Rahman et al., 2016). Consequently, the elevated concentration of D-Ala would thereby inhibit oxacillin from reaching its target. Upon the exogenous inclusion of FmtA, there was no change in colony formation observed for the oxacillin concentrations tested, which could be attributed to the occurrence of opposing forces: a reduction in cell autolysis, as well as a decrease in steric hinderance of oxacillin due to the removal of D-Ala.

MRSA strains N315 and MU50 were subjected to varying concentrations of oxacillin to assess the role of D-alanylation in β-lactam resistance. The MU50 strain was significantly more resistant compared to N315. In contrast to MSSA strains, the MIC of oxacillin for N315, in the presence of exogenous FmtA, was reduced to 2 μg/ml, representing a 4-fold decrease relative to N315 without FmtA exposure. We believe that the reduction in antibiotic resistance in N315, upon incubation with FmtA, is linked to the delocalization of PBP2a, the primary resistance mechanism in MRSA strains. Previously, our group has indicated that an *in vitro* interaction occurs between WTAs and PBP2a, which could potentially be observed *in vivo*, leading to the belief that WTAs are essential for optimal localization of PBP2a (Qamar and Golemi-Kotra, 2012). We postulate

that the D-Ala modification on WTAs plays a role in this localization process. Consequently, hydrolysis of the bond between D-Ala and WTA may result in partial delocalization of PBP2a, thereby increasing susceptibility, as oxacillin is targeting other PBPs to weaken the peptidoglycan. A similar theory was proposed by Coupri et al. (2021). Conversely, no change in the oxacillin MIC was observed for MU50 following FmtA treatment. This likely reflects the reduced cross-linking characteristic of VISA strains (Cui et al., 2000), which could indicate lower PBP activity, thus limiting oxacillin binding to these PBPs regardless of FmtA presence. Additionally, an elevated WTA and D-Ala synthesis observed in some VISA strains (Hort et al., 2021) may further prevent any reduction in antibiotic resistance as seen in MU50.

In conclusion, our studies have revealed several key aspects of *S. aureus* physiology. Firstly, FmtA has been demonstrated to remove D-Ala from WTAs in *S. aureus* and other Gram-positive bacteria *in vivo*. Secondly, alterations in *S. aureus* physiology, particularly in relation to viability, resulting from FmtA-mediated hydrolysis of the D-Ala-WTA bond, are observed exclusively under conditions of bacterial stress. Within such stress-inducing environments, the viability of *S. aureus* may either increase or decrease in the presence of FmtA, contingent upon two factors: the type of *S. aureus* strain being studied and the type of applied stressor, whether it be an antibiotic or another antimicrobial agent.

Future Directions

We hypothesize that the decreased MIC of oxacillin for the N315 strain is attributable to the partial delocalization of PBP2a following the removal of D-Ala from WTA. To validate this hypothesis, further experimental investigation is required. Future studies should focus on evaluating whether PBP2a undergoes delocalization upon co-incubation with FmtA and oxacillin. This can be achieved by coupling fluorescence markers to PBP2a, enabling the visualization of its potential delocalization. Additionally, similar experiments could be conducted to investigate whether the synthesis or localization of PBP enzymes, including PBP2a, is altered in VISA strains, such as MU50. Insights from these VISA studies could reveal whether the reduction in peptidoglycan cross-linking correlates with diminished PBP activity, which would justify the MIC of MU50 remaining unchanged following the removal of D-Ala. A reduction in PBP activity or

synthesis would theoretically be accompanied by a diminished oxacillin activity, given that PBPs are the primary targets of oxacillin antibiotics (Bush and Bradford, 2016).

Our investigation into FmtA-mediated D-Ala removal has revealed that the loss of D-Ala from *S. aureus* WTAs can have both advantageous and detrimental effects on cell viability. However, further research into the FmtA-D-Ala interaction and its impact on *S. aureus* physiology may deepen our understanding. In our study, oxacillin was employed as the representative β-lactam antibiotic in the MIC assays. While oxacillin effectively indicates changes in β-lactam MICs, future studies incorporating a broader range of β-lactams, including cephalosporins, are necessary for a more comprehensive assessment of MIC alterations in MSSA and MRSA strains. As demonstrated by published research, different β-lactams do not exhibit the same MICs for the same *S. aureus* strains. N315 and SA 113 strains exhibit varied MICs depending on the specific cephalosporin or β-lactam tested (Beltramini et al., 2009; Göhring et al., 2011; Ubukata et al., 1989). Consequently, the extent of MIC alteration in both MSSA and MRSA strains may vary, with certain β-lactams potentially demonstrating greater synergy or antagonism with FmtA, resulting in either enhanced or reduced antibiotic resistance. Furthermore, exploring the use of vancomycin, a cornerstone antibiotic in the treatment of MRSA infections over the past half century, could yield additional insights. Vancomycin is employed for the use against a wide range of bacterial strains where β-lactams are no longer effective (Rose et al., 2022). It would be of significant interest to observe how the activity of heavily relied-upon antibiotics like vancomycin change following exogenous FmtA incubation and D-Ala removal in MRSA strains, such as MU50 and N315.

The physiological alterations in RN4220 *S. aureus* resulting from D-Ala removal were observed under both antibiotic and antimicrobial protein exposure as well as in nutrient-rich, stress-free environments. However, there are numerous additional stressors to which *S. aureus* can be subjected, potentially yielding relevant data regarding cell viability and physiological changes following FmtA incubation. *S. aureus*, like other bacteria, have specific optimal growth conditions, including temperature, salt concentration, and nutrient availability (Missiakas and Schneewind, 2013). Deviations from these optimal conditions are likely to induce cellular stress, resulting in either adaptation or cell death. Future studies could explore *S. aureus* viability assays in which FmtA is incubated under conditions that deviate from these optimal requirements. These experiments would investigate whether FmtA-mediated D-Ala removal influences the survival of *S. aureus* under a sub-optimal temperature, salt concentration, or pH condition. The D-Ala

incorporation into the cell envelope of *S. aureus* is maintained, provided that alterations in temperature, pH, and salt concentration do not exceed defined parameters (Hurst et al., 1975; Koch et al., 1985; MacArthur and Archibald, 1984).

It would be worthwhile to investigate whether other strains of *S. aureus*, including MSSA and MRSA strains, exhibit a D-Ala/Pi ratio comparable to the RN4220 strain analyzed in this study. Should variations be observed, would it likely result from differences in ribitol subunits or D-Ala modifications? The possible occurrence of either of these two WTA differentiations would further enhance our understanding of the physiological distinctions across different *S. aureus* strains.

Several limiting factors are associated with the research conducted in this thesis, particularly in the growth and lysis experiments. In these experiments, only the wild-type strain RN4220 was used to assess viability alterations resulting from D-Ala removal by FmtA. In future studies, mutant strains may serve as appropriate controls to further evaluate changes in *S. aureus* physiology following FmtA incubation. For instance, the RN4220 Δ*fmtA* strain, in which the *fmtA* gene has been deleted, would provide valuable insights into cellular behavior when an increased number of D-Ala modifications are present on WTAs. It would also help us understand how the absence of this gene affects cell growth or lysis upon exogenous addition or absence of FmtA. Additionally, utilizing RN4220 Δ*dltA* cells would help elucidate growth and lysis patterns in the complete absence of D-Ala modifications on WTAs. In this thesis, FmtA was employed to remove D-Ala from WTAs; however, as a control variable, it would be beneficial to examine how cell viability is affected when the cells can no longer synthesize D-Ala. These mutant strains would provide essential data on the role of FmtA in *S. aureus* physiology.

Furthermore, we introduced experiments conducted on planktonic *S. aureus* cells treated with FmtA. However, as discussed, *S. aureus* is capable of forming stationary biofilms during its life cycle, a process regulated by controlling the quantity of both the WTAs and the FmtA protein (Qamar and Golemi-Kotra, 2012). Altering D-Ala WTA content through exogenous FmtA incubation may lead to noticeable changes in *S. aureus* biofilm development. Future experiments could be designed in two ways. First, cells could be incubated with FmtA to assess how D-Ala removal influences biofilm formation, similar to Qamar and Golemi-Kotra (2012). Second, FmtA incubation could be performed after biofilm formation to evaluate its impact on biofilm integrity. Additional variables, such as antibiotics, could be introduced to explore potential synergistic effects. An important question to consider during experimental planning is whether FmtA can

effectively penetrate the extracellular matrix and remove D-Ala from WTAs. Given that biofilms are integral for *S. aureus* survival and are influenced by D-Ala-modified WTAs, further investigation into the role of FmtA in biofilm formation would be highly valuable.

References

Beltramini, A. M., Mukhopadhyay, C. D., & Pancholi, V. (2009). Modulation of cell wall structure and antimicrobial susceptibility by a *Staphylococcus aureus* eukaryote-like serine/threonine kinase and phosphatase. *Infection and Immunity*, *77*(4), 1406–1416.

Bush, K., & Bradford, P. A. (2016). B-lactams and β-lactamase inhibitors: An overview. *Cold Spring Harbor Perspectives in Medicine*, *6*(8).

Coupri, D., Verneuil, N., Hartke, A., Liebaut, A., Lequeux, T., Pfund, E., & Budin-Verneuil, A. (2021). Inhibition of d-alanylation of teichoic acids overcomes resistance of methicillin-resistant *Staphylococcus aureus*. *Journal of Antimicrobial Chemotherapy*, *76*(11), 2778–2786.

Cui, L., Murakami, H., Kuwahara-Arai, K., Hanaki, H., & Hiramatsu, K. (2000). Contribution of a thickened cell wall and its glutamine nonamidated component to the vancomycin resistance expressed by *Staphylococcus aureus* MU50. *Antimicrobial Agents and Chemotherapy*, *44*(9), 2276–2285.

Göhring, N., Fedtke, I., Xia, G., Jorge, A. M., Pinho, M. G., Bertsche, U., & Peschel, A. (2011). New role of the disulfide stress effector YjbH in β-lactam susceptibility of *Staphylococcus aureus*. *Antimicrobial Agents and Chemotherapy*, *55*(12), 5452–5458.

Hort, M., Bertsche, U., Nozinovic, S., Dietrich, A., Schrötter, A. S., Mildenberger, L., Axtmann, K., Berscheid, A., & Bierbaum, G. (2021). The role of β-glycosylated wall teichoic acids in the reduction of vancomycin susceptibility in vancomycin-intermediate *Staphylococcus aureus*. *Microbiology Spectrum*, *9*(2).

Hurst, A., Hughes, A., Duckworth, M., & Baddiley, J. (1975). Loss of D-alanine during sublethal heating of *Staphylococcus aureus* S6 and magnesium binding during repair. *Journal of General Microbiology*, *89*(2), 277–284.

Koch, H. U., Döker, R., & Fischer, W. (1985). Maintenance of D-alanine ester substitution of lipoteichoic acid by reesterification in *Staphylococcus aureus*. *Journal of Bacteriology*, *164*(3), 1211–1217.

MacArthur, A. E., & Archibald, A. R. (1984). Effect of culture pH on the D-alanine ester content of lipoteichoic acid in *Staphylococcus aureus*. *Journal of Bacteriology*, *160*(2), 792–793.

Missiakas, D. M., & Schneewind, O. (2013). Growth and laboratory maintenance of *Staphylococcus aureus*. *Current Protocols in Microbiology*, *Chapter 9*, Unit–9C.1.

Mistretta, N., Brossaud, M., Telles, F., Sanchez, V., Talaga, P., & Rokbi, B. (2019). Glycosylation of *Staphylococcus aureus* cell wall teichoic acid is influenced by environmental conditions. *Scientific Reports*, *9*(1).

Peschel, A., Vuong, C., Otto, M., & Götz, F. (2000). The D-alanine residues of *Staphylococcus aureus* teichoic acids alter the susceptibility to vancomycin and the activity of autolytic enzymes. *Antimicrobial Agents and Chemotherapy*, *44*(10), 2845–2847.

Qamar, A., & Golemi-Kotra, D. (2012). Dual roles of FmtA in *Staphylococcus aureus* cell wall biosynthesis and autolysis. *Antimicrobial Agents and Chemotherapy*, *56*(7), 3797–3805.

Rahman, M. M., Hunter, H. N., Prova, S., Verma, V., Qamar, A., & Golemi-Kotra, D. (2016). The *Staphylococcus aureus* methicillin resistance factor FmtA is a d-amino esterase that acts on teichoic acids. *mBio*, *7*(1).

Rose, W., Volk, C., Dilworth, T. J., & Sakoulas, G. (2022). Approaching 65 years: Is it time to consider retirement of vancomycin for treating methicillin-resistant *Staphylococcus aureus* endovascular infections? *Open Forum Infectious Diseases*, *9*(5).

Ubukata, K., Nonoguchi, R., Matsuhashi, M., & Konno, M. (1989). Expression and inducibility in *Staphylococcus aureus* of the mecA gene, which encodes a methicillin-resistant *S. aureus*-specific penicillin-binding protein. *Journal of Bacteriology*, *171*(5), 2882–2885.

Walsh, S., Shah, A., & Mond, J. (2003). Improved pharmacokinetics and reduced antibody reactivity of Lysostaphin conjugated to polyethylene glycol. *Antimicrobial Agents and Chemotherapy*, *47*(2), 554–558.

Appendix: Raw Data, Standards, and CFU/ml Plates

Appendix A: Florescent Enzyme Coupled Assay D-Ala Standard

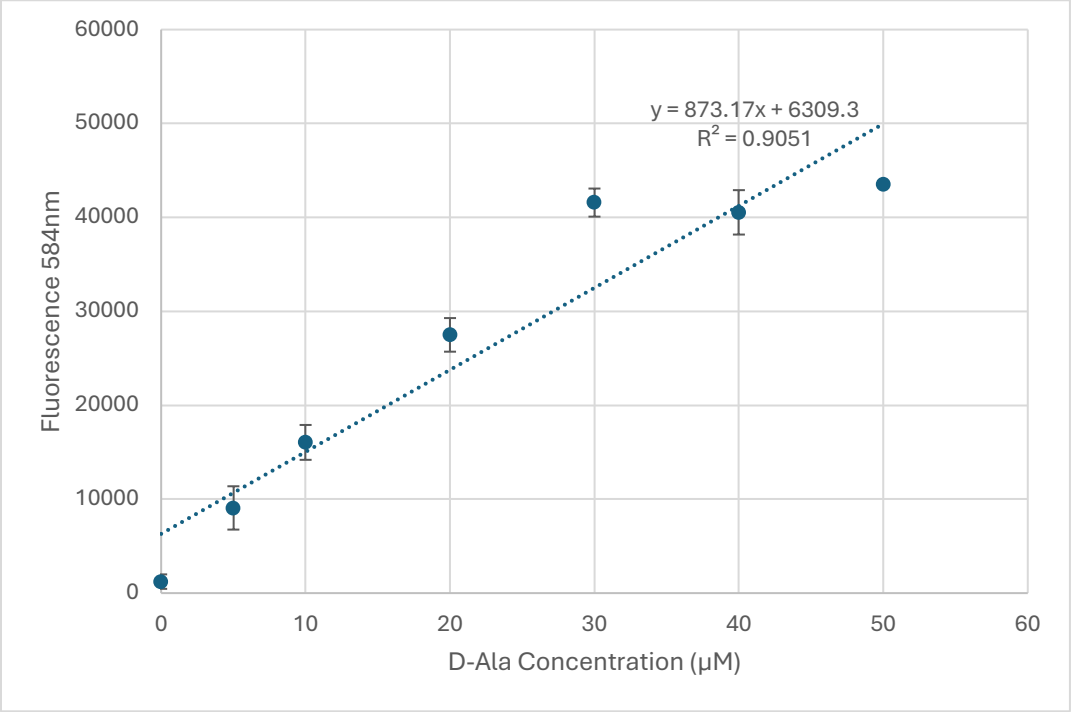

Figure 27. Illustration of the fluorescent enzyme coupled assay D-Ala standard graph. The graph displays the equation derived from the fluorescent values recorded at various concentrations of the D-Ala amino acid. As a result of the correlation between resorufin fluorescence and D-Ala concentration, the graph indicates that amplified resorufin fluorescence corresponds to increased D-Ala concentration in solution. A 563 nm excitation wavelength was utilized followed by an emission wavelength of 584 nm to record the values. The standard graph was utilised to quantify the sum of D-Ala released from isolated WTA of *S. aureus* RN4220. The standard D-Ala fluorescence assay was repeated twice, with three replicates for each trial, and the mean fluorescence intensity was calculated and plotted with ± standard deviation based on the data from these two trials.

Appendix B: ^{1}H-NMR D-Ala Standard Graph

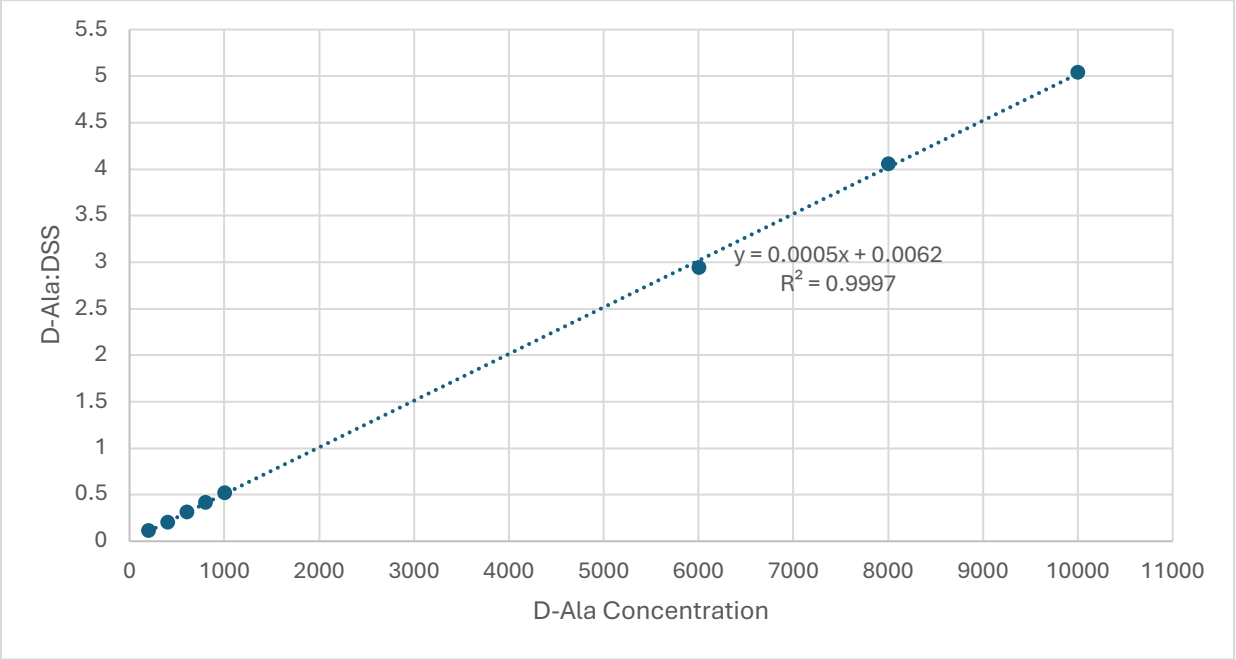

Figure 28. ^{1}H-NMR D-Ala standard, illustrating D-Ala concentrations ranging from 200 µM to 10 mM. The graph displays the ratio of D-Ala to DSS at each concentration, based on peak height integration. This standard curve serves to quantify the total D-Ala concentration in isolated WTA samples based on ^{1}H-NMR. Standard deviation is approximately 3% - 5%.

Appendix C: ^{1}H-NMR *S. aureus* RN4220 D-Ala Release Negative Control

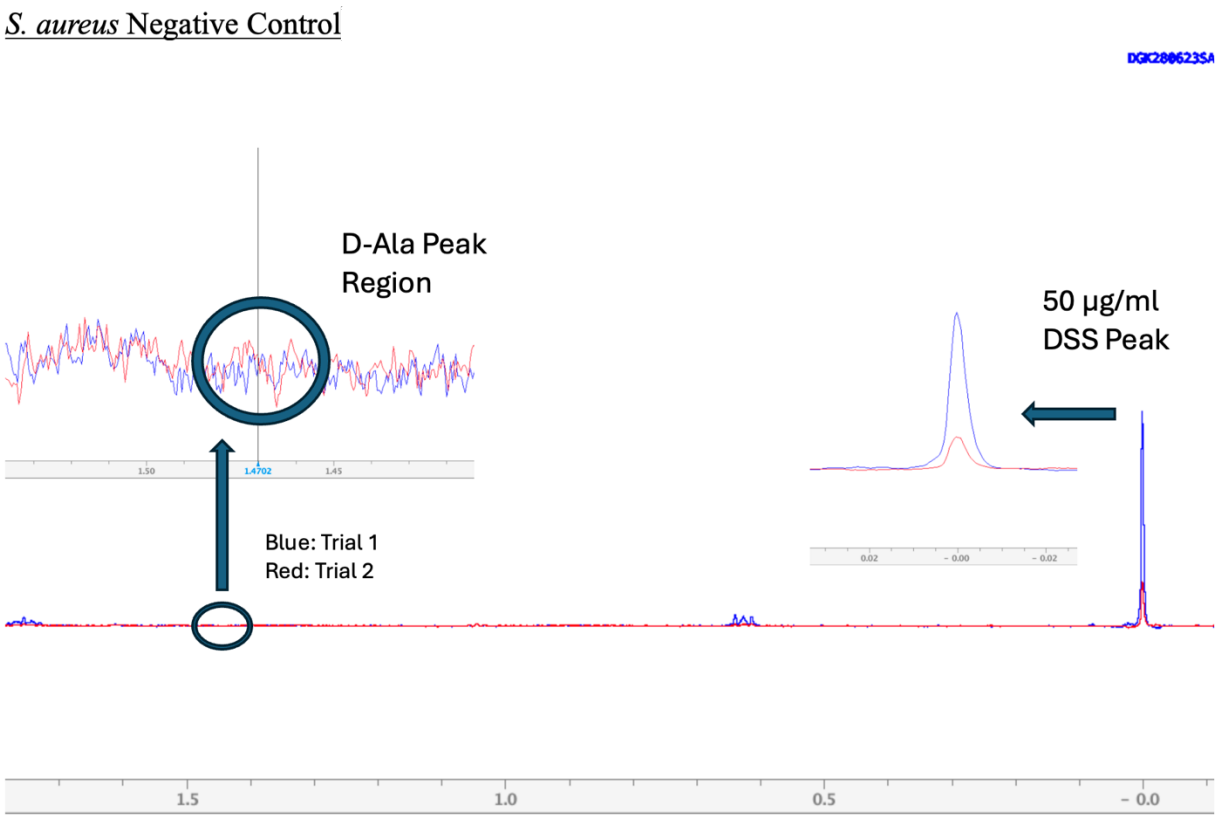

Figure 29. ^{1}H-NMR data depicting D-Ala release from RN4220 cells incubated with no FmtA. This figure is a partial ^{1}H-NMR spectrum for RN4220 D-Ala release without FmtA incubation and portrays two trials conducted. The D-Ala peak region is located at 1.47 ppm. Blue spectrum: Trial 1, red spectrum: Trial 2.

Appendix D: RN4220 WTA Molecular Weight Calculations

The molecular weight of the RN4220 *S. aureus* was calculated by incorporating the contributions from the glucosamine modifications (40 units estimated) (Jenni and Berger-Bächi, 1998), ribitol-phosphate backbone (40 units estimated), D-Ala residues (10 units estimated), and the linker unit comprised of glycerol-phosphate (2-3 units estimated) and both N-Acetylglucosamine and N-Acetylmannosamine (1 unit each) (Kojima et al., 1985). This figure summarizes the molecular weight of each WTA component, and the calculation performed to obtain the total average molecular weight of WTA based on the D-Ala data recorded in Table 3.

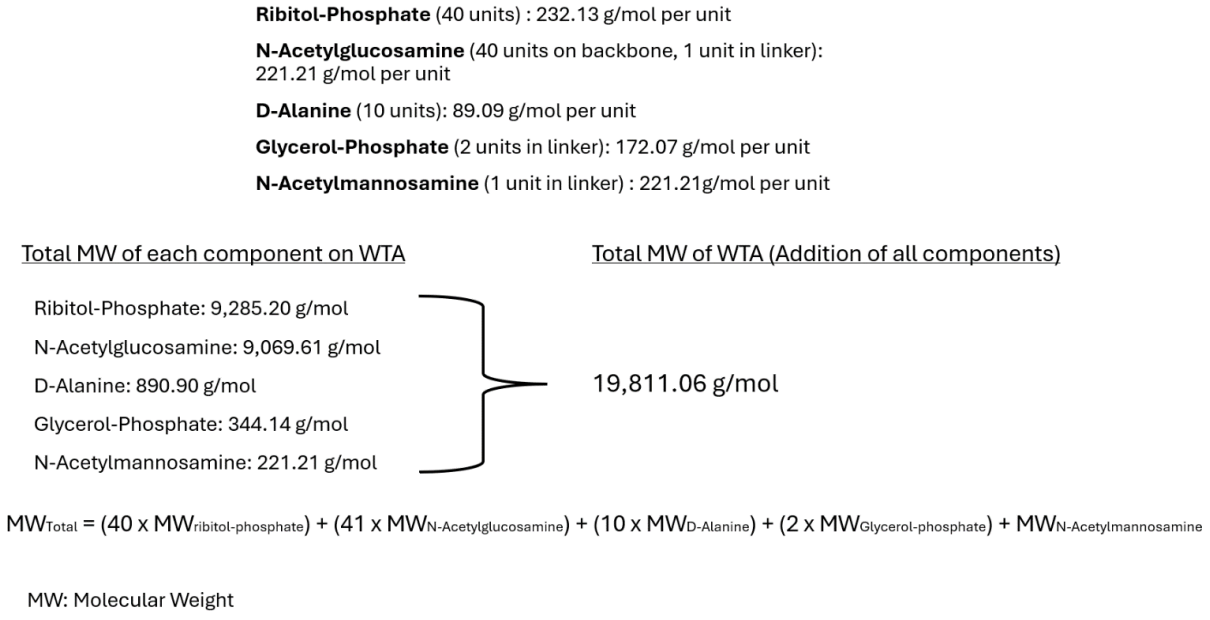

Figure 30. The average total molecular weight of WTA, derived from the sum of its integral components. Each component's molecular weight is presented alongside the number of repetitions within the polymer. The molecular weight of each component was multiplied by its respective repetition count, and the resulting values were combined to determine the total molecular weight.

Appendix E: *S. aureus* RN4220 One Hour Incubation with FmtA Prior to Growth in TSB Media

Table 5. OD_{600} measurements were recorded from three independent trials representing *S. aureus* RN4220 growth dynamics over time. The RN4220 cells were subjected to 10 µM or 20 µM FmtA to elucidate potential alterations in growth patterns attributed to D-Ala removal from WTAs. Cell pellets were initially cultured, normalized by weight for consistency in each trial, incubated with the desired concentration of FmtA for one hour, and allowed to grow in optimal TSB media for a total of 360 minutes. Measurements were recorded every 40 minutes as growth occurred at 37°C. The values for each trial are listed, alongside the mean ± standard deviation.

RN4220 + 10 µM FmtA (OD 600 nm)					
Time (min)	Trial 1	Trial 2	Trial 3	Average	Standard Deviation ±
40	0.03	0.02	0.02	0.02	0.00
80	0.07	0.06	0.08	0.07	0.01
120	0.19	0.23	0.22	0.21	0.02
160	0.67	0.81	0.67	0.71	0.08
200	1.60	1.93	1.64	1.72	0.18
240	2.63	2.81	2.70	2.71	0.09
300	3.78	3.87	3.29	3.65	0.31
360	4.82	3.72	4.34	4.30	0.55
Bacterial Pellet Weig	65.3 mg	54.7 mg	60.4 mg		
RN4220 without FmtA (OD 600 nm)					
Time (min)	Trial 1	Trial 2	Trial 3	Average	Standard Deviation ±
40	0.03	0.02	0.02	0.02	0.00
80	0.08	0.09	0.09	0.09	0.01
120	0.25	0.26	0.21	0.24	0.02
160	0.81	0.79	0.69	0.76	0.06
200	1.92	1.97	2.16	2.02	0.13
240	2.91	2.82	3.04	2.92	0.11
300	3.54	3.41	4.05	3.67	0.34
360	5.45	5.27	4.01	4.91	0.79
Bacterial Pellet Weig	65.8 mg	55 mg	59.6 mg		
RN4220 + 20 µM FmtA (OD 600 nm)					
Time (min)	Trial 1	Trial 2	Trial 3	Average	Standard Deviation ±
40	0.02	0.02	0.03	0.02	0.00
80	0.09	0.07	0.09	0.08	0.01
120	0.30	0.26	0.28	0.28	0.02
160	0.92	0.83	0.83	0.86	0.05
200	1.67	1.70	1.63	1.67	0.03
240	3.00	2.72	2.70	2.81	0.17
300	4.40	4.77	4.32	4.50	0.24
360	3.09	6.17	3.53	4.26	1.67
Bacterial Pellet Weig	55.9 mg	44 mg	57.1 mg		
RN4220 without FmtA (OD 600 nm)					
Time (min)	Trial 1	Trial 2	Trial 3	Average	Standard Deviation ±
40	0.03	0.02	0.03	0.03	0.01
80	0.14	0.06	0.12	0.11	0.04
120	0.45	0.24	0.38	0.36	0.11
160	1.18	0.78	1.08	1.01	0.21
200	2.03	1.60	1.91	1.85	0.22
240	3.49	2.58	3.16	3.08	0.46
300	4.21	4.66	4.33	4.40	0.23
360	4.89	4.09	3.88	4.29	0.54
Bacterial Pellet Weig	56.3 mg	43.2 mg	56.2 mg		

Table 6. CFU/ml calculations were derived from three independent trials representing *S. aureus* RN4220 growth dynamics over time. The RN4220 cells were subjected to 10 μM or 20 μM FmtA to elucidate potential alterations in growth patterns attributed to D-Ala removal from WTAs. Cell pellets were initially cultured, normalized by weight for consistency in each trial, incubated with the desired concentration of FmtA for one hour, and allowed to grow in optimal TSB media for a total of 360 minutes. At 40-minute intervals, an aliquot of each solution was serially diluted and plated onto TSB-Agar plates. Subsequently, these plates were incubated at 37ºC for 16 hours to facilitate colony formation. CFU/ml was determined by enumeration of the colonies observed on the agar at every time point. The results were recorded for each trial, averaged, and displayed alongside ± standard deviation calculations.

RN4220 + 10 μM FmtA (CFU/ml)					
Time (min)	Trial 1	Trial 2	Trial 3	Average	Standard Deviation ±
40	8.00E+06	6.67E+06	8.00E+06	7.56E+06	7.70E+05
80	1.20E+07	4.00E+06	8.00E+06	8.00E+06	4.00E+06
120	2.87E+07	1.67E+07	1.67E+07	2.07E+07	6.93E+06
160	5.73E+07	5.60E+07	5.93E+07	5.76E+07	1.68E+06
200	1.73E+08	2.20E+08	2.67E+08	2.20E+08	4.67E+07
240	5.33E+08	4.67E+08	6.40E+08	5.47E+08	8.74E+07
300	8.07E+08	7.60E+08	8.27E+08	7.98E+08	3.42E+07
360	7.53E+08	6.80E+08	8.93E+08	7.76E+08	1.08E+08
Bacterial Pellet Weight	65.3 mg	54.7 mg	60.4 mg		
RN4220 without FmtA (CFU/ml)					
Time (min)	Trial 1	Trial 2	Trial 3	Average	Standard Deviation ±
40	6.00E+06	2.67E+06	8.00E+06	5.56E+06	2.69E+06
80	8.00E+06	9.33E+06	1.13E+07	9.56E+06	1.68E+06
120	2.93E+07	2.47E+07	3.27E+07	2.89E+07	4.02E+06
160	7.87E+07	6.00E+07	8.87E+07	7.58E+07	1.46E+07
200	2.93E+08	3.40E+08	4.27E+08	3.53E+08	6.77E+07
240	6.53E+08	5.60E+08	7.47E+08	6.53E+08	9.33E+07
300	7.20E+08	8.07E+08	8.47E+08	7.91E+08	6.48E+07
360	8.00E+08	6.93E+08	8.87E+08	7.93E+08	9.68E+07
Bacterial Pellet Weight	65.8 mg	55 mg	59.6 mg		
RN4220 + 20 μM FmtA (CFU/ml)					
Time (min)	Trial 1	Trial 2	Trial 3	Average	Standard Deviation ±
40	8.67E+06	4.67E+06	8.67E+06	7.33E+06	2.31E+06
80	1.40E+07	7.33E+06	1.47E+07	1.20E+07	4.06E+06
120	3.60E+07	3.07E+07	3.53E+07	3.40E+07	2.91E+06
160	8.73E+07	7.27E+07	8.33E+07	8.11E+07	7.58E+06
200	4.00E+08	2.93E+08	4.93E+08	3.96E+08	1.00E+08
240	6.87E+08	6.13E+08	8.13E+08	7.04E+08	1.01E+08
300	6.40E+08	6.47E+08	8.73E+08	7.20E+08	1.33E+08
360	7.93E+08	7.20E+08	8.33E+08	7.82E+08	5.75E+07
Bacterial Pellet Weight	55.9 mg	44 mg	57.1 mg		
RN4220 without FmtA (CFU/ml)					
Time (min)	Trial 1	Trial 2	Trial 3	Average	Standard Deviation ±
40	8.67E+06	5.33E+06	1.60E+07	1.00E+07	5.46E+06
80	2.13E+07	8.00E+06	1.33E+07	1.42E+07	6.71E+06
120	4.13E+07	2.93E+07	3.53E+07	3.53E+07	6.00E+06
160	1.09E+08	6.67E+07	1.00E+08	9.18E+07	2.22E+07
200	4.80E+08	2.40E+08	5.53E+08	4.24E+08	1.64E+08
240	6.93E+08	4.80E+08	8.00E+08	6.58E+08	1.63E+08
300	6.40E+08	5.27E+08	8.00E+08	6.56E+08	1.37E+08
360	7.47E+08	4.07E+08	8.33E+08	6.62E+08	2.26E+08
Bacterial Pellet Weight	56.3 mg	43.2 mg	56.2 mg		

Appendix F: *S. aureus* RN4220 Growth with Continuous FmtA Incubation in TSB Media

Table 7. The OD_{600} absorbance values of three independent replicates of the same initial trial were recorded to assess the growth kinetics of *S. aureus* RN4220 over time under constant exogenous FmtA exposure. RN4220 cells were cultured, washed, and resuspended in TSB media containing 20 µM FmtA. The cells were grown at 37°C and the OD_{600} measurements were taken at 40-minute intervals for a total duration of 300 minutes. A control group was included, comprising of cells without exposure to the FmtA enzyme, for comparative analysis. The dataset includes values for individual replicates, the mean of the three replicates, and the ± standard deviation for each time point.

RN4220 + 20 µM FmtA (OD 600nm)					
Time (min)	Replicate 1	Replicate 2	Replicate 3	Average	Standard Deviation (±)
40	0.07	0.077	0.075	0.07	0.00
80	0.094	0.106	0.1	0.10	0.01
120	0.153	0.155	0.159	0.16	0.00
160	0.285	0.284	0.293	0.29	0.00
200	0.472	0.499	0.486	0.49	0.01
240	0.699	0.748	0.712	0.72	0.03
300	0.808	0.794	0.79	0.80	0.01
RN4220 with no FmtA (OD 600nm)					
Time (min)	Replicate 1	Replicate 2	Replicate 3	Average	Standard Deviation (±)
40	0.06	0.056	0.057	0.06	0.00
80	0.072	0.067	0.072	0.07	0.00
120	0.125	0.121	0.123	0.12	0.00
160	0.246	0.246	0.251	0.25	0.00
200	0.411	0.42	0.409	0.41	0.01
240	0.642	0.673	0.662	0.66	0.02
300	0.747	0.748	0.733	0.74	0.01

Table 8. The CFU/ml values of three independent replicates of the same initial trial were recorded to assess the growth kinetics of *S. aureus* RN4220 over time under constant exogenous FmtA exposure. RN4220 cells were cultured, washed, and resuspended in TSB media containing 20 μM FmtA. The cells were grown at 37ºC, and every 40 minutes, an aliquot of the cell culture was diluted and plated onto TSB-Agar plates. The plates were subsequently incubated for 16 hours at 37ºC, after which colony enumeration was performed to calculate CFU/ml for each time point. This growth assay was conducted for a total of 300 minutes. A control group was included, comprising of cells without exposure to the FmtA enzyme, for comparative analysis. The dataset includes values for individual replicates, the mean of the three replicates, and the ± standard deviation for each time point.

RN4220 + 20 μM FmtA (CFU/ml)					
Time (min)	Replicate 1	Replicate 2	Replicate 3	Average	Standard Deviation (±)
40	1.00E+07	1.02E+07	1.08E+07	1.03E+07	4.16E+05
80	1.60E+07	1.68E+07	1.56E+07	1.61E+07	6.11E+05
120	6.40E+07	5.80E+07	6.00E+07	6.07E+07	3.06E+06
160	1.44E+08	1.52E+08	1.62E+08	1.53E+08	9.02E+06
200	6.80E+08	6.20E+08	7.20E+08	6.73E+08	5.03E+07
240	1.22E+09	1.22E+09	1.18E+09	1.21E+09	2.31E+07
300	2.20E+09	2.20E+09	2.24E+09	2.21E+09	2.31E+07
RN4220 with no FmtA (CFU/ml)					
Time (min)	Replicate 1	Replicate 2	Replicate 3	Average	Standard Deviation (±)
40	1.10E+07	9.80E+06	1.04E+07	1.04E+07	6.00E+05
80	1.52E+07	1.52E+07	1.44E+07	1.49E+07	4.62E+05
120	5.60E+07	6.60E+07	6.20E+07	6.13E+07	5.03E+06
160	1.44E+08	1.44E+08	1.52E+08	1.47E+08	4.62E+06
200	6.40E+08	6.60E+08	7.00E+08	6.67E+08	3.06E+07
240	1.26E+09	1.14E+09	1.12E+09	1.17E+09	7.57E+07
300	2.04E+09	2.00E+09	1.88E+09	1.97E+09	8.33E+07

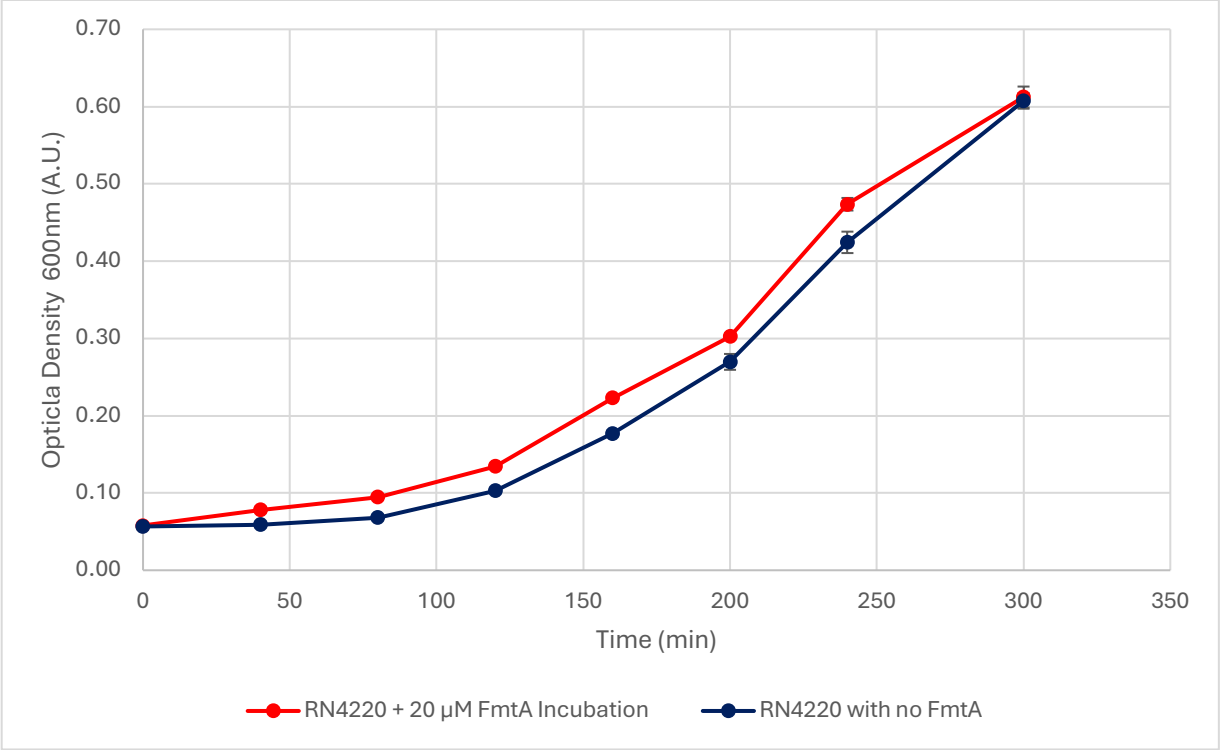

Figure 31. A second trial depicting the mean OD_{600} values of RN4220 bacterial cultures incubated with 20 µM FmtA compared to control cultures without FmtA for the entirety of growth. Following an initial wash with 50 mM sodium phosphate buffer (pH 7.2), the cells were resuspended in TSB medium. Absorbance measurements were recorded every 40 minutes, with both cultures displaying exponential growth over a 300-minute period at 37°C. The plotted values represent the average results from a single trial (three replicates of the same trial), with ± standard deviation error bars calculated from these replicates.

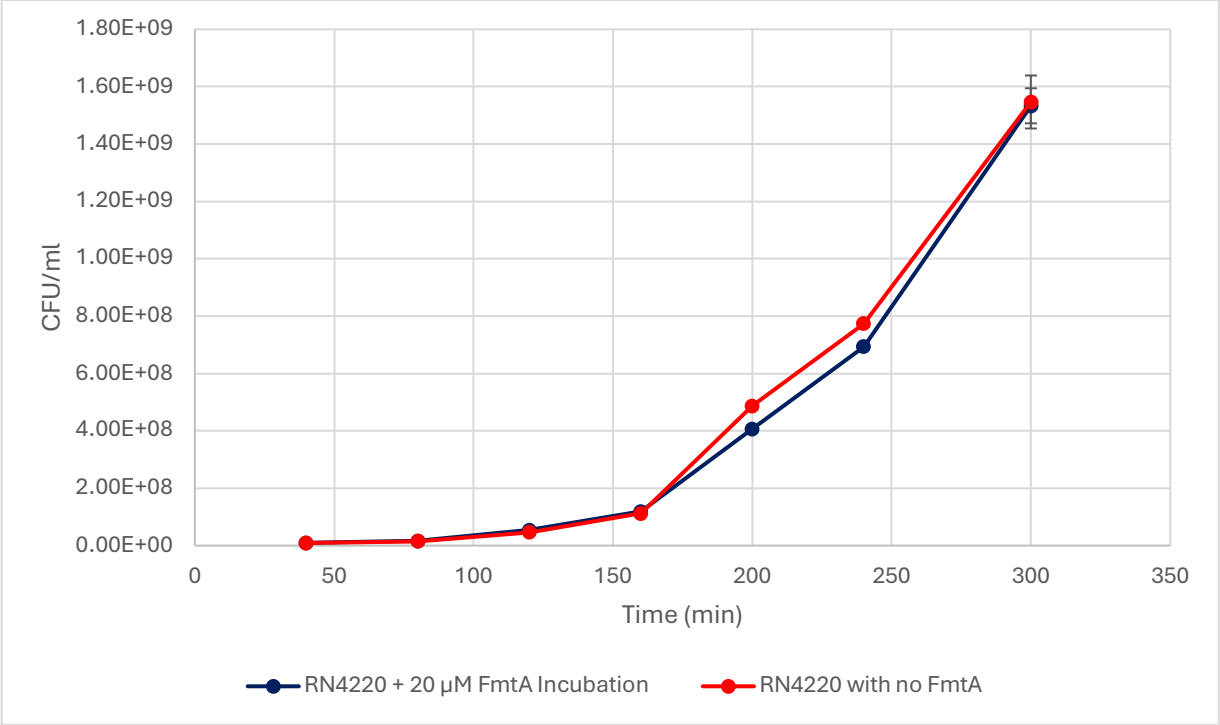

Figure 32. A second trial depicting the average CFU/ml of RN4220 cells plated onto TSB-Agar plates at 40-minute intervals over a 300-minute period from bacterial cultures incubated with or without 20 µM FmtA at 37°C. The cells were initially washed with 50 mM sodium phosphate buffer (pH 7.2) and resuspended in TSB medium. Aliquots of 5 µl from dilutions ranging from 10^{-3} to 10^{-5} were plated in triplicate to obtain a precise average of colony formation at each time point. Plates were incubated at 37°C for 13 hours to facilitate colony development. The graph presents the mean results from a single trial (three separate colony formations of the same trial), with ± standard deviation error bars calculated from these three replicates for each time point.

Appendix G: OD_{600} and CFU/ml of RN4220 Cell Growth Incubated with FmtA and Lysozyme

Table 9. OD_{600} measurements for RN4220 *S. aureus* cells incubated with and without 20 μM FmtA, after which both solutions were subjected to 500 μg/ml lysozyme. OD_{600} readings were recorded over time, demonstrating a growth pattern in both conditions after 360 minutes. Three trials were conducted and averaged. The initial weights of the RN4220 cell pellets were normalized prior to incubation with FmtA, and the data was presented together with ± standard deviation calculated from the three trials. The raw data from each trial is listed.

RN4220 + 20μM FtmA + Lysozyme (OD 600nm)					
Time (min)	Trial 1	Trial 2	Trial 3	Average	Standard Deviation (±)
0	0.01	0.01	0.01	0.01	0.00
40	0.02	0.03	0.04	0.03	0.01
80	0.10	0.13	0.12	0.12	0.01
120	0.36	0.44	0.35	0.38	0.05
160	1.01	1.17	1.00	1.06	0.10
200	1.70	2.09	1.85	1.88	0.20
240	2.18	3.22	2.96	2.79	0.54
300	3.32	4.16	4.17	3.89	0.49
360	3.73	4.49	4.82	4.35	0.56
Bacterial Pellet Weights:	56 mg	57 mg	55 mg		
RN4220 + Lysozyme with no FmtA (OD 600nm)					
Time (min)	Trial 1	Trial 2	Trial 3	Average	Standard Deviation (±)
0	0.01	0.01	0.01	0.01	0.00
40	0.03	0.03	0.04	0.03	0.01
80	0.13	0.12	0.14	0.13	0.01
120	0.46	0.42	0.44	0.44	0.02
160	1.14	1.14	1.16	1.15	0.01
200	2.01	2.05	2.23	2.10	0.11
240	2.54	3.35	3.23	3.04	0.44
300	3.54	4.30	4.11	3.98	0.39
360	4.07	4.83	5.04	4.65	0.51
Bacterial Pellet Weights:	56 mg	57 mg	55 mg		

Table 10. Quantification of the CFU/ml for RN4220 *S. aureus* cells incubated with and without 20 μM FmtA, after which both conditions were treated with 500 μg/ml lysozyme. Over a 240-minute time interval, both conditions exhibited increased formation of colonies on TSB-Agar plates. The experiment was conducted in triplicate, and the initial weights of the RN4220 cell pellets were normalized prior to FmtA incubation. The data was averaged and presented with ± standard deviation calculated from the three trials. The raw data from each trial is listed.

RN4220 + 20μM FmtA + Lysozyme (CFU/ml)					
Time (min)	Trial 1	Trial 2	Trial 3	Average	Standard Deviation (±)
40	7.33E+06	1.73E+07	1.67E+07	1.38E+07	5.59E+06
80	1.13E+07	1.53E+07	1.20E+07	1.29E+07	2.14E+06
120	4.33E+07	5.67E+07	5.53E+07	5.18E+07	7.34E+06
160	2.67E+08	3.60E+08	3.27E+08	3.18E+08	4.73E+07
200	6.53E+08	6.20E+08	6.07E+08	6.27E+08	2.40E+07
240	9.33E+08	9.53E+08	9.93E+08	9.60E+08	3.06E+07
300	1.06E+09	1.09E+09	1.16E+09	1.10E+09	5.18E+07
360	1.10E+09	1.12E+09	1.37E+09	1.20E+09	1.49E+08
Bacterial Pellet Weights:	56 mg	57 mg	55 mg		
RN4220 + Lysozyme with no FmtA (CFU/ml)					
Time (min)	Trial 1	Trial 2	Trial 3	Average	Standard Deviation (±)
40	1.00E+07	1.00E+07	1.27E+07	1.09E+07	1.54E+06
80	1.53E+07	1.53E+07	1.53E+07	1.53E+07	0.00E+00
120	5.13E+07	5.27E+07	5.13E+07	5.18E+07	7.70E+05
160	3.87E+08	3.80E+08	4.00E+08	3.89E+08	1.02E+07
200	6.80E+08	7.07E+08	7.27E+08	7.04E+08	2.34E+07
240	1.00E+09	9.73E+08	1.03E+09	1.00E+09	2.67E+07
300	9.73E+08	1.14E+09	1.19E+09	1.10E+09	1.12E+08
360	1.19E+09	1.33E+09	1.19E+09	1.24E+09	7.70E+07
Bacterial Pellet Weights:	56 mg	57 mg	55 mg		

Appendix H: OD_{600} and CFU/ml of RN4220 Cell Lysis in the Presence of Lysozyme

Table 11. The lysis rate of *S. aureus* RN4220 measured using OD_{600} absorbance following incubation with 20 µM FmtA. Cell lysis was induced by treatment with 350 µg/ml lysozyme enzyme. Cultured cells were normalized by weight for each trial, incubated with FmtA, and resuspended in nutrient free 1x PBS buffer. Lysis was monitored over a period 240 minutes with measurements recorded every 40 minutes. A control without FmtA treatment was performed alongside the FmtA incubated sample for comparison. The table exhibits the raw values recorded in conjunction with the average of all three trials and ± standard deviation calculations.

S. aureus RN4220 + Lysozyme + 20 µM FmtA (OD 600nm)					
Time (min)	Trial 1	Trial 2	Trial 3	Average	Standard Deviation (±)
0	0.39	0.40	0.40	0.40	0.01
40	0.36	0.35	0.35	0.35	0.01
80	0.33	0.31	0.31	0.32	0.01
120	0.32	0.29	0.29	0.30	0.02
160	0.30	0.27	0.27	0.28	0.01
200	0.28	0.24	0.25	0.26	0.02
240	0.26	0.23	0.22	0.24	0.02
Bacterial Pellet Weight	59.1 mg	57.3 mg	56.8 mg		
RN4220 + Lysozyme (OD 600nm)					
Time (min)	Trial 1	Trial 2	Trial 3	Average	Standard Deviation (±)
0	0.36	0.37	0.39	0.37	0.01
40	0.33	0.32	0.33	0.33	0.01
80	0.32	0.30	0.30	0.31	0.01
120	0.28	0.28	0.28	0.28	0.00
160	0.28	0.26	0.27	0.27	0.01
200	0.26	0.23	0.25	0.25	0.01
240	0.25	0.21	0.23	0.23	0.02
Bacteial Pellet Weight	59.2 mg	57.6 mg	56.9 mg		

Table 12. The lysis rate of *S. aureus* RN4220 was depicted by CFU/ml calculations following incubation with 20 μM FmtA. Cell lysis was induced by treatment with 350 μg/ml lysozyme enzyme. Cultured cells were normalized by weight for each trial, incubated with FmtA, and resuspended in nutrient free 1x PBS buffer. Lysis was monitored over a period of 240 minutes segmented into 40-minute intervals where aliquots of the solutions were plated onto TSB-Agar plates after a series of serial dilutions. The plates were incubated at 37ºC for 16 hours and CFU/ml was subsequently assessed by recording the number of colonies grown for each time point. The colony counts were an indicator of the level of viable cells remaining in solution. A control without FmtA treatment was performed alongside the FmtA incubated sample for comparison. The table exhibits the raw values recorded in conjunction with the average of all three trials and ± standard deviation calculations.

RN4220 + Lysozyme + 20 μMFmtA (CFU/ml)					
Time (min)	Trial 1	Trial 2	Trial 3	Average	Standard Deviation (±)
0	3.93E+08	3.87E+08	3.00E+08	3.60E+08	5.21E+07
40	9.53E+07	1.15E+08	1.25E+08	1.12E+08	1.52E+07
80	9.67E+07	1.24E+08	9.87E+07	1.06E+08	1.52E+07
120	9.87E+07	1.15E+08	1.15E+08	1.10E+08	9.62E+06
160	7.53E+07	9.93E+07	1.05E+08	9.33E+07	1.59E+07
200	7.13E+07	9.47E+07	8.67E+07	8.42E+07	1.19E+07
240	8.20E+07	9.53E+07	6.93E+07	8.22E+07	1.30E+07
Bacterial Pellet Weight	59.1 mg	57.3 mg	56.8 mg		
RN4220 + Lysozyme (CFU/ml)					
Time (min)	Trial 1	Trial 2	Trial 3	Average	Standard Deviation (±)
0	3.67E+08	4.27E+08	4.07E+08	4.00E+08	3.06E+07
40	8.20E+07	1.39E+08	1.17E+08	1.12E+08	2.86E+07
80	9.07E+07	1.37E+08	1.25E+08	1.18E+08	2.42E+07
120	8.40E+07	1.28E+08	1.24E+08	1.12E+08	2.43E+07
160	8.33E+07	9.47E+07	1.03E+08	9.36E+07	9.71E+06
200	6.60E+07	1.05E+08	1.06E+08	9.22E+07	2.27E+07
240	7.40E+07	8.87E+07	8.13E+07	8.13E+07	7.33E+06
Bacteial Pellet Weight	59.2 mg	57.6 mg	56.9 mg		

Appendix I: OD_{600} and CFU/ml of RN4220 Cell Lysis Incubated with FmtA and Lysostaphin

Table 13. OD_{600} measurements for RN4220 *S. aureus* cells incubated with and without 20μM FmtA, after which both solutions were subjected to 0.25 μg/ml lysostaphin. OD_{600} readings were recorded over time, demonstrating a lysis pattern in both conditions until the 120–160-minute interval. Three trials were conducted and averaged. The initial weights of the RN4220 cell pellets were normalized prior to incubation with FmtA, and the data was presented together with ± standard deviation calculated from the three trials. The raw data from each trial is listed.

RN4220 + 20μM FmtA + Lysostaphin (OD 600nm)					
Time (min)	Trial 1	Trial 2	Trial 3	Average	Standard Deviation (±)
0	0.40	0.42	0.41	0.41	0.01
40	0.22	0.20	0.24	0.22	0.02
80	0.08	0.09	0.09	0.09	0.00
120	0.06	0.06	0.06	0.06	0.00
160	0.06	0.06	0.06	0.06	0.00
200	0.06	0.06	0.05	0.06	0.00
240	0.06	0.06	0.05	0.06	0.00
Bacteral Pellet Weights	57 mg	57.5 mg	55 mg		
RN4220 + Lysostaphin without FmtA (OD 600nm)					
Time (min)	Trial 1	Trial 2	Trial 3	Average	Standard Deviation (±)
0	0.39	0.42	0.38	0.39	0.02
40	0.23	0.23	0.27	0.24	0.02
80	0.10	0.10	0.12	0.11	0.01
120	0.06	0.06	0.07	0.06	0.00
160	0.05	0.05	0.05	0.05	0.00
200	0.05	0.05	0.05	0.05	0.00
240	0.05	0.05	0.05	0.05	0.00
Bacteral Pellet Weights	57 mg	57.5 mg	55 mg		
RN4220 without Lysostaphin or FmtA (OD 600nm)					
Time (min)	Trial 1	Trial 2	Trial 3	Average	Standard Deviation (±)
0	0.43	0.41	0.43	0.42	0.01
40	0.36	0.37	0.40	0.38	0.02
80	0.36	0.36	0.38	0.37	0.01
120	0.39	0.36	0.37	0.38	0.01
160	0.41	0.35	0.37	0.37	0.03
200	0.42	0.37	0.41	0.40	0.03
240	0.40	0.40	0.42	0.41	0.01
Bacteral Pellet Weights	57 mg	57.5 mg	55 mg		

Table 14. Quantification of the CFU/ml for RN4220 *S. aureus* cells incubated with and without 20μM FmtA, after which both conditions were treated with 0.25 μg/ml lysostaphin. Over a 240-minute time interval, both conditions exhibited increased lysis as fewer colonies were detected on the TSB-Agar plates. The study was conducted in triplicate, and the initial weights of the RN4220 cell pellets were normalized prior to FmtA incubation. The data was averaged and presented with ± standard deviation calculated form the three trials. The raw data from each trial is listed.

RN4220 + 20μM FmtA + Lysostaphin (CFU/ml)					
Time (min)	Trial 1	Trial 2	Trial 3	Average	Standard Deviation (±)
0	1.93E+08	4.27E+08	2.27E+08	2.82E+08	1.26E+08
40	4.73E+07	5.27E+07	9.47E+07	6.49E+07	2.59E+07
80	4.67E+06	6.20E+06	1.33E+07	8.07E+06	4.63E+06
120	5.40E+05	7.07E+05	1.52E+06	9.22E+05	5.24E+05
160	2.67E+04	3.33E+04	9.33E+04	5.11E+04	3.67E+04
200	2.73E+03	4.93E+03	6.73E+03	4.80E+03	2.00E+03
240	4.67E+02	8.67E+02	8.67E+02	7.33E+02	2.31E+02
Bacteral Pellet Weights	57 mg	57.5 mg	55 mg		
RN4220 + Lysostaphin without FmtA (CFU/ml)					
Time (min)	Trial 1	Trial 2	Trial 3	Average	Standard Deviation (±)
0	1.73E+08	4.40E+08	2.13E+08	2.76E+08	1.44E+08
40	8.80E+07	9.27E+07	1.15E+08	9.87E+07	1.46E+07
80	1.67E+07	3.40E+07	3.27E+07	2.78E+07	9.65E+06
120	2.00E+06	2.11E+06	2.13E+06	2.08E+06	7.06E+04
160	6.87E+05	9.80E+05	9.87E+05	8.84E+05	1.71E+05
200	1.71E+04	1.89E+04	2.03E+04	1.88E+04	1.61E+03
240	3.33E+03	4.40E+03	1.73E+03	3.16E+03	1.34E+03
Bacteral Pellet Weights	57 mg	57.5 mg	55 mg		

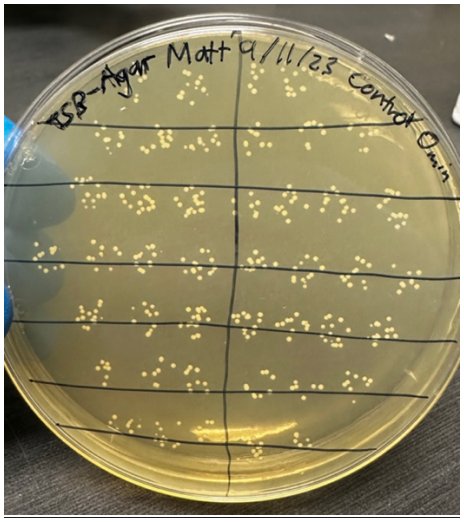

Figure 33. Quantification of *S. aureus* RN4220 colonies formed on the TSB-Agar plates, in the absence of FmtA and lysostaphin. This plate was cultured to confirm that these cells were not able to multiply in a 50 mM Tris-HCl solution devoid of nutrients. The number of colonies were assessed by enumeration of the growth from a 10^{-5} serially diluted solution. The initial time point (0 minutes) is represented in the first row, with subsequent rows corresponding to further incubation intervals (every 40 minutes) for a total of 240 minutes.

Appendix J: Confirmation of the Oxacillin MIC Against Several *S. aureus* Strains by Colony Formation on TSB-Agar Plates Following FmtA Incubation

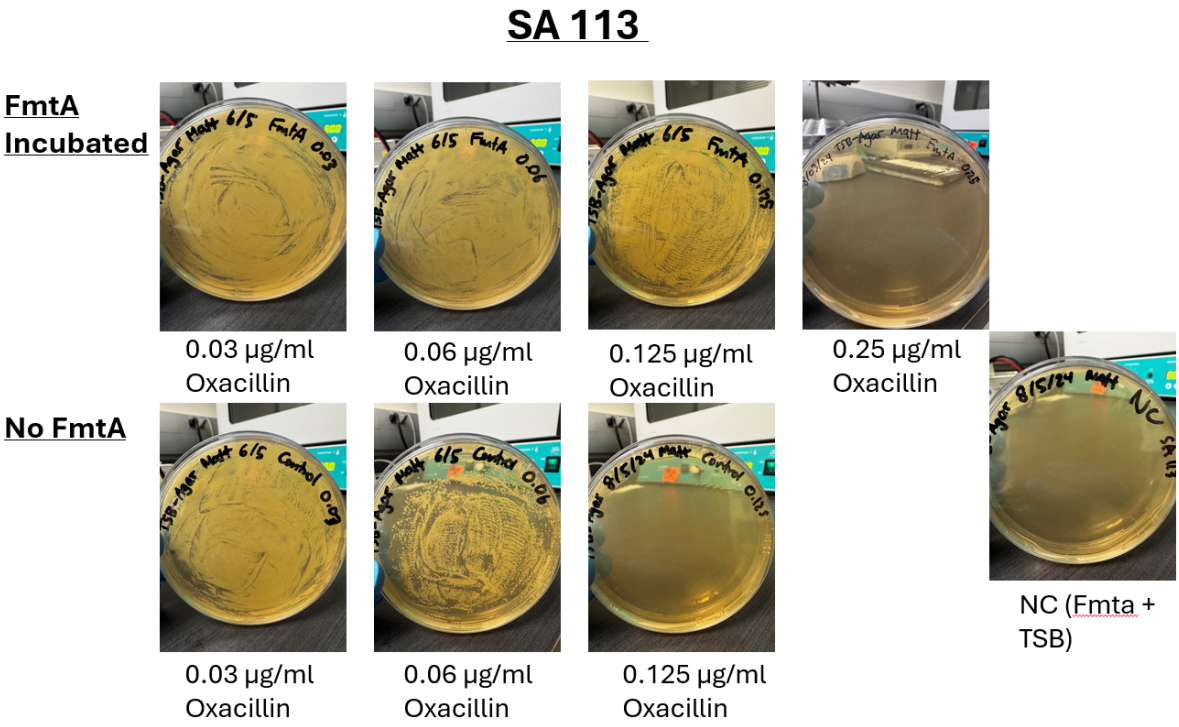

Figure 34. The modification of the oxacillin MIC against *S. aureus* SA 113 was evaluated by colony formation on TSB-Agar plates under the absence of or incubation with 20µM exogenous FmtA. Initial growth was conducted in 96-well culture plates containing SA 113, varying concentrations of oxacillin, and either FmtA or 50 mM sodium phosphate buffer (pH 7.2). Aliquots from these solutions were subsequently cultured onto these TSB-Agar plates to validate the MIC determined from the 96-well plate. These plates were incubated at 37°C for 22 hours, after which colony formation was assessed to determine the presence or absence of viable cells for each oxacillin-containing solution. For the SA 113 strain, solutions containing oxacillin concentrations ranging from 0.03 to 0.25 µg/ml were tested. The negative control (NC) containing FmtA and TSB was included to ensure the purity of FmtA.

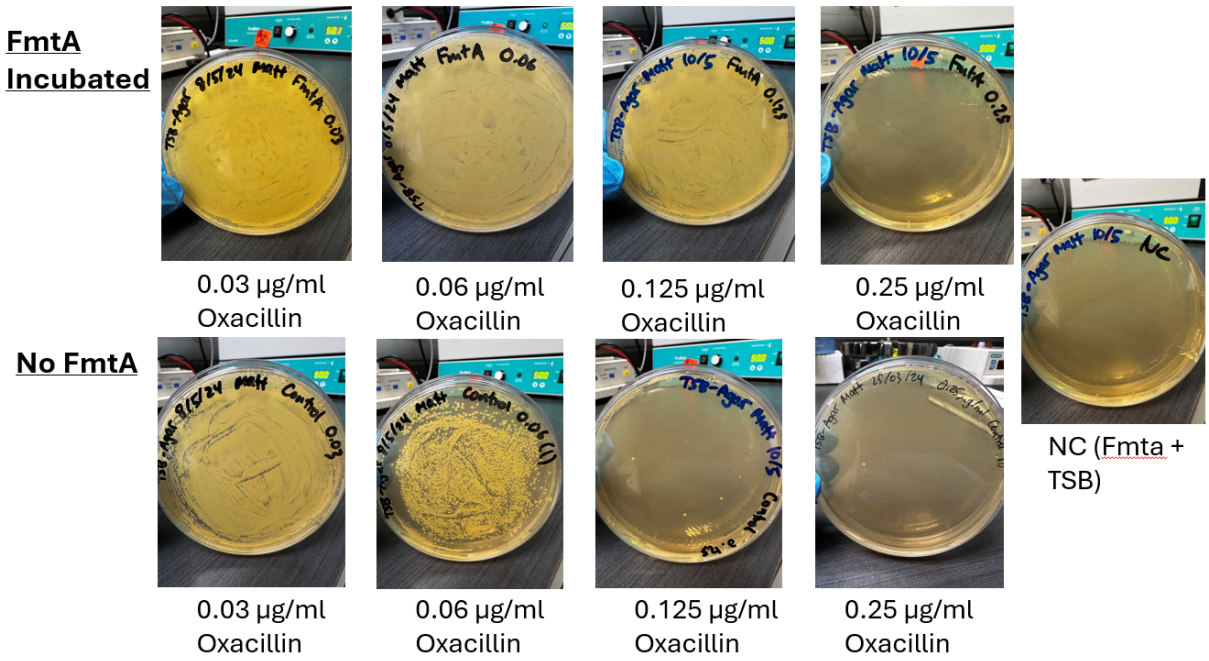

Figure 35. The modification of the oxacillin MIC against *S. aureus* MSSA 1112 was evaluated by colony formation on TSB-Agar plates under the absence of or incubation with 20µM exogenous FmtA. Initial growth was conducted in 96-well culture plates containing MSSA 1112, varying concentrations of oxacillin, and either FmtA or 50 mM sodium phosphate buffer (pH 7.2). Aliquots from these solutions were subsequently cultured onto these TSB-Agar plates to validate the MIC determined from the 96-well plate. These plates were incubated at 37°C for 22 hours, after which colony formation was assessed to determine the presence or absence of viable cells for each oxacillin-containing solution. For the MSSA 1112 strain, solutions containing oxacillin concentrations ranging from 0.03 to 0.25 µg/ml were tested. The negative control (NC) containing FmtA and TSB was included to ensure the purity of FmtA.

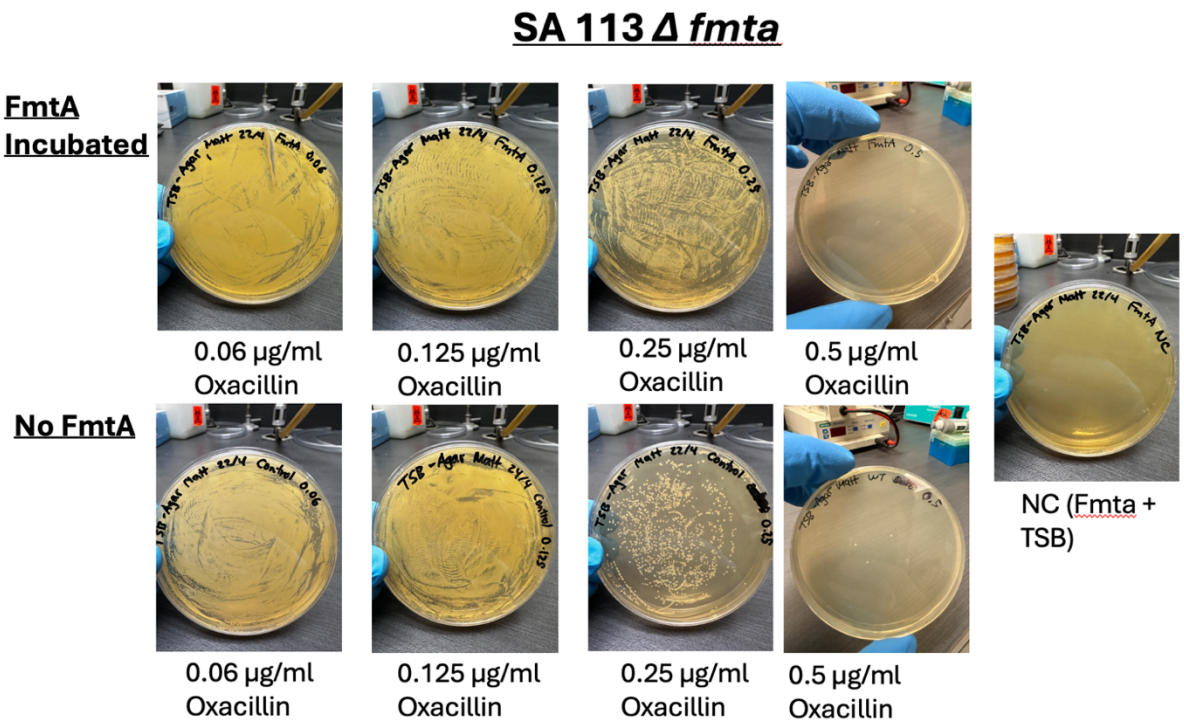

Figure 36. The modification of the oxacillin MIC against *S. aureus* SA 113 *Δfmta* was evaluated by colony formation on TSB-Agar plates under the absence of or incubation with 20µM exogenous FmtA. Initial growth was conducted in 96-well culture plates containing SA 113 *Δfmta*, varying concentrations of oxacillin, and either FmtA or 50 mM sodium phosphate buffer (pH 7.2). Aliquots from these solutions were subsequently cultured onto these TSB-Agar plates to validate the MIC determined from the 96-well plate. These plates were incubated at 37°C for 22 hours, after which colony formation was assessed to determine the presence or absence of viable cells for each oxacillin-containing solution. For the SA 113 *Δfmta* strain, solutions containing oxacillin concentrations ranging from 0.06 to 0.5 µg/ml were tested. The negative control (NC) containing exogenous FmtA and TSB was included to ensure the purity of FmtA.

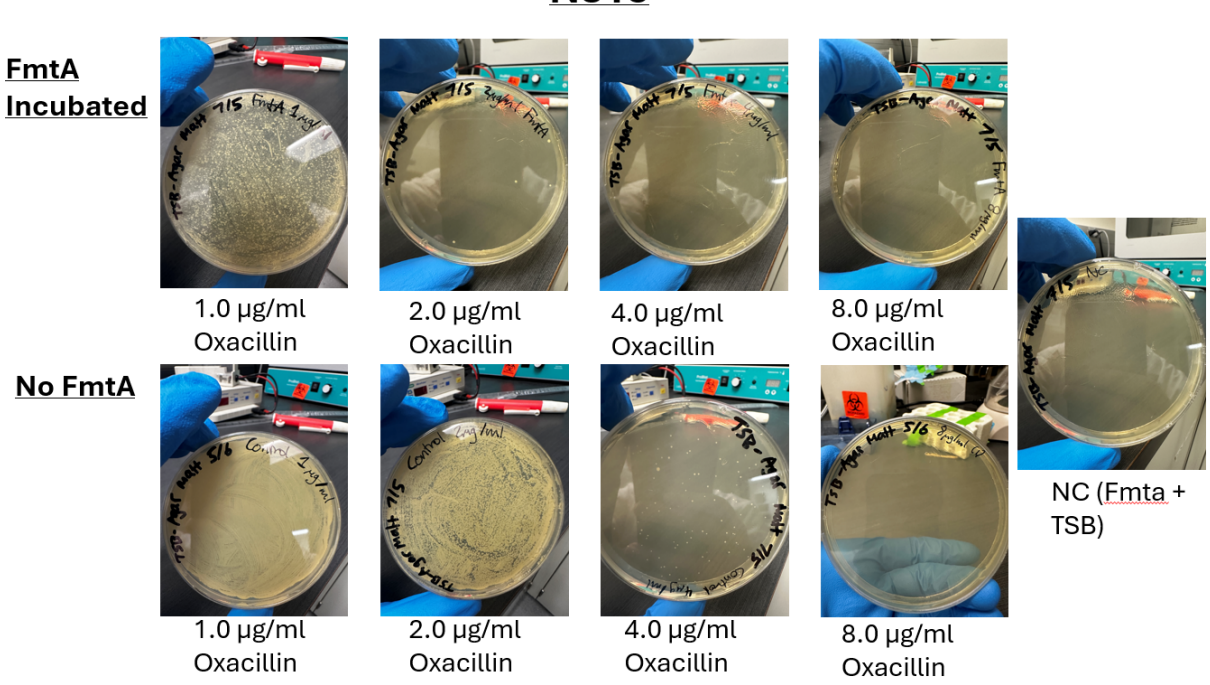

Figure 37. The modification of the oxacillin MIC against *S. aureus* N315 was evaluated by colony formation on TSB-Agar plates under the absence of or incubation with 20µM exogenous FmtA. Initial growth was conducted in 96-well culture plates containing N315, varying concentrations of oxacillin, and either FmtA or 50 mM sodium phosphate buffer (pH 7.2). Aliquots from these solutions were subsequently cultured onto these TSB-Agar plates to validate the MIC determined from the 96-well plate. These plates were incubated at 37°C for 22 hours, after which colony formation was assessed to determine the presence or absence of viable cells for each oxacillin-containing solution. For the N315 strain, solutions containing oxacillin concentrations ranging from 1.0 to 8.0 µg/ml were tested. The negative control (NC) containing FmtA and TSB was included to ensure the purity of FmtA.

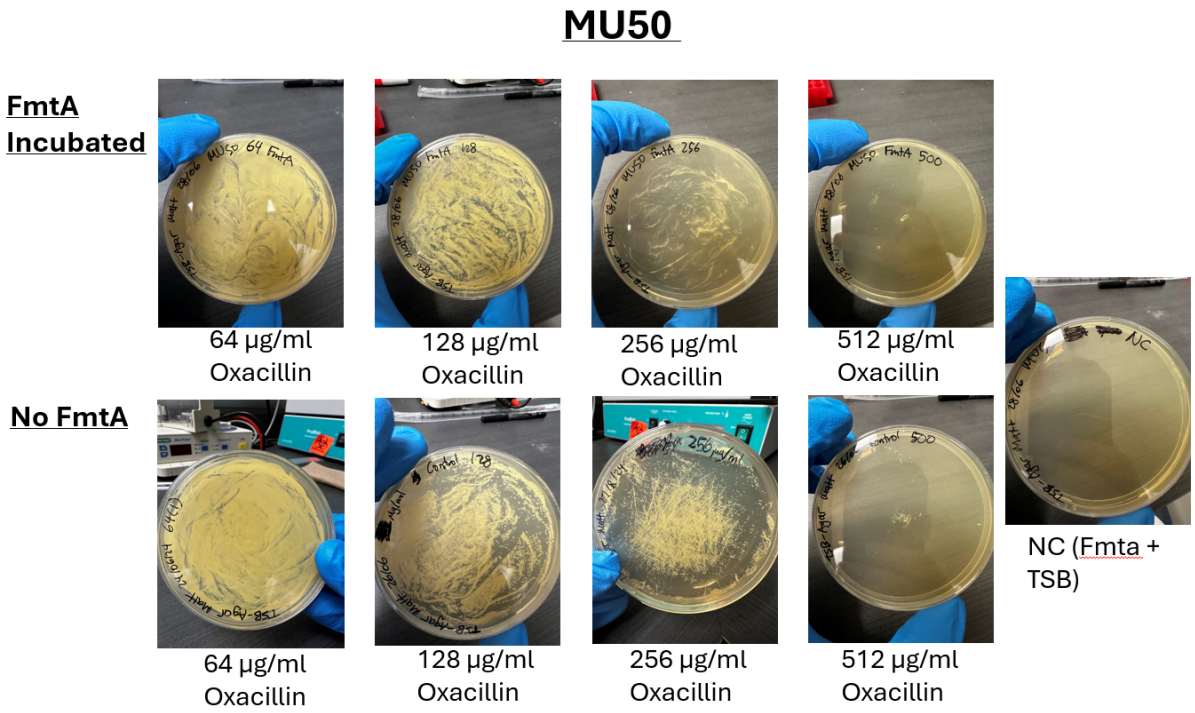

Figure 38. The modification of the oxacillin MIC against *S. aureus* MU50 was evaluated by colony formation on TSB-Agar plates under the absence of or incubation with 20µM exogenous FmtA. Initial growth was conducted in 96-well culture plates containing MU50, varying concentrations of oxacillin, and either FmtA or 50 mM sodium phosphate buffer (pH 7.2). Aliquots from these solutions were subsequently cultured onto these TSB-Agar plates to validate the MIC determined from the 96-well plate. These plates were incubated at 37°C for 22 hours, after which colony formation was assessed to determine the presence or absence of viable cells for each oxacillin-containing solution. For the MU50 strain, solutions containing oxacillin concentrations ranging from 64 to 512 µg/ml were tested. The negative control (NC) containing FmtA and TSB was included to ensure the purity of FmtA. The agar containing 512 µg/ml oxacillin solutions had aberrations for both FmtA-containing and FmtA-absent plates. The visible deposition on the plates is not indicative of bacterial growth.

References

Jenni, R., & Berger-Bächi, B. (1998). Teichoic acid content in different lineages of Staphylococcus aureus NCTC8325. *Archives of Microbiology*, *170*(3), 171–178.

Kojima, N., Araki, Y., & Ito, E. (1985). Structure of the linkage units between ribitol teichoic acids and peptidoglycan. *Journal of Bacteriology*, *161*(1), 299–306.